

TECHNISCHE UNIVERSITÄT MÜNCHEN

Institut für Wasserchemie und Chemische Balneologie

Lehrstuhl für Analytische Chemie

**Immunoanalytical Determination of Mycotoxins in Food with an
Automatized Instrumental Platform**

Jimena Celia Saucedo-Friebe

Vollständiger Abdruck der von der Fakultät für Chemie der Technischen Universität München zur Erlangung des akademischen Grades eines

Doktors der Naturwissenschaften

genehmigten Dissertation.

Vorsitzender: Univ.-Prof. Dr. M. Schuster

Prüfer der Dissertation: 1. Univ.-Prof. Dr. R. Niessner

2. Univ.-Prof. Dr. P. Schieberle

Die Dissertation wurde am 11.04.2011 bei der Technischen Universität München eingereicht und durch die Fakultät für Chemie am 07.07.2011 angenommen.

Für Lars

This work was made possible by the generous funding of the Federal Ministry of Education and Research (BMBF, project No. 0315036) and of Eurofins Wej Contaminants GmbH. The experimental work was conducted under the kind supervision of Prof. Dr. Reinhard Niessner during the time comprising August 2008 to July 2010.

Part of the research presented in this work has already been published:

J.C. Saucedo-Friebe, Xaver Y.Z. Karsunke, Susanna Vazac, Scarlett Biselli, Reinhard Niessner, Dietmar Knopp, *Regenerable immuno-biochip for screening ochratoxin A in green coffee extract using an automated microarray chip reader with chemiluminescence detection*, Anal. Chim. Acta **2011**, 689(2), 234-242.

During her doctoral work, the author collaborated in the following original scientific papers:

Z. Lin, J.C. Saucedo-Friebe, J. Lin, R. Niessner, D. Knopp, *Double-codified nanogold particles based automated flow-through CLEIA for 2,4-dinitrotoluene* Anal. Methods **2010**, 2(7), 824-830.

D. Tang, J.C. Saucedo, Z. Lin, S. Ott, E. Basova, I. Goryacheva, S. Biselli, J. Lin, *Magnetic nanogold microspheres-based lateral flow immunodipstick for rapid detection of aflatoxins in food*, Biosens. Bioelectron. **2009**, 25(2), 514-518.

M. Rieger, C. Cervino, J.C. Saucedo, R. Niessner, D. Knopp, *Efficient hybridoma screening technique using capture antibody based microarrays*, Anal. Chem. **2009**, 81(6), 2373-2377.

C. Cervino, J.C. Saucedo, R. Niessner, D. Knopp, *Mycotoxin analysis by automated flow-through immunoassay with chemoluminescence readout*, Luminescence **2008**, 23(4), 206-207.

I would like to express my heartfelt thanks to my mentor, Prof. Dr. Reinhard Niessner, for the interesting topic and the uninterrupted support offered during the time of my PhD. I would also like to thank Prof. Dr. Dietmar Knopp for the fruitful discussions and the generous guidance in the realization of this project.

My gratitude also goes to Xaver Karsunke, Susanna Vazac, Dr. Philipp Stolper, Dr. Christian Cervino, and Dr. Sung Zhe, for the memorable times, the invaluable help, and the excellent group atmosphere that made my stay at the Institute unforgettable.

To Dr. Natalia Ivleva I thank for her help with the microscopy pictures and for much, much more.

I am thankful to Klaus Wutz for the critical review of my scientific article and for the excellent discussion opportunities.

To my colleagues and friends from the IWC community I am indebted because they were always there for me when I most needed them, for a good time, or a good laugh, for insightful advice or a helping hand.

The students that worked under my supervision earned a permanent place in my heart. Without them, this work would not have been possible.

I would like to thank Dr. Jürgen Groll for the generous samples of Star-PEG prepolymers.

Dr. Michael Weller has my gratitude for the helpful and friendly advice that took me a step further in the experimental research.

I would also like to thank Dr. Scarlett Biselli of Eurofins WEJ Contaminants and her helpful team for providing the mycotoxin contaminated food samples and the official mycotoxin norms.

Finally, I am indebted to my family, Rocío, Juan Manuel, Regina, Roland, Patricia and Daniel, for this wonderful place that I take always with me, which is called Home.

Table of Contents

1	Introduction and Problem Stating	1
2	Theoretical Background	3
2.1	Ochratoxin A: Relevance and Analytics	3
2.1.1	Mycotoxins: Definition, Origin and Importance.....	3
2.1.2	OTA, Generalities	5
2.1.3	OTA, Toxicity Assessment	6
2.1.4	OTA Contamination in Foods: Impact and Legislation.....	7
2.1.5	Mycotoxin Analytics: Challenges and Trends	9
	Sample and sample preparation.....	10
	Extraction	10
	Sample Clean-up	11
	Detection	15
2.2	Chemical Immobilization of Receptors on Biosensors	25
2.2.1	Diversity and Challenges in Sensor Miniaturization.....	25
2.2.2	Physical Adsorption	26
2.2.3	Covalent Immobilization.....	26
2.2.4	Receptor Immobilization: Affinity Binding.....	31
2.2.5	Receptor Immobilization: Analyte Derivatization	32
2.2.6	Arraying Methods: Analyte Deposition Techniques.....	34
2.3	Solid Phase Peptide Synthesis (SPPS)	36
2.3.1	Generalities and Principle of SPPS	36
2.3.2	Activating Reagents in Fmoc Chemistry	39
2.3.3	SPPS Solid Supports	41
2.3.4	Side Reactions in SPPS	42
	Racemization at the α -Carbon.....	42

Diketopiperazine Formation.....	43
Aspartimide Formation	43
3 Results and Discussion	45
3.1 Customization and Characterization of the MCR 3	45
3.1.1 MCR 3: General Description and Characteristics	45
3.1.2 The Flow-Cell Work Surface	50
3.1.3 Analyte Chemical Modification for Immobilization.....	52
3.1.4 Reactive Surface Characterization: Contact Spotting	55
3.1.5 Optimization of Surface Regeneration Conditions	56
3.1.6 Signal Decrease with Surface Regeneration	60
3.1.7 Additional Surface Modifications: Star-PEG.....	63
3.1.8 Instrumentation: Flow Cell Characteristics.....	65
3.1.9 Instrumentation: Optimized Assay Conditions	68
3.2 MCR 3-Based OTA Determination in Green Coffee	71
3.2.1 HPLC Testing of Blank Green Coffee	71
3.2.2 Comparison of Four Available Anti-OTA Antibodies.....	75
3.2.3 Optimization of Assay Conditions with Coffee Extract.....	78
3.2.4 MCR 3 OTA Measurements in Green Coffee Extract: Search for an Adequate Positive Control.....	80
3.2.5 Dose-Response Curves in Buffer and in Green Coffee Extract.....	83
3.2.6 Real Sample Measurements	91
3.2.7 Comparison of the Developed MCR 3 Method with Other Available Methods for OTA Screening in Coffee	96
3.3 Towards Multiple Toxin Screening and Shorter Measuring Times with the MCR 3.....	102
3.3.1 Simultaneous Detection of AFB ₁ and OTA, Proof of Principle	102

3.3.2	Dual Signal Stability with Peanut Extract.....	104
3.3.3	Further Developments in MCR 3 Assay Formats for Reducing Measuring Time.....	107
4	Summary and Outlook.....	112
5	Experimental.....	117
	Instruments.....	117
	Software.....	118
	Antibodies and Antigens.....	118
	Chemicals.....	119
	Miscellaneous.....	121
	Buffer solutions.....	122
	Standard Procedures.....	123
	MCR 3 code for green coffee assay.....	135
6	Abbreviations.....	140
7	Bibliography.....	142

1 Introduction and Problem Stating

“It is recommended that efforts should continue to reduce OTA-contamination of foods. Monitoring programs to describe known sources of exposure and to identify potential emerging sources are recommended as the re-evaluation of OTA indicated that infants and children, as well as distinct segments of the population representing high consumers of certain locally-produced food specialties, may have high rates of exposure to OTA.”

This closing remark was expressed by the Scientific Panel on Contaminants in the Food Chain of the European Food Safety Authority (EFSA) in 2006 and is still considered valid as the end of the year 2010 approaches. Ochratoxin A (OTA), a potent fungal nephrotoxin, can be extremely harmful to humans and to domestic animals if ingested even in very low quantities. It may be present in cereals and cereal products, dried fruit, coffee, nuts, pulses, beer, wine, and even animal tissue, as it can move up along the food chain when contaminated feed is used in stock breeding. Global awareness of the problem and good agricultural practices can reduce the OTA content in foods, but because its producing fungi are ubiquitous and may infest crops in any stage of growing, harvesting, or storage, a certain extent of contamination is still unavoidable.

Strict limits on OTA maximum contamination values have been adopted in countries all over the world for several raw and processed agricultural products. In order to ensure safe access to food sources, the OTA content must not exceed a few parts per million, or between 3 and 10 μg OTA per kg of product, for most of the relevant food commodities. Limits in a similar range have also been imposed for other mycotoxins of importance such as patulin, zearalenone, the aflatoxins and the trichothecenes. Both locally produced foods and imported goods are subjected to these controls. Since the beginning of 1960, the need for efficient mycotoxin screening in food samples has been fulfilled by an ever-growing number of analytical methods. Frequently, and given the diversity of agricultural products and mycotoxins that may contaminate them, these methods are not only toxin-specific, but matrix-specific as well. Several of them are based on a combination of immunoaffinity enrichment, liquid chromatography, and either spectrophotometric or mass spectrometric detection. Although highly efficient, they are labor-intensive, require the expertise of highly trained personnel and their use is constrained to specialized research facilities. Therefore, field applications have also been developed that are far more adequate for “on-the-spot” testing, mostly relying on a version of the Enzyme Linked Immunosorbent Assay (ELISA). The

ELISA is based on the specific interaction between the analyte of interest and an exquisitely selective sensing molecule, an antibody. It is suitable for the fast screening of raw food extracts because the antibodies used are able to bind to their targets with exquisite affinity and selectivity. This characteristic is needed for the screening because mycotoxin concentration in raw food extracts is usually several orders of magnitude lower than that of other bulk components. Therefore ELISAs also represent a cost effective, viable alternative for the screening of OTA and other mycotoxins in complex food samples.

The Munich Chip Reader 3 (MCR 3) designed at the Institute of Hydrochemistry and Chair for Analytical Chemistry of the Technische Universität München is an instrument developed to carry out a miniaturized version of the ELISA in a fully automated way. It was first tested for the simultaneous detection of several antimicrobial residues in raw milk, as it offers the possibility of carrying out parallel assays in one single sample. It is the primary aim of this work to explore the possibilities that this technology has to offer in the field of mycotoxin screening. In particular, emphasis is made on the screening of OTA in green coffee samples. World imports of this universal commodity are estimated to reach 5510 tons for the 2000-2010 decade and as much as 2035 tons are expected to be traded in the European Community. Furthermore, according to the Food and Agriculture Organization of the United Nations (FAO), 15.6% of the total European import trade will be conducted in Germany. Therefore, a fast screening method capable of delivering reliable results would be highly desirable, since green coffee shipments are not allowed in the market without undergoing strict controls that guarantee them free of OTA, and therefore safe for the consumer. Additionally, the possibility to measure simultaneously more than one toxin in other relevant samples, particularly the combination OTA and aflatoxin B₁ (AFB₁), will also be tested in an effort to take full advantage of the multiplexing possibilities that this technology has to offer. In order to reach these goals, an adequate method for the covalent immobilization of the sensor toxin receptors has to be designed. The optimum programming of the assay, as well as the most time saving assay strategy will also be tested.

2 Theoretical Background

2.1 Ochratoxin A: Relevance and Analytics

2.1.1 Mycotoxins: Definition, Origin and Importance

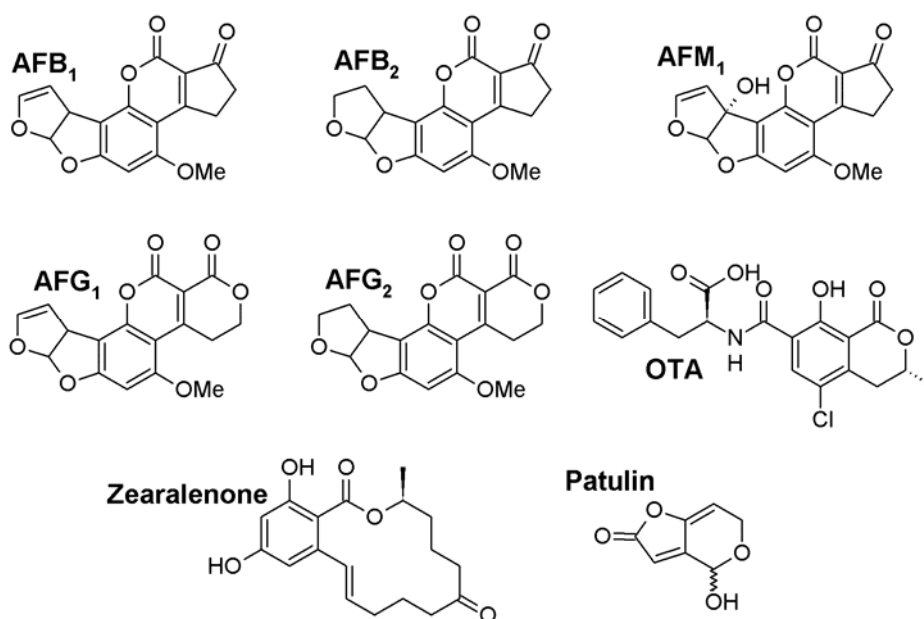
Mycotoxins (from the Greek “μύκηζ”, or “fungus”, and the Latin “toxicum”, or “poison”) are substances of fungal origin that find their way into the food chain by contaminating important agricultural products. The ubiquitous fungi that produce them are considered crop pathogens and belong mainly to the genera *Fusarium*, *Aspergillus* and *Penicillium*. When these fungi infest crops, agricultural productivity is negatively affected. However, the major threat presented to humans consists of the deleterious effects that some of their fungal secondary metabolites, the mycotoxins, exert on human health. The dire consequences of mycotoxin crop contamination are exemplified in recordings dating back as early as the 10th century. One of them describes how at least 40 000 people died in the south of France after intense suffering and hallucination. Most likely, the cause was the ergot fungi (*Claviceps purpurea* and other species) infestation of large crops of rye, which was then eaten in the form of bread.

The defining moment that gave rise to modern mycotoxicology and the realization that human food could be contaminated with mycotoxins came several centuries later, during the so-called “Turkey-X disease outbreak” in the UK, in 1960. Researchers perplexed by the death of thousands of farm turkeys found the fungus *Aspergillus flavus* as contaminant of imported bird feed. One of its metabolic products was finally isolated and proven to be responsible for the outbreak: the previously unknown, highly carcinogenic substance, AFB₁.

Since 1960, some hundreds of mycotoxins have been isolated and characterized. Only a few of them are of importance to food safety, posing serious risks to human health. According to Shephard, the major food-borne mycotoxins are the aflatoxins B₁, B₂, G₁, G₂ and M₁, the fumonisins B₁, B₂ and B₃, the trichothecenes deoxynivalenol and T-2 toxin, zearalenon, OTA, and patulin.^[1] A summary of the food products prone to a specific type of mycotoxin contamination and the chemical structure of some mycotoxins is given in table 1 and in figure 1.

Table 1 Mycotoxins of relevance and some of their characteristics.^[1]

Mycotoxin	Fungal species	Food commodity
Aflatoxins B ₁ , G ₁ , B ₂ and G ₂	<i>Aspergillus flavus</i> , <i>Aspergillus parasiticus</i>	Maize, wheat, rice, figs, sorghum, ground nuts, tree nuts
Aflatoxin M ₁	Metabolite of AFB ₁ in mammals	Milk, milk products
Fumonisin B ₁ , B ₂ and B ₃	<i>Fusarium verticillioides</i> <i>Fusarium proliferatum</i>	Maize, maize products, sorghum, asparagus
Deoxynivalenol	<i>Fusarium graminearum</i> <i>Fusarium culmorum</i>	Cereal, cereal products
T-2 toxin	<i>Fusarium sporotrichioides</i> <i>Fusarium poae</i>	Cereal, cereal products
Zearalenone	<i>Fusarium graminearum</i> <i>Fusarium culmorum</i>	Cereal, cereal products
Ochratoxin A	<i>Aspergillus ochraceus</i> <i>Penicillium verrucosum</i>	Cereals, dried vine fruit, wine, coffee
Patulin	<i>Aspergillus carbonarius</i> <i>Penicillium expansum</i>	Apples, apple juice

**Figure 1** Selected mycotoxins of importance.

In order to reduce mycotoxin ingestion by humans, the FAO and the World Health Organization (WHO) have periodically commissioned panels of experts to assess mycotoxin contamination, prevention and control. As a result, a series of recommendations, including maximum levels of contamination for a broad range of products have been issued. Most countries around the world have followed suit, adapting these recommendations into laws and official regulations. In general, research efforts in the field of mycotoxins in the last 50 years have been aimed at understanding the biochemical mode of action of the most significant mycotoxins, their implications for human health and in the development of analytical methods for their detection in relevant quantities.

2.1.2 OTA, Generalities

Ochratoxin A (OTA), or 7-carboxy-5-chloro-8-hydroxy-3,4-dihydro-3*R*-methylisocoumarin-*L*- β -phenylalanin, (figure 2), is a harmful fungal metabolite and a common contaminant of several agricultural products. It is the most toxic compound of the mycotoxin family generically referred to as “the ochratoxins”, and therefore the member that draws the most attention. Other members in this family include ochratoxin C (ethyl ester of OTA), ochratoxin B (dechlorinated product of OTA), ochratoxin α and ochratoxin β (isocoumarin derivatives of OTA and OTB), substances comparatively less toxic to humans and domestic animals also frequently mentioned in the literature.

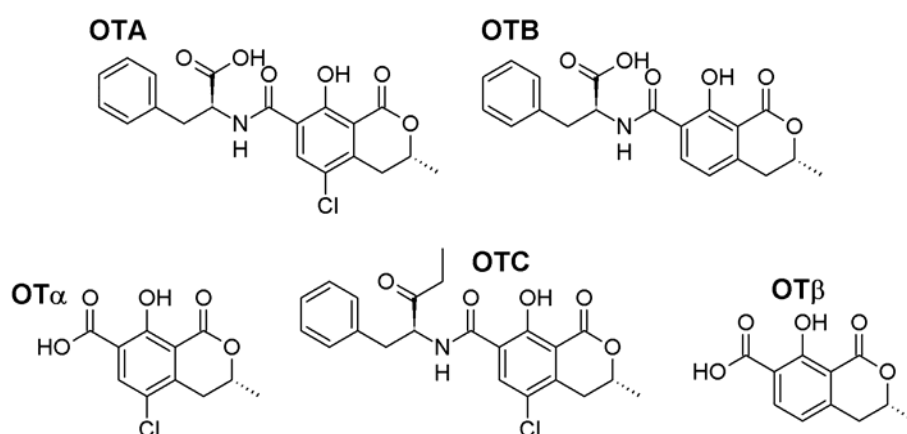


Figure 2 Members of the ochratoxin family.

Most mycotoxins, OTA included, are usually referred to as “fungal secondary metabolites”. This means that their production is highly dependent on the environmental conditions and that it only takes place after the fungus has completed its initial growth phase.^[2] The biochemical

synthesis of OTA has not been fully elucidated; nevertheless the final synthetic step involves the formation of an amide bond between α -OTA and phenylalanine.^[3, 4] Several ochratoxin-producing mould strains have been isolated, among them *Penicillium verrucosum* (previously known as *Penicillium viridicatum*), *Penicillium nordicum* and at least 19 species of *Aspergillus*.^[5] OTA and its derivatives are only produced at a narrow range of warm temperatures (15 to 37 °C), high humidity and sufficient nutrient availability, conditions found all too often in crop storage facilities.^[6] The major agricultural commodities of significant importance to humans where OTA contamination is frequently encountered are grains, green coffee and cocoa beans, spices, grape products and dried fruit. Because of the toxin's long half-life and relative stability, OTA is able to move upwards in the food chain, making it still biologically available in edible animal products, for example meat (particularly pork) and milk. Beer, wine and roasted coffee have also shown traces of OTA, as they are manufactured from raw foodstuffs that may have been contaminated in the less processed stage.^[7-10] Mould infestation of food commodities can occur anywhere in the production chain, whether during harvesting, storage, transportation and even transformation. Once formed, OTA is difficult to remove as well.

2.1.3 OTA, Toxicity Assessment

The International Agency for Research on Cancer (IARC) has classified OTA as a type 2b potential human carcinogen.^[11] It has also been confirmed that OTA causes renal toxicity, nephropathy and immunosuppression in several experimental animals.^[12] Moreover, OTA is strongly suspected to be the cause of the irreversible and fatal kidney disease known as Balkan nephropathy, common in populations living in the river regions of the Balkan Peninsula.^[13] Countless research efforts have been focused on clarifying the molecular cause of OTA toxicity, not necessarily free from controversy and debate.^[3, 13] Although the multiple ways in which OTA affects living organisms are not fully understood, the general consensus can be summarized as follows. OTA is mainly absorbed through the gastrointestinal system, permeates to blood serum and undergoes bioconcentration in the kidneys (to a lower extent in the liver, muscle and fat).^[14] Its capacity to induce renal tumors in animal models is either the result of a direct formation of DNA adducts (genotoxicity), of a secondary effect that induces cell proliferation after chronic toxic damage (epigeneticity), or a combination of both mechanisms. OTA also induces oxidative stress in the mitochondria and might cause indirect DNA damage by interfering with the cytochrome P450 system, or by interacting with other

mitochondrial peroxidases.^[15-18] Whether OTA is classified as human genotoxic in the future is not only of concern to global public health, but would impact legal attitudes toward the establishment of more stringent contamination limits of food products and would have a huge influence on economic interests in trade countries, as well as on the food and beverage industry. The importance of the discussion is well reflected by the multiple re-evaluations in the WHO and FAO sittings that have periodically reevaluated the risks posed by OTA.^[19-21]

2.1.4 OTA Contamination in Foods: Impact and Legislation

Because of its direct impact on the human health of consumers, the European Union (EU) and several other governments around the world have established stringent maximum residual limits (MRL) for OTA in a variety of food commodities. These are estimated by evaluating a mean dietary exposure to OTA and defining a provisional tolerable weekly intake (PTWI). A joint EU-WHO study involving data from Canada, Germany, Japan and three African countries decisively showed that cereals are the most important contributors to OTA in the human diet.^[22] The next major contributors include wine and coffee, as can be appreciated from figure 3.

Contribution of each food commodity to the mean European total dietary intake of OTA (data from France, Norway & Sweden. 2002)

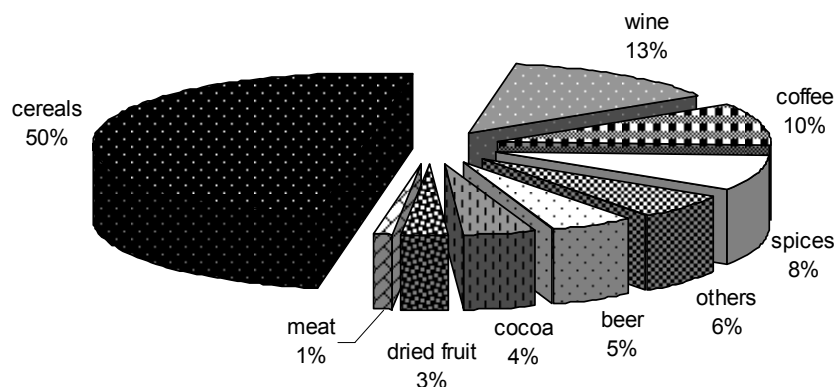


Figure 3 Major contributors to OTA intake in the European diet.

Based on these data, the averaged dietary exposure of Europeans was calculated at 8–17 ng per kg body weight (BW) per week, an intake considered within the established PTWI of 100 ng per kg BW.^[23] Nevertheless, these figures represent averaged data and some populations may be at greater risk of ingesting greater OTA quantities than others.

Maximum limits of OTA vary among different countries, but efforts to harmonize most of the individual existing legislation are the subject of intense cooperation between states and supranational commissions. In 2003 approximately 100 countries in the world had adopted specific regulations concerning mycotoxin content in foods, among them OTA.^[24] In the meantime, the EU has unified regulations for at least 50 combinations of mycotoxins and food products through its organizations such as the European Food Safety Authority (EFSA), the Scientific Cooperation on Questions relating to Food, and the Rapid Alert System for Food and Feed.^[25] The Mercado Común del Sur (MERCOSUR) also has adopted unified legislation for its member states Argentina, Uruguay, Paraguay and Brazil. Moreover, established contamination limits also differ from product to product, depending on risk assessment factors and taking into consideration the local PTWI, which can vary from population to population.

In Germany, and particularly in Bavaria, the Bayrisches Landesamt für Gesundheit und Lebensmittelsicherheit harmonized its legislation with the EU with regard to OTA in 2007. Table 2 summarizes the current maximum permissible contamination values in several products of importance.

Table 2 OTA MRLs in food and food commodities. EU and Germany legislation^[26]

Food	MRL OTA, $\mu\text{g kg}^{-1}$	Food	MRL OTA, $\mu\text{g kg}^{-1}$
raw cereal, rice, buckwheat	5	soluble & instant coffee	10
processed cereal products	3	beverages from wine, wine, grape must	2
dried vines	10	grape juice & nectar, grape juice ingredients, reconstituted juice	2
dried figs	8	cereal products (infants, young children)	0.5
dried fruits	2	baby formula, baby dietary supplements	0.5
roasted coffee	5		

Until now, no maximum limit has been set for OTA in green coffee, dried fruits (excepting vines), cacao or cacao derived products, fortified wine (port, sherry), spices or licorice, but future risk evaluations will determine whether this measure is necessary.

2.1.5 Mycotoxin Analytics: Challenges and Trends

In general, it can be said that current legislation is very clear concerning consumer protection against the deleterious effects of mycotoxins. Nevertheless, the adherence to existing legal considerations, the quality control of vulnerable products, as well as the prevention of economical damage present a complex challenge to producers and to surveillance institutions alike. Highly desirable as it may be, the elimination of mycoflora from crops is not a realistic perspective, although the reduction of contamination has proven successful through the adoption of global prevention strategies. The now concluded FAO/WHO program “Enhancement of Coffee Quality through the Prevention of Mould Formation” is a good example of such a global initiative.^[27]

The problem presented by mycotoxin contamination assessment is complex: for instance, the presence of the *bona fide* mycotoxin-producing fungi is not necessarily an indicator of that the harmful compounds are present. In particular, OTA may be present in the parts-per-billion (ppb) to parts-per-million (ppm) range in complex matrices, which may be hard to eliminate for analytical purposes and usually interfere with the determination. Therefore, the need for developing fast, efficient and cost-effective methods for OTA screening and quantification is still present.

In general, the analytical procedures for the determination of mycotoxins in food products can be summarized in the following steps^[28]:

- Sampling and sample preparation
- Extraction
- Sample cleanup
- Detection

Some of the relevant aspects of each step will be discussed with more detail in this section.

Sample and sample preparation

The mycotoxins OTA and the aflatoxins tend to be distributed inhomogeneously in contaminated goods, the so-called “hot-spots”. This further complicates sampling procedures, which should be at the same time practicable and representative of big trade volumes. EU directives are responsible for describing the requirements of sampling procedures as well. For example, the EU Directive 1998/53/EC establishes that for OTA analysis, a sample of 10 kg of material must be drawn from the bulk.^[29] Furthermore, for laboratory preparation, the sample must be homogenized, a condition difficult to achieve. For this purpose, the “water slurry” technique is the most viable. This consists of blending the sample material with a set amount of water.^[30] Sample preparation usually includes the reduction of the homogenized water slurry to a workable amount, since the original size exceeds the capacities of the analytical lab. A new method for the sampling of large raw food products is the “Discovery” technology.^[31] This instrument presents a cylindrical chamber, similar to a front-loading drying machine, where the goods are placed and spinned under controlled pressure, cycling, temperature and air input, in order to release particles from inspected items. One instrument load can process up to 150 kg of material. Samples can be analyzed and identified using standard methods after collecting the trapped particles from the filters. The “Discovery” is novel because it reduces the sampling time, and because the inspection of large volumes of raw stuffs allows for more statistically significant outcome results. The method has already been put to the test for OTA determination in green coffee and cocoa beans.

Extraction

For OTA analysis, the liquid sample or the homogenized slurry must be extracted before further steps in the analysis follow, as is the case with most mycotoxin analytical methods. During method development, factors such as extraction time, temperature, solvent pH, solvent composition and sample to solvent ratio have to be taken into consideration. When the quantitative, simultaneous extraction of multiple toxins is required, the method development can become even more complex. For example, cereals contaminated with OTA may show traces of aflatoxins as well. Aflatoxins have no ionizable groups and are more effectively extracted with non-polar solvents, or at least with a high proportion of organic solvent in a water mixture. If simultaneous extraction of OTA and aflatoxins is the goal, it has to be taken into consideration that the individual conditions for optimal extraction of one type of toxins may not be the same as for other. On the other hand, OTA is an amphiphilic molecule with two ionizable groups, a carboxylic acid and a phenol (pK_a 4.4 and 7.2-7.3, respectively), a

characteristic that can be used advantageously when the preferred mixtures of organic solvent and water are used for extraction.^[32] For OTA extraction, two trends can be appreciated, a water-based approach or an organic approach. In the first case, acetonitrile (ACN) or methanol (MeOH) are usual components of the extracting solution and usually the addition of sodium bicarbonate is necessary to keep the toxin soluble by providing a pH above both pK_a values. For organic solvent-based extraction, chloroform, dichloromethane (DCM), toluene or a mixture of them are employed and the solution needs to be acidified with hydrochloric or phosphoric acid,^[8] since non-polar, organic solvents dissolve the unprotonated form of the analyte better. Although chlorinated solvents are efficient for extraction, they are harmful to the environment and to the laboratory personnel and “greener” solvent alternatives are preferred when possible. A certified extraction method for OTA in roasted coffee is provided by the Deutsche Industrie Norm (DIN) and is a good example of a water-based extraction carried out under basic conditions.^[33]

The transfer of the toxin from the solid sample (or slurry) to the liquid phase is regularly achieved by means of mechanical shaking, the simplest tool available. Newer technologies present the added advantage of shorter extraction times, the diminished use of solvent and the possibility of automation. For example, the accelerated solvent extraction method (ASE) originally developed by the company Dionex confines the sample to a pressurized chamber (500 to 300 psi) and makes use of organic solvents at high temperatures (50-200 °C). The effective time required can be as short as 5 min, as opposed to the 30 min to 1 h necessary for mechanical shaking.^[34] Procedures for the determination of OTA in rice and bread have already been published using this fast technology.^[35]

Sample Clean-up

The ratio of bulk to toxin in a contaminated food sample can be as high as 1 to 10⁹. The determination of contaminants at these low levels presents the analytical chemist with difficulties in isolating the analyte of interest and separating it from the co-extracted interfering impurities. Therefore, clean-up methods for trace analysis serve two purposes: the enrichment of the target in the final liquid phase and the removal of matrix-associated interferences in the original sample. Immunoaffinity cleanup and solid phase extraction are relevant to mycotoxin analysis and will be discussed further.

Immunoaffinity purification relies on the recognition between an epitope (the analyte) and an antibody, a finely tuned interaction for spatial complementarity of specific chemical

groups. The principle of immunoaffinity chromatography (IAC) is presented in figure 4. First, the column (or “cartridge”) needs to be conditioned, which means that a solution with the same composition as the sample to be applied is to be flushed extensively along the packing material. After washing and conditioning of the IAC column with appropriate buffer, the extract is applied and the target will bind to the specific antibodies. Next, the column is rinsed to remove the matrix components, but the target remains bound to their specific antibody. Finally, elution is carried out as the final step by applying an organic solvent (e.g. MeOH or ACN), which will denature the antibody-analyte complex and will cause the analyte to be released. The solution can then be analyzed by the method of choice.

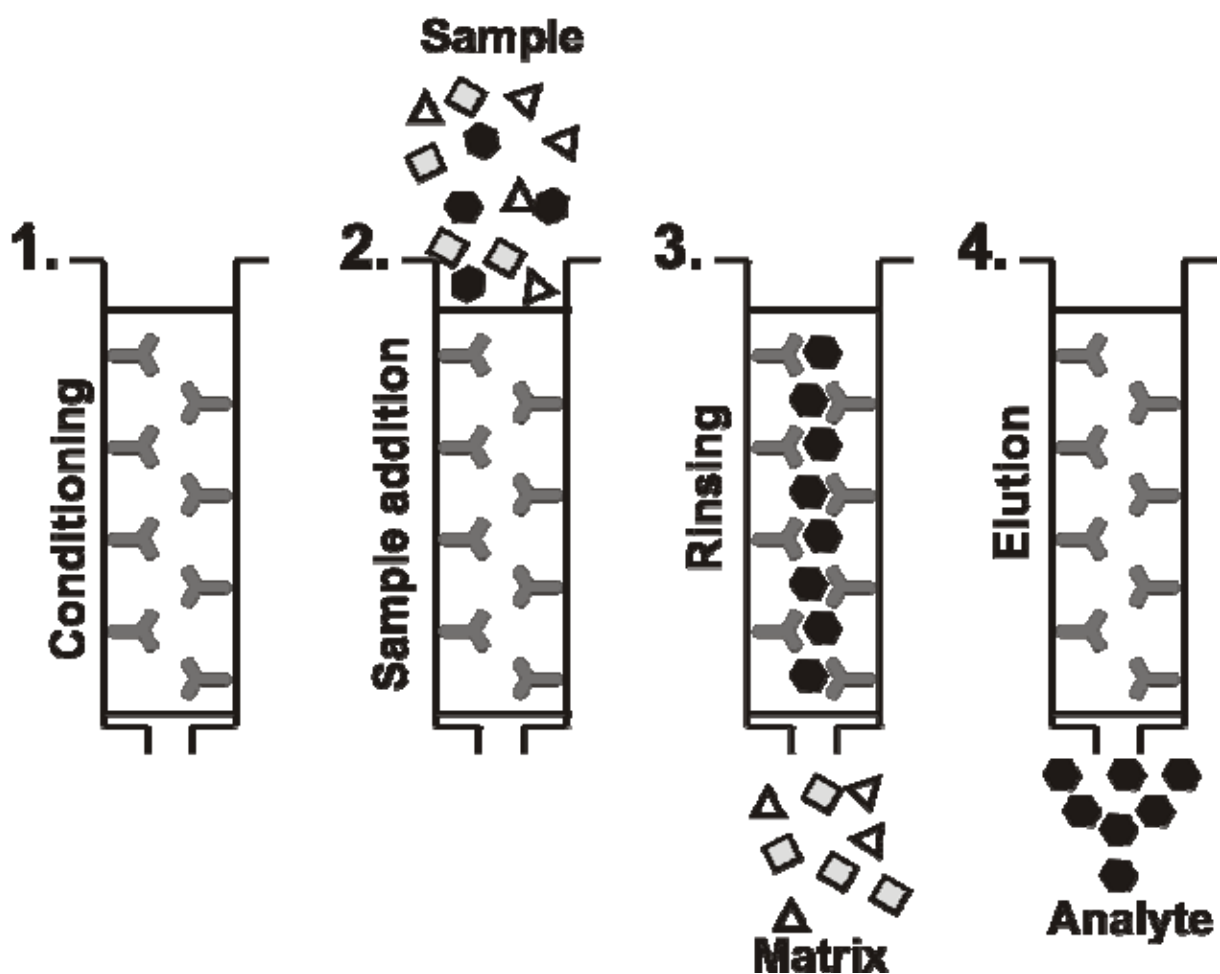


Figure 4 Immunoaffinity chromatography principle.

Commercially available immunoaffinity columns have found widespread use for a variety of assays involving environmental samples, food products or biological fluids because they can be used with basic laboratory equipment and are proven to efficiently remove sample interferences. In the field of food safety, the development of cartridges that contain antibodies specific to more than one toxin has also been promoted. Some advantages are the effective

and specific purification of mycotoxins in a few, uncomplicated steps, the economic use of organic solvents and the improved chromatographic performance in further analysis.^[25] A method for the simultaneous enrichment of 11 mycotoxins in maize, among them OTA, used a commercially available immunoaffinity column from Vicam.^[36] Nevertheless, the main disadvantage of immunoaffinity column cleanup is the high cost associated with each determination. Although often mentioned in the literature^[37], the re-use of commercial IAC cartridges is not encouraged by the producing companies for obvious reasons. Bulky antibodies can only reach low coupling densities when linked to the solid support of the cartridge, therefore limiting the amount of OTA that can be recovered from a sample. Another drawback is the restricted use of non-aqueous solvents that could denature the antibodies and disrupt the analyte interaction, causing early break-through of the toxin from the column and introducing errors in the determination.

Solid phase extraction (SPE) with its small, pre-packed cartridges is a cost-effective cleanup method that relies on the same 4-step principle of immunoaffinity enrichment. In a first variation of the method, a solid support, frequently silica, is modified with functional groups that interact with the analyte of interest. The modifying groups may be hydrophobic, hydrophilic, ionizable, or a combination of any of these. Case-by-case appropriate analyte eluting conditions may be screened according to the application by testing different pH, temperature, flow rate and eluent composition. Three specific solid-phase modifications are frequently used for OTA enrichment in coffee samples: C-18, phenyl and aminopropyl. Procedures that use the first two modifications (C-18, phenyl, or a mixture of the two groups) require a basic pH in the extract (pH in the range of 8.5), which favors the single-charged ionic form of OTA, and a hydrophobic or π - π interaction with the solid support. In the method from Nesheim, described for the clean-up of green coffee extracts, the final elution step is carried out with an acidified ethyl acetate/methanol mixture.^[38] In contrast, the elution of OTA in the method of Hinkel is brought about with a water/MeOH mixture.^[39] Both methods make use of an organic solvent mixture for the final elution, in order to disrupt the hydrophobic interaction of OTA with the solid phase.

Alternatively, when an aminopropyl-derivatized solid phase cartridge is used, the retention mechanism is ionic and the working pH of the sample must be ideally such that both the solid support and the analyte are respectively in their positive and negatively charged state. In the method described by Sibanda, OTA-containing coffee was enriched from a roasted coffee extract by applying the later to an aminopropyl cartridge at a basic pH and eluting with

sodium bicarbonate solution and MeOH. The method was successful in retaining interfering substances derived from the roasting process that had made the HPLC-based OTA analysis difficult.^[40]

Additionally, an example of a mixed-effect adsorbent for SPE cleanup has proven to be a good substitute of IAC enrichment and the cleaned extract can be directly injected in an HPLC unit for analysis. Both green and roasted coffee beans have been tested for this method. The mixed adsorbent solid phase consists of a polymeric reversed-phase substituted with quaternary amine groups that exhibit also anion exchange functionalities^[41]. The technology has been further developed in the Mycosep® series^[42], where the multifunctional SPE cartridge with a support mixture of charcoal, ion-exchange resins and other materials allows for an efficient, one-step cleanup of the extract.^[43] Nevertheless, these highly specialized sorbents are sold as a one-time use and cost practically the same as an immunoaffinity column.

Molecularly imprinted polymers (MIPs) for mycotoxin separation have become an active area of research in the last ten years because of the promise for inexpensive, reusable supports. These materials are produced by carrying out polymerization and cross-linking reactions on monomers to which an analog of an analyte has been supplemented. The analogue molecule does not bind covalently to the polymerized matrix; it nevertheless provides a 3-D “template” to form cavities that are complementary in size, shape and functional group orientation to the target analyte. To make this cavity available, the analogue used for forming the cavity must be removed from the polymerized matrix. The polymer matrix also has to be sturdy enough to maintain its functional structure even at the changing pH/solvent conditions needed for analyte elution. This characteristic is generally hard to achieve, therefore MIP technology for mycotoxin separation is still only of interest for researchers and has not found its way into other applications. OTA analogues that might serve as templates for MIP production have been synthesized mainly by research groups.^[44, 45] For most of the published literature, the difference between mycotoxin retention in the bulk polymer and in the template-modified polymer is only minimal, unless the analyte itself is used as a template.^[46-48] Nevertheless, apart from the toxicological risks and limited availability of OTA, residual bleeding of the template could introduce errors in sample analysis, since 100% template removal is usually difficult to achieve. Therefore, for this variation of the technique, reproducibility is still considered a challenge.^[49]

Detection

Methods routinely used today for the simultaneous separation and detection of OTA in food samples are mainly based on reverse-phase high performance liquid chromatography (RP-HPLC), thin-layer chromatography (TLC) or immunoaffinity-based assays, such as the enzyme-linked immunosorbent assays (ELISA).^[50] For clarity in the discussion, a distinction will be made between chromatographic methods (such as HPLC and TLC) and immunoanalytical methods (such as ELISA), although it is understood that chromatography-based methods may rely on clean-up steps that make use of antibodies, such as IAC enrichment. In chromatographic methods, the detection of the toxin is always associated with an intrinsic property of the analyte, such as its fluorescence, absorbance, the change in the IR that it produces, or its m/z ratio, and its concentration is directly proportional to any of these properties. In contrast, immunoanalytical detection is based on the interaction between an antigen (the analyte of interest) and an immunoglobulin, or antibody, raised against the antigen. The detection is indirect in the sense that the measured signal is the consequence of a two-molecule interaction, an interaction between the probing molecule and the analyte. Furthermore, we will divide this last type of methods in those that do not require a reporter molecule (e.g. surface plasmon resonance), and those that do (e.g. an enzyme, an antibody-enzyme complex, or a fluorophore tag).

Chromatographic methods: HPLC. HPLC is relevant because not only is it at the core of many standard, validated procedures for several combinations of food matrices and toxins, but it is also employed as a validating method for newly developed screening techniques. Among other reasons for the popularity of HPLC techniques, solvent compatibility can be cited, as the traditional extraction solvents used for mycotoxin extraction (ACN, MeOH, water) are also well tolerated by this type of instrumentation. The validated methods for OTA detection developed by the Association of Official Analytical Chemists (AOAC) and the European Commission (EC) rely on IAC clean-up followed by HPLC with fluorescence detection (FD); however, a disadvantage is that they address only a moderate number of food commodities, among them coffee^[51-53], and their capability for multianalyte detection is limited. Nevertheless, the fluorescence detection of OTA after HPLC separation is still very popular due to its sensitivity, selectivity, ease of use and moderate cost in contrast to the mass spectrometer alternative. Usually, post-elution derivatization of OTA with ammonia increases the fluorescence signal significantly, which improves limits of detection (LOD).^[9] Alternatively, when peak identity is in question, the on-line esterification of OTA with

BF₃/MeOH causes the OTA chromatographic peak to disappear and is considered the ultimate proof of identity.^[40]

Although highly reliable and reproducible, HPLC-based methods present the following drawbacks: they are generally cost-intensive, they require trained personnel and their use is restricted to the laboratory environment. Moreover, the complexity of the sample mixture almost always requires a previous clean-up procedure, as described in the former sections. Exceptionally, if detection is performed by means of a mass spectrometer in tandem mode, IAC may be replaced by a less specific type of SPE. In combination with a highly diluted sample extract, this choice may suffice to reduce matrix effects.^[54] By applying this strategy, the determination of 39 mycotoxins in wheat and maize (including OTA) with a single extraction step and subsequent liquid chromatography-tandem mass spectrometry analysis (LC-MS/MS) was possible.^[55] An HPLC-MS example of OTA detection in coffee has been provided by Ventura^[41] in combination with an SPE cleanup step. LC-MS/MS was also successfully applied for OTA detection in beer with an LOD and LOQ of 0.4 and 0.8 µg kg⁻¹ respectively.^[56] The use of MS detection offers significant advantages to analytical chemists not only for its ability to quantitate low levels of mycotoxins, but also because it provides indisputable proof of identity of the separated analyte in the shape of the characteristic fragment ions. Moreover, the relatively recent development of atmospheric pressure ionization for sample introduction in the MS detector makes the sequential coupling of instrumental chromatographic separation and mass spectrometry analysis very straightforward.

Although MS detection clearly presents advantages above other methods, the cost of the equipment involved makes this cutting-edge technology prohibitively expensive for most small laboratory facilities and not applicable for on-the-spot screening. Nevertheless, tandem MS is the leading detection system when multitoxin detection is to be carried out.

Chromatographic methods: TLC. Despite the instrumental developments of liquid chromatography instrumentation, TLC methods are potentially comparable to HPLC in their efficacy and validated procedures for the determination of OTA in several food matrices, including green coffee, have been available for at least 35 years.^[57] This form of chromatography applied to mycotoxin analysis is still the method of choice in most of the developing countries^[1] because it offers the advantage of simultaneous analyte detection and its costs are very moderate. TLC may even be used for quantitative toxin detection if coupled to densitometry analysis, or it may also be used as a fast, screening method, previous to the

application of more sophisticated instrumental analysis. On a cautionary note, it is still difficult to draw comparisons between the performance of different TLC procedures, complicating standardization, since this methodology presents high coefficients of variation (CVs) in the properties measured (typically the R_f). Another major disadvantage is that because of TLC's low separating power, interference derived from co-extracted substances limits the reliability of the method. This effect can be diminished by using an initial cleanup procedure such as SPE or IAC. A literature example of OTA quantification in green coffee by TLC was able to detect the toxin in a range of 1.8 to 109 $\mu\text{g kg}^{-1}$. The method effectively used immunoaffinity clean-up of the extract and a densitometer for detection.^[58]

As with most forms of chromatography, the high performance variation of TLC is also available. Multitoxin determination with high performance thin layer chromatography (HPTLC) is possible as well.^[59] It is clear that this cost-effective, on-site alternative to HPLC is still a powerful mycotoxin screening method that requires little instrumentation.^[50]

Immunoanalytical methods: the competitive assay format. All of the immunoaffinity-based analytical methods have their origin in the pioneer work of Georges Köhler and César Milstein that made the immortalization of antibody-producing cell lines possible.^[60] This ground-breaking research was worthy of the Nobel Prize in Physiology or Medicine, awarded to the scientists in 1984. Since then, these molecules have become accessible to countless applications. The previously discussed IAC is one example that relies on a constant source of antibodies of known specificity. As tools for sample analysis, monoclonal antibodies are also used in various types of methodologies of which the ELISA is one popular application. Immunoassays in ELISA formats are very diverse and several classifications among all the different types are possible. Some classification criteria include whether the assay takes place in bulk solution (homogeneous), or at an interface (heterogeneous), whether a tracer is needed (enzyme/fluorophore labeled or label-free), and for the heterogeneous methods, whether the assay is direct (antibody immobilized on the solid phase) or indirect (analyte immobilized on the solid phase). In the following section, attention will be focused on competitive assay formats because only these can be applied to the detection of small molecules, such as mycotoxins (<1000 Da).^[61] The distinguishing feature of a competitive assay, also known as inhibition assay, is the limited availability of specific antibody binding sites for the recognition of a target analyte. Because of the finely tuned, specific interaction between an antigen (the analyte) and its antibody, even complex samples can be analyzed with little or no sample preparation at all. It is important to mention that immunoanalytical methods usually

rely on the establishment of chemical equilibrium (or at least a steady state of mass transfer) between the analyte in its various forms and the specific antibody, a requirement that may be crucial to assay reproducibility.

Labeled immunoanalytical methods. The traditional ELISA consists of an immunoanalytical method characterized by the physical separation of the probing molecule from the bulk of the sample, and by the use of an enzymatic tracer. The function of the tracer is to generate a signal after antibody-antigen binding has taken place. Two formats are available, the direct format and the indirect format, both schematized in figure 5.

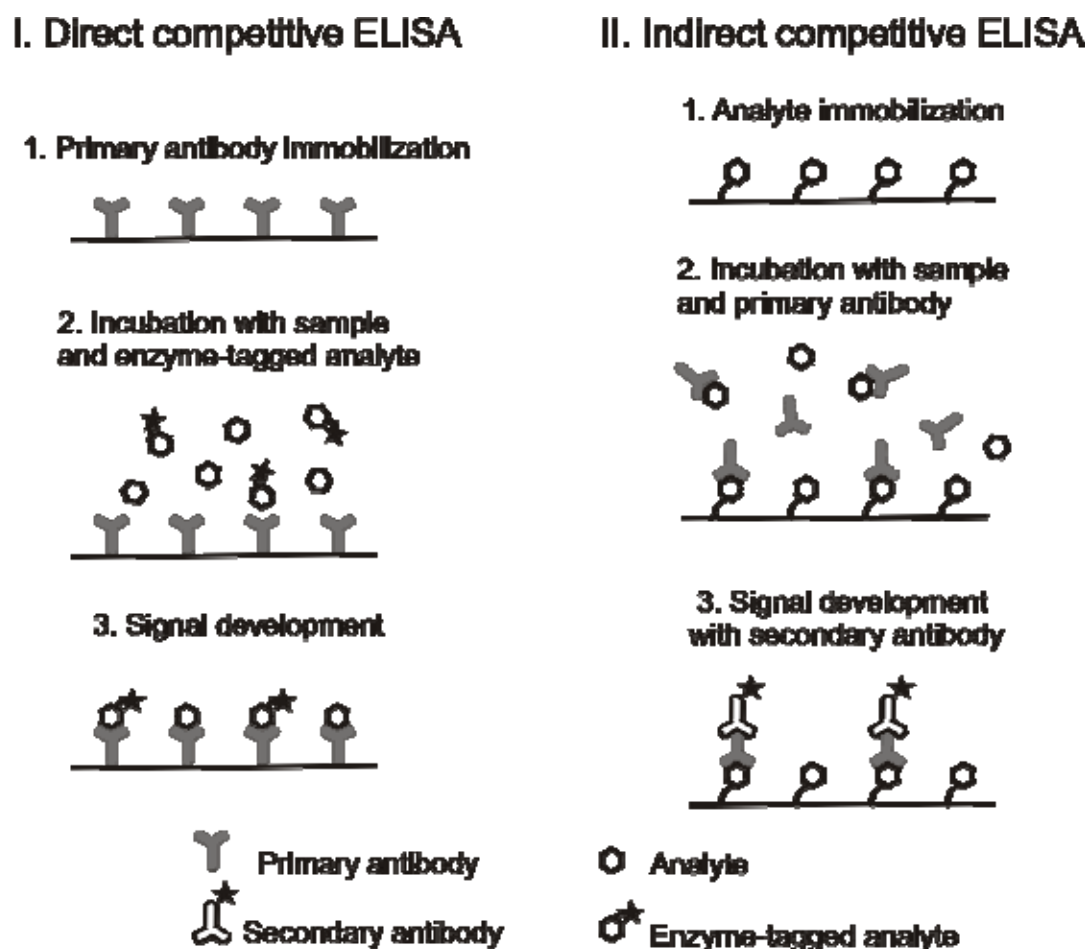


Figure 5 Schematized ELISA in direct and indirect format.

In a direct ELISA, a specific capture antibody is immobilized on a solid support that can take the shape of either a polystyrene microtiter plate (MTP), or a so-called “dip-stick”. The crude extract (the sample) or a standard of known analyte concentration (the calibrant) are placed respectively into contact with the immobilized antibody and mixed with a constant amount of the enzyme-tagged version of the target analyte. Competition takes place between the tagged and the plain analyte for a limited number of receptor antibody sites that will become

occupied upon establishment of chemical equilibrium. When the original mixture is washed, the analytes will remain bound to the receptor. Substrate addition generates a signal of intensity proportional to the amount of bound toxin-analyte conjugate.

On the other hand, the indirect assay format uses a modified version of the analyte to “fix” it to the solid support, instead of the receptor antibody used for the direct assay. This modified version of the analyte usually consists of a protein covalently coupled to it. In this case, a mixture of the sample containing the analyte (or the calibrant) and the specific antibody is incubated on the microtiter plate, so that the immobilized and the free versions of the analyte compete for the binding sites of the free antibody. After equilibrium is established and the mixture is washed from the surface, the antibody bound to the immobilized analyte will remain attached to the solid support. This antibody may already be marked with an enzyme, or alternatively, a secondary, enzyme-marked antibody can be added that will bind to the primary, specific antibody in an additional step. In the direct and indirect ELISAs, signal generation is the result of the final step: the addition of a substrate and its enzymatic conversion into a detectable product. Larger signals indicate the presence of lower analyte concentration in the original sample, and vice versa. In general, signal behavior for immunocompetition takes the shape of the following mathematical equation:

$$y = A_2 + \frac{A_2 - A_1}{1 + (x/x_0)^p}$$

where

y is the signal intensity (chemiluminescence, fluorescence, absorbance...),

A_1 is the signal intensity at zero analyte concentration (maximum intensity),

A_2 is the signal intensity at very high analyte concentration (minimum intensity),

x_0 is the analyte concentration needed to produce half signal intensity, and

p is a parameter that gives the change in signal intensity at x_0

A detailed plot of signal intensity as a function of analyte concentration can be seen in figure 6, where the parameters of the equation have also been indicated.

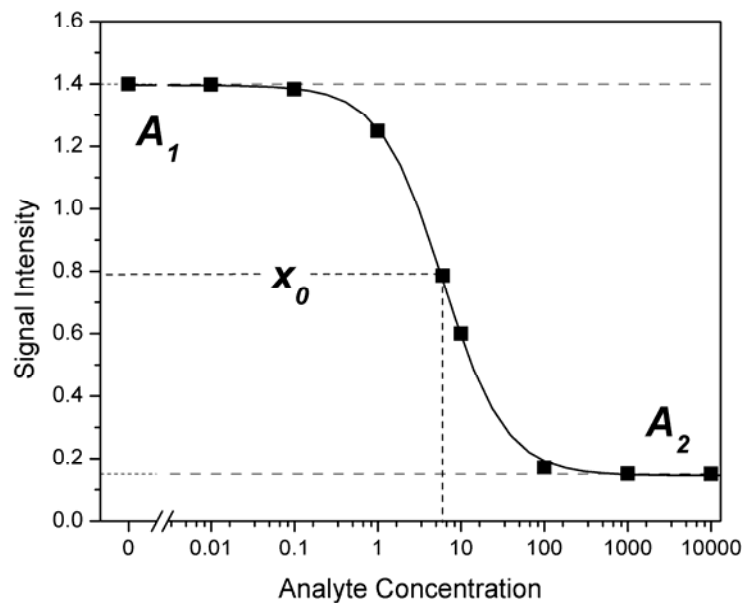


Figure 6 Dose-response curve of a typical competitive ELISA with the relevant parameters.

In both methods, covalent conjugation of the analyte to a protein (be it a protein for analyte immobilization, or an enzyme) is carried out mostly by coupling to primary amino or carboxylate groups present on the protein's accessible surface. For microtiter plate-based ELISAs, the immobilization is the result of weak unspecific interactions, such as van der Waals forces or π - π stacking, between the antibody or the protein-analyte conjugate with a hydrophobic polystyrene surface. A protein generally used for analyte coupling is bovine serum albumin (BSA). The most popular enzyme choices for ELISAs are horseradish peroxidase (HRP) and alkaline phosphatase (AP) because of their high turnover numbers associated with substrate conversion. Depending on the type of substrate added, the enzymes can catalyze either a chromogenic reaction (HRP, AP), where the property measured will be the absorbance, or a chemiluminescent reaction (HRP), where light will be generated for recording.^[62] Signal detection can be achieved with a spectrophotometer, if the reaction produces a chromogene, or with a charged-coupled device (CCD) camera, if the reaction gives a chemiluminescent product.

The combination of highly specific antibody-antigen interactions and the signal amplification conceded by enzyme catalysis makes ELISA-based methods very attractive for mycotoxin screening in food samples. The main advantages of the ELISA technique are the possibility to analyze raw extracts (little or no clean-up necessary), the moderate cost of the analysis, the relative simplicity of the method and the compatibility with field-portable applications.

Simultaneous detection of different mycotoxins is still dependent on an adequate extraction method that must be adapted to the type of food product, as is the case with other technologies. Nevertheless, an additional requirement must be fulfilled, namely that the antibodies used do not cross-react with their respective targets. In other words, that only one toxin is recognized by one antibody. In practice, and for toxins with very similar chemical structures (for example the aflatoxins), cross-reactivity cannot be altogether avoided. In this case, the determined concentration will reflect not the individual concentration of a particular toxin, but a total concentration of the sum of all the toxins that cross-react with the antibody.

In general, ELISAs can provide rapid quantitative and semi-quantitative analytical results, although for more challenging quantitative applications the presence of matrix effects can cause some limitations. These may originate from a number of factors including other co-extracted compounds (such as lipids, carbohydrates, tannins, polyphenols and pigments), extraction pH and solvent composition, and sample processing that might interact in an unspecific way with the antibodies. Matrix effects introduce errors in the analytical result, but may be overcome by measures such as extract clean-up, extract dilution or addition of detergents.^[1] It is worth mentioning that detection limits of ELISA procedures cannot be improved by concentrating the sample extract because the interfering components will still be present in the same proportion to the analytes as before concentration.^[63]

Among others, examples of ELISA assays developed for the screening of OTA in cereals^[64], spices^[65] and wine^[66] are available. Fuji et al.^[67, 68] have recently reported a method where back-extraction of a green coffee extract into chloroform diminishes the matrix interferences and affords reliable results. The method was tested on real contaminated samples and showed good correlation against a validated HPLC-based methodology. Nevertheless, classical plate-based ELISAs are not suitable for on-site screening and their use is constrained to the laboratory environment.

Miniaturized versions of both ELISA supports and adequate readout systems have also been developed in the last ten years, of which the Naval Research Laboratory Array Biosensor is a good example.^[69] This application for point-of-measurement employs specific fluorescently labeled antibodies and consists on a glass optical waveguide with the size of a microscope slide, onto which mycotoxin-protein conjugates have been patterned. After competition and binding, laser light reflected along the wave guide causes evanescent fluorescence excitation of the surface-bound antibodies. The signal is recorded by a charge coupled device. The portable self-contained platform weighs 7 kg and allows for the measurement and processing

of samples in connection with a portable computer. Applications for OTA determination have been reported for grains, roasted coffee and wine^[70], with measuring ranges along the 5 to 100 $\mu\text{g kg}^{-1}$ interval, depending on the food matrix tested. Parallel detection of OTA and deoxynivalenol has also been reported for barley, wheat, cornmeal and maize, although this application was prior to the development of the self-contained platform.^[71]

Dip-sticks, otherwise known as immunoassay-based lateral flow devices (LFDs), are compact and inexpensive ELISA applications that can be used as field-tests for mycotoxin screening and detection of contamination at or above a pre-set limit.^[72] Remarkably, they do not require any additional instrumentation for their use, other than the test strip, which consists of a thin piece of flexible support, where gold nanoparticles coupled to specific antibodies have been adsorbed. When the bottom of the dip-stick comes into contact with the liquid sample, the analyte binds to the gold-coupled antibody and migrates along the flexible support of the strip. Nanoparticle-coupled antibodies that did not bind to the analyte contained in the liquid sample also migrate up to an upper boundary, where the analyte of interest has been immobilized as well. These non-occupied antibodies will become attached to the control line. The user identifies this event because a pink line derived from the gold nanoparticles becomes visible. Contamination below a set limit is shown as the appearance of color on the strip when running a dip-stick assay. A control that ensures the correct migration of the antibodies is also desirable. An example of this type of ELISA format applied to coffee screening is given by Liu et al.^[73] The test generates a positive result for OTA concentrations below 5 $\mu\text{g L}^{-1}$, in a time of 10 minutes. The simultaneous detection of the two mycotoxins OTA and zearalenone with this assay format has also been reported in the literature.^[74] The limits of detection obtained for corn (no cleanup step necessary) was similar to those determined for coffee samples.

Another type of immunoassay rapidly gaining in importance is the fluorescence polarization immunoassay (FPIA). In contrast to ELISAs, FPIAs are carried out in the homogeneous phase. In this case, a user-supplemented fluorescently-labeled toxin competes with the toxin originally present in the sample for the binding sites of a specific antibody. The property measured, the fluorescence polarization value (FP), is related to the molecular rotation rate, which is ultimately dependent on the effective molecular volume of the fluorophore. Upon antibody binding of the marked toxin, this value undergoes a change, and so does the orientation of the fluorescence polarization signal.^[75] The change in the signal is proportional to the amount of bound antibody-toxin complex, so that the same mathematical model

described in the previous section for ELISA can be applied both for system calibration and for sample measurement. Such an assay type has been described for the quantification of OTA in barley samples^[74] and in wine.^[76] The reached limits of detection were respectively reported as 3 $\mu\text{g L}^{-1}$ and 1 $\mu\text{g L}^{-1}$. For barley, no cleanup step was necessary, but matrix interferences in wine made the use of SPE unavoidable.

Label-free immunoanalytical methods. Two emerging techniques have overcome the need to use enzymatic or fluorescent labels for the measuring of antibody-antigen binding events: surface plasmon resonance (SPR), and optical waveguide lightmode spectroscopy (OWLS). Both technologies have also been adopted in the field of competitive immunoassays, and in particular for the detection of mycotoxins. The working principle consists of the excitation of a surface with light, where the toxin of interest has been immobilized either directly, or in the form of a protein conjugate. Binding of a specific antibody pumped over the surface is detected as a change in the surface properties, which means to say that the measurement is continuous and it happens in real time, until no significant change in the signal can be detected (e.g. when saturation of the binding sites is completed).

SPR occurs at the interface between two transparent materials of different refractive index, for example water and glass. A beam of monochromatic, plane-polarized light is aimed at the surface with the higher refractive index and will be entirely reflected at values larger than a critical incident angle. Nevertheless, the electromagnetic field component of the plane-polarized light will still penetrate a short distance (approx. 200 nm) into the lower refractive index medium and create an exponentially decreasing evanescent wave. A thin gold layer placed between the two transparent media, causes the “loss” of some of the energy to the metal layer. At a specific incidence angle, resonance energy transfer from the evanescent wave to the loosely held electrons of the gold layer takes place and the intensity of the reflected light drops to a minimum. The resonance conditions for the phenomenon to occur (i.e. the SPR angle) are strongly influenced by the mass of the molecule immobilized, and so binding of an antibody to an immobilized mycotoxin can be detected at the time when the event takes place.^[77] A sensitive photodetector array measures changes of the SPR angle in the form of response units. Using such a sensor, van der Gaag et al. have developed a method for the simultaneous detection of multiple mycotoxins within a time frame of 25 min. Detection limits of 0.2, 0.01, 0.1, 5.0, and 0.5 ppb for aflatoxin B₁, zearalenone, OTA, and fumonisin B₁ were reported for a prototype of buffered solution (no real matrix was used in this proof-of-principle experiment).^[78]

The operating principle of OWLS sensors is similar to that of SPR sensors: linearly polarized light is coupled into a waveguide (a transparent surface, for example silica) at two well defined incident angles. These incoupling angles are sensitive to changes in the refractive index within the evanescent field above the surface of the waveguide and allow for the determination of layer thickness and coverage (or mass) of the adsorbed or bound material with ultra high sensitivity.^[79] Adanyi has reported the use of OWLS technology for simultaneous OTA and AFB₁ measurement in grain samples within the 0.5 to 10 µg L⁻¹ measuring range.^[80]

2.2 Chemical Immobilization of Receptors on Biosensors

2.2.1 Diversity and Challenges in Sensor Miniaturization

Miniaturization of immunoanalytical biosensors and the wide use of microarray technology applied for their fabrication have brought about new ways to immobilize analytes as diverse as proteins, DNA or small molecules to different types of supports. To this end, derivatization strategies and physical methods designed to deliver the analyte of interest to the sensor have been extensively explored. In particular, the immobilization techniques used today for biosensors with immunoaffinity recognition at their core have been adapted from the blooming field of DNA microarray technology. Whether an antibody, a protein-hapten conjugate or a small molecule is to be immobilized for an assay setup, the physical confinement of the bound analyte to a small and delimited area needs to be counter-balanced by a sufficiently high analyte density that is necessary to obtain a detectable signal, especially when complex matrices are being screened. Whatever the detection method used in combination with a particular biosensor, one of the most challenging problems consists in the non-specific protein adsorption to the biosensor's surface that causes significant deterioration of the signal-to-noise ratio.^[81] The problem is ever more pressing when the sensors are to be used in complex, multicomponent solutions, such as biological fluids, environmental samples or food extracts. Therefore, in addition to immobilization strategies, surface passivating techniques also have to be developed. Furthermore, the support materials for biosensor fabrication are very diverse: they include metals (gold, silver, copper or nickel)^[82, 83] and metal oxides (indium tin oxide, titanium oxide, niobium oxide)^[84, 85], silica-based substrates such as glass, fused silica or quartz, polymers or a combination of some of these^[86]. Consequently, immobilization techniques are specific to each type of substrate. The choice of solid support depends on factors such as the detection method used, the type of substance that will come into contact with the sensor, and the preferred analyte immobilization strategy.

This section will give an overview of some existing techniques for both molecule immobilization to chemically modified surfaces and for the reduction of unspecific interactions that are detrimental to most immunoaffinity-based assays. It will differentiate between three main models of molecule immobilization: physical adsorption, covalent attachment via reactive groups, and affinity-based techniques, given their relevance in the fabrication of immunoaffinity-based biosensors. Realizing the importance that miniaturization

has acquired in the last few years, this section will also briefly consider some methods for the transfer of the receptors to the modified surfaces. Finally, two new analyte modification techniques will be described in the context of covalent immobilization for biosensor fabrication.

2.2.2 Physical Adsorption

One of the most commonly employed immobilization methods is the physical adsorption of antibodies and proteins on a surface, which is driven by weak attraction forces such as ion-pairing, hydrophobic interactions and hydrogen bonding. Historically, this has been the method of choice in microtiter plate-based ELISA, discussed in section one.^[87] Along polystyrene, other surfaces can be employed, including cellulose derivatives and Nylon.^[88] Glass and silicon treated polyethylene imine (PEI), a polyelectrolyte, have also been used successfully for antibody immobilization.^[89] Physical adsorption methods for receptor immobilization are straight-forward and widely used, but most of them suffer from loss of activity with time, particularly when proteins are concerned. Since immobilization is unspecific, spatial orientation of receptors is also difficult to achieve. Loss of functionality is a problem, and immobilized receptor antibodies may slowly denature at the solid-liquid interface. In classical microtiter plate-based ELISA, the reusability of the functionalized surface is for these very reasons out of the question. Covalent immobilization techniques present an alternative, especially when small receptors are to be attached to a surface. This feature also offers the possibility to fabricate reusable biosensors.

2.2.3 Covalent Immobilization

Covalent immobilization strategies are particularly suitable when receptors are to be constrained to small areas, yet achieve high enough surface densities required for detectable binding. Particularly in the case of SPR, OWLS and other lateral flow applications, where the immobilized molecules are exposed to a constant flow perpendicular to the plane of attachment, simple adsorption would cause leaching with time and discard the possibility of sensor regeneration. In most cases where covalent immobilization is desired, it is the receptor surface that needs to be chemically activated to provide anchoring groups for the molecule to be attached.

Silanization is the preferred derivatization strategy for silica-based substrates (glass, quartz, fused silica), as it affords a surface suitable for the covalent immobilization of receptors. To this end, microscopic glass slides represent a suitable substrate choice as a biosensor platform because of their moderate costs, excellent optical properties, inertness, temperature stability, availability and non-porosity.^[90, 91] Mercaptopropyltrimethoxysilane, (MPTS) aminopropyltriethoxysilane (APTS) and glycidoxypropyltrimethoxysilane (GOPTS) are the three types of alkoxy silanes frequently used for silanization (figure 7).

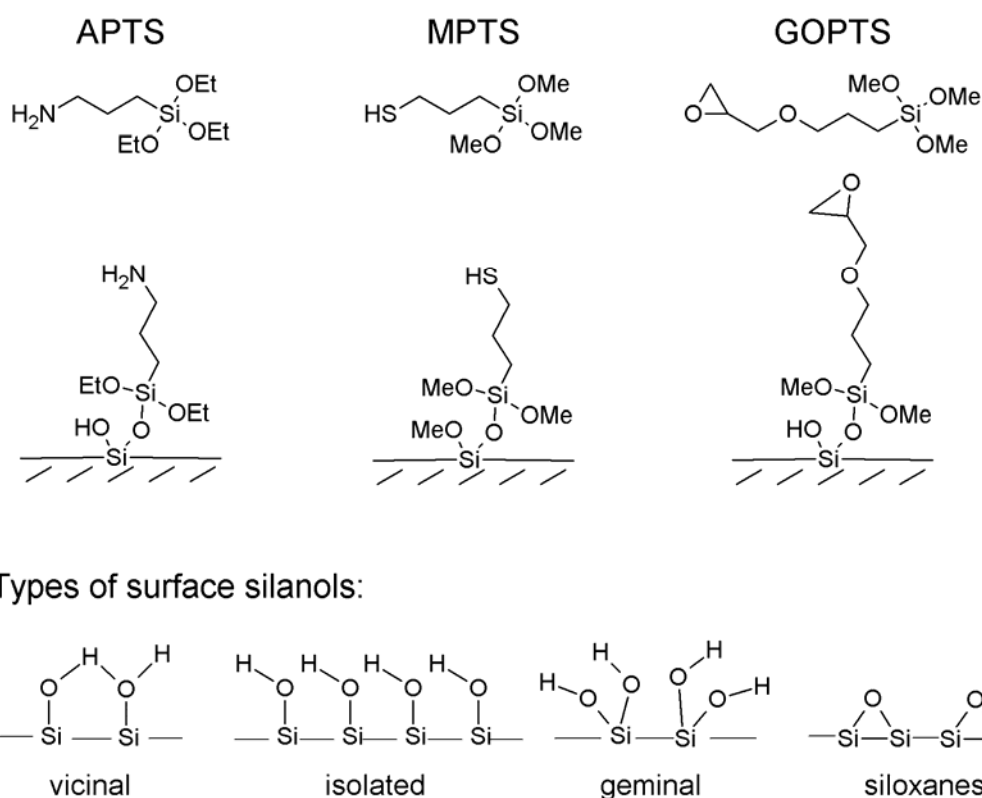


Figure 7 Silanes frequently used for surface modification.

Silanization occurs when the methoxy groups in the alkoxy silane condense with the surface silanol groups of a glass or silica surface. Although opinions are divided whether trace amounts of water are necessary or not for the process to occur, it is generally accepted that silane monolayers are preferably formed under moisture-free conditions. In order to obtain reproducible results, silanization should be conducted under a controlled atmosphere. Moreover, of the four types of silanols available on a quartz or glass surface, only the geminal and isolated types are reactive towards condensation^[92], as seen in figure 7. Thorough glass clean-up procedures and etching with strong acids or bases must be performed on the substrates in order to make as many reactive silanols as possible available.

Silanes provide moderate resistance against non-specific protein adsorption, a spacer to separate the immobilized molecule from the sensor surface, and suitable reactive groups for the coupling of diverse functionalities. In particular, silanization with GOPTS is often preferred from MPTS and APTS because it affords higher coupling densities^[93] and the terminal epoxy groups can react with a wider variety of chemical nucleophiles without the need of further derivatization (e.g. the need for an additional hetero, or homobifunctional linker). The chemical versatility of GOPTS-treated surfaces is schematized in figure 8.

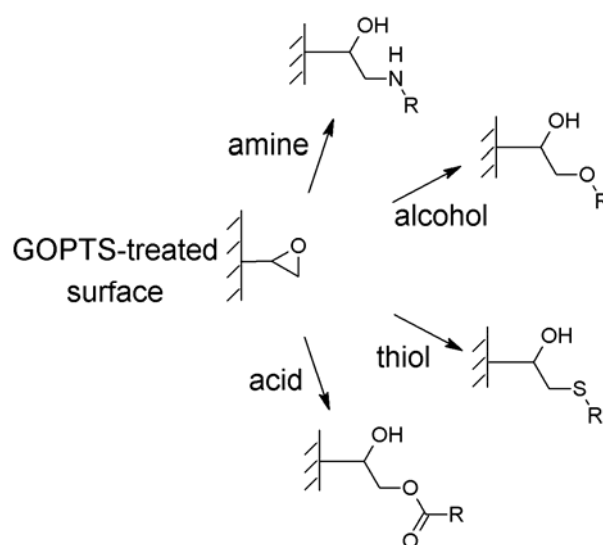


Figure 8 GOPTS-treated surface versatility for reagent immobilization.^[94]

In contrast to other trialkoxysilanes with short aliphatic chains, it is generally accepted that GOPTS forms stable monolayers, even when applied as a pure substance.^[95-97] The terminal reactive epoxy functionality of GOPTS is also moderately stable in water solutions at neutral or slightly alkaline pH, yet reactive to thiol or amine-containing compounds. This characteristic allows for the attachment of biological molecules that require water-based buffer systems or a water-saturated atmosphere in order to remain functional (for example proteins). A good example of covalent protein-hapten immobilization on a GOPTS derivatized glass slide is given by Knecht et. al.^[98] In this application, the immunoaffinity-based detection and quantification of 10 different antibiotic residues in milk under an indirect competitive assay format is described.

Further functionalization of a GOPTS-derivatized surface is also possible after the molecule of interest has been covalently immobilized, for example with a substance that controls nonspecific adsorption on the remainder of the substrate. Alternatively, the passivating

substance may be reacted first to the GOPTS layer, and then further functionalized for specific analyte binding.^[99]

PEG surface derivatization. For a biosensor to remain functional, especially in the presence of complex matrices such as biological fluids, or food extracts, it is necessary to suppress non-specific protein adsorption in order to reach the desired sensitivity and selectivity. Polyethylene glycol (PEG) derivatization is a useful strategy to counteract attractive forces between proteins and surfaces. PEG is a non-branched polymer able to form linear “brushes” when arranged in a densely packed conformation. The effects that make PEG distinctly protein repellent in aqueous environments are still not entirely understood. Nevertheless, it is usually agreed that the shielding properties of PEG are generally attributed to 1) steric hindrance that prevents proteins from diffusing to the underlying substrate; 2) its hydrophilicity and large exclusion volume that makes it difficult for proteins to interact with the linear chain; and 3) its chain flexibility, which accounts for a physical barrier that is hard to compress or collapse. The protein repelling effect of PEG is most effective when the packing density is high and when the molecular weight of the linear chain is greater or equal to 2 kDa.^[84, 100]

PEG has been shown to successfully confer protein resistance to a variety of surfaces, among them glass and gold.^[101] As already discussed in section one, gold surfaces are of importance for SPR or OWLS techniques.

PEG is commercially available in several forms and suitable for the most diverse applications: it can be obtained with a wide variety of end functional groups (amino, carboxyl, alcohol, and thiol, either in the homobifunctional or the heterobifunctional variation) and in a broad range of molecular weights.^[102] The most commonly used variants include end amino or carboxylic groups because these are amenable with standard activation techniques such as carbodiimide activation (carboxylic acid) or succinimidyl activation (primary amino groups) and allow for a sequential building of a reactive layer, suitable for further analyte immobilization. The requirement after using such activation techniques is that the analyte to be covalently coupled contains a nucleophilic group in its structure, for example a primary amine. If nucleophilic groups are not already present, they can be introduced by performing a chemical modification, provided it does not influence the ability of the original molecule to be recognized by an antibody. Additionally, a last factor that must be taken into consideration when patterning an activated surface with a receptor, is that some unreacted groups will still remain after the

coupling. These must be adequately “quenched” as a final step in the sensor production, otherwise they could potentially influence the sensor’s response.

Star-PEG surface derivatization. Another alternative to simultaneously modify a material with a protein-repellent layer and introduce reactive groups suitable for further receptor attachment is the use of star-shaped polyethylene glycol coatings (star-PEG).^[103] The star-PEG surface modification is achieved by applying pre-polymers that cross-link with a modified surface and with themselves, generating a layer of densely packed, star-shaped motives that provide high coverage. The resulting star-PEG coating is ultrathin (3 to 50 nm layer thickness) and highly homogeneous.^[104, 105] By modifying the pre-polymers with different end functional groups it is possible to create a variety of coatings suitable for several surfaces. The structure of the pre-polymers consists of a sorbitol core modified with six arms of a copolymer of ethylene glycol and propylene glycol (4:1 ratio), each arm displaying a molecular mass of 2 kDa. Available end-branch functional groups include acrylate, suitable for the modification of synthetic materials, and isocyanate, which can be used for a wide variety of biological applications due to its distinctive reactivity towards amino groups.

In particular, the primary aliphatic isocyanate groups of the star-PEG pre-polymers undergo two types of reaction: they can hydrolyze and ultimately decarboxylate to the primary amine, or they can react with other amino groups to form a stable urea bond. Since the conversion to amino groups is a much slower process than the urea bond formation, cross linking between the pre-polymers or with an amino-derivatized surface takes place after initiation of the reaction, until steric effects prevent it from proceeding any further. Isolated, unreacted isocyanate groups remain available on the densely packed surface for further coupling for a limited amount of time (approximately 9 hours), allowing the surface to be patterned with the analyte of interest.^[106] Worthy of emphasis is that receptor molecules containing amino groups such as antibodies, peptides or other small analytes can be reacted and coupled to the star-PEG film without the need of previous chemical activation of either the receptor or the surface. The final deactivation step needed in the case of other surface-modifying strategy can be altogether avoided as well, since isocyanate groups spontaneously decarboxylate. Alternatively, after sufficient time is allowed so that every isocyanate group is converted to the amine, additional functionalization can be performed, as in the case of the linear amino-PEG addressed previously. Furthermore, the star-PEG method for surface functionalization is compatible with the use of water solutions and with the mild conditions necessary to preserve

the function of biomolecules. For these main reasons, it is very amenable to the fabrication of biosensors.

2.2.4 Receptor Immobilization: Affinity Binding

Affinity recognition is a type of interaction that can also be used as a strategy for the anchoring of a recognition element on a biosensor surface. The avidin-biotin complex formation, a universal tool used in combination with countless biotechnological applications, has been explored to this effect as well.^[107] The binding between avidin (or streptavidin, the bacterial equivalent), a tetrameric protein, and biotin exhibits the highest known affinity between a protein and its ligand, with an affinity constant K_{aff} in the order of $10^{-15} \text{ M}^{[108]}$, making this non-covalent interaction one of Nature's strongest, along with the binding of complementary DNA strands. Avidin and streptavidin-modified surfaces provide a scaffold for selective receptor immobilization, useful in the fabrication of immunoanalytical biosensors. The principle consists on patterning a surface, for example a silanized glass slide, with a streptavidin or avidin layer, followed by the immobilization of a biotinylated receptor, be it an antibody or a small molecule. The receptor so immobilized is to be used in an immunoassay. One variation of this technique even makes use of a PEG-derivatized biotin as base-layer in order to reduce unspecific protein interactions. Alternatively, an activated biotin may also be attached to an amino-PEG layer. Other variations of this type of immobilization include functionalizing the solid surface with biotin and then patterning conjugates of streptavidin.^[109, 110] A picture of the affinity-binding principle can be seen in figure 9.

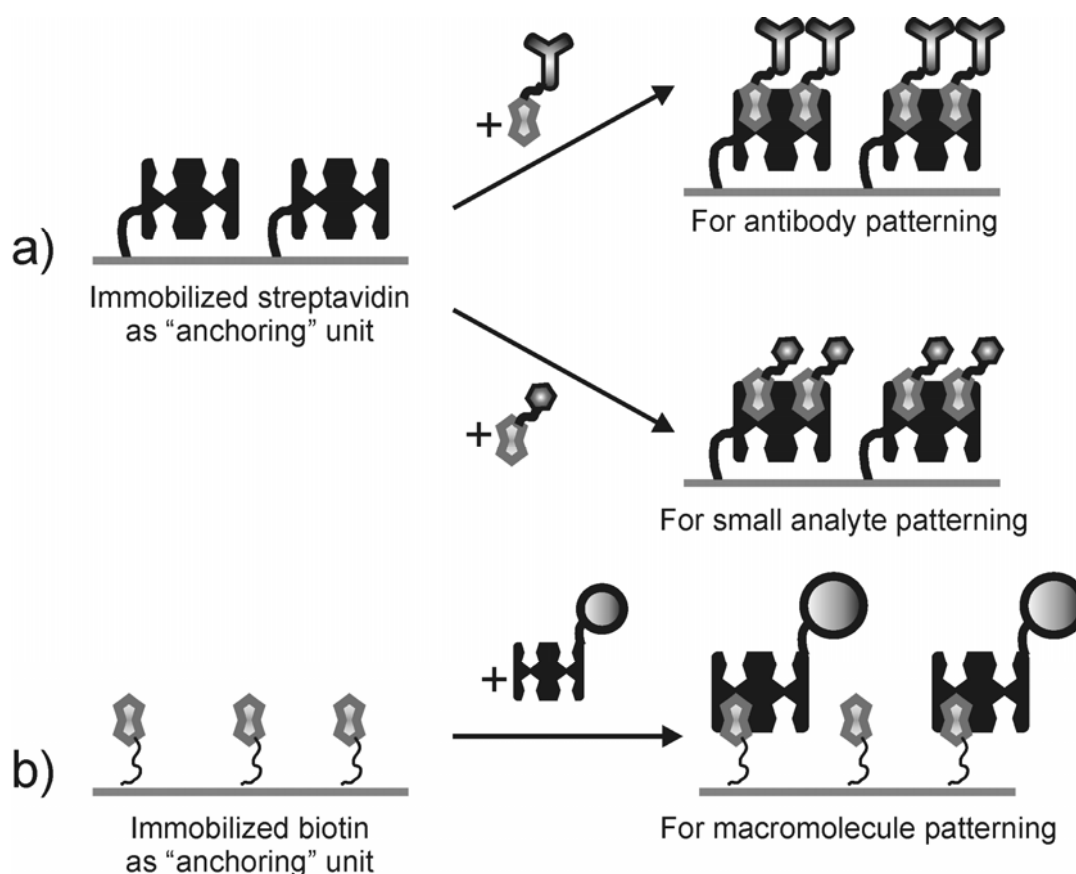


Figure 9 Affinity immobilization of small molecules, of antibodies and of macromolecules.

Examples of this type of affinity patterning in the fabrication of mycotoxin biosensors are available from the Naval Research Laboratory. Deoxynivalenol, OTA and AFB₁ were first covalently coupled to the amino-end of a biotin-PEG-amine construct and then patterned on an avidin-derivatized surface. The sensor thus obtained was used in an indirect competitive ELISA format.^[70, 71] Other examples of affinity immobilization on biosensor surfaces include the binding of antibodies, whether they be covalently coupled to streptavidin first and then “captured” by a biotin-derivatized surface, or else biotinylated first and then attached to a streptavidin-modified surface.^[101] These may be used for direct competitive ELISA sensing methods, among other applications.

2.2.5 Receptor Immobilization: Analyte Derivatization

Another receptor immobilization strategy complementary to the ones described previously is the direct (chemical) activation of a receptor molecule in order to bind it to a derivatized surface. Covalent immobilization strategies are considered advantageous in comparison to non-covalent, unspecific immobilization because they offer increased signal reproducibility in

the fabrication of the biosensors and the possibility to reuse the surface. For this end, the chemistry is very broad and it is not our intention to exhaustively describe it, only to cite some new interesting examples. The goal when using chemical immobilization, regardless of the strategy preferred, remains the same: to produce a receptor molecule that maintains its spatial configuration and/or its relevant chemical groups on the support, in order to be recognized by the sensitive, antibody-binding reaction. Of course, a quick and efficient reaction to the surface of interest is also desired. Among some novel techniques is the use of “click chemistry”^[111, 112], which consists on the Cu(I) mediated Huisgen cycloaddition of an azide-derivatized molecule to an alkyne functionality (figure 10).^[113]

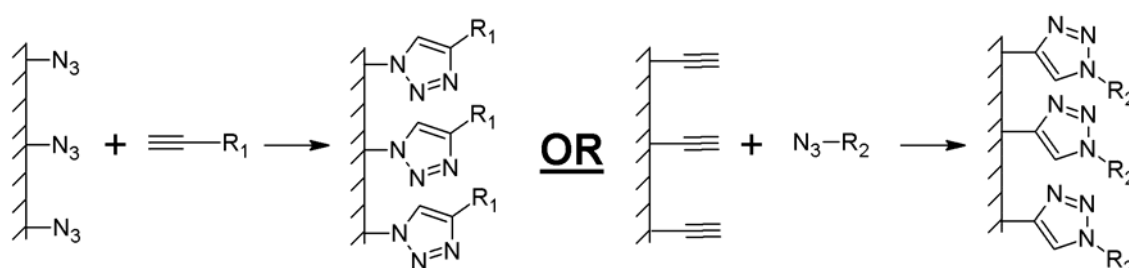


Figure 10 “Click” chemistry: immobilization of molecules modified with an azide or an alkyne motif.

The fast reaction has already been used to immobilize azide-modified bioactive proteins onto polymeric and glass substrates^[114, 115], for the generation of sugar microarrays^[116], and for DNA-oligonucleotide immobilization on glass substrates^[117, 118], as some examples of interesting applications in the biosensor field. One significant advantage of azide functionalization is that it keeps or contributes to a molecule’s hydrophilicity, which makes it compatible with most biological systems.

On a similar note, peptides can also be directly immobilized to a surface without further derivatization, provided that they contain suitable reactive groups such as amino-groups, or carboxylic acids, or they may require the introduction of tags for coupling. In particular, peptide arrays on solid surfaces used for high throughput screening in the pharmaceutical sciences have also become popular in the last ten years.^[119] Combinatorial chemistry and improved immobilization on solid supports can account for the efficient selection of drug targets in libraries of as many as thousands of compounds.^[120] In all these examples, peptides are a target on themselves, as it is usually screened for a particular peptide sequence that is recognized by molecular marker. Nevertheless, peptides can also be used for modifying other molecules, i.e. as “linkers” for immobilizing other analytes. After all, their building units, the

amino acids, already contain chemical groups that are well-suited for covalent immobilization, such as $-NH_2$, $-COOH$, $-OH$ and $-SH$. These functionalities were originally the focus of attention for the immobilization of native proteins. By modifying a small receptor of non-protein origin with a peptide moiety, it is possible to take advantage of all the surface immobilization chemistry, already tested for proteins. It is for this reason that the topic “Solid Phase Peptide Synthesis” will be discussed in more detail in the next chapter. This is, after all, a technique that was extensively used for the coupling of mycotoxins to the functionalized glass microscopic slides used as biosensors in the present work.

2.2.6 Arraying Methods: Analyte Deposition Techniques

Practical aspects of biosensor manufacturing involve not only the choice of suitable immobilization strategies, but also the physical method most suitable to transfer the analytes to the small surfaces required. The purpose of most microarray fabrication devices is the efficient deposition of small amounts of analytes on a solid support, in a uniform arrangement. In general, the instruments available can achieve this in two different ways: by contact transfer of a solution containing the analyte or by non-contact deposition such as photochemical printing, electroprinting and spraying.^[121] As a generalization, the available commercial devices are appropriate for handling water-based solutions of the analytes, since the technological developments in this field originally focused in the arraying of biomolecules such as proteins and DNA. Contact transfer is also applicable to both soft substrates (nitrocellulose, nylon, and cellulose), and to rigid supports (glass, metals, synthetic materials, etc.).

Pin printing methods belong to the contact transfer techniques that are widely used in the industry and by research laboratories. In brief, the principle consists in dipping a pin in an analyte solution, then transferring a small amount or droplet to the substrate by means of a robotic arm. Deposition of a small droplet takes place when the pin is accelerated and decelerated against the surface (“pin tapping”). Since surface tension and adsorption forces play a major role in this process, the humidity and temperature must be precisely controlled to obtain homogeneous, reproducible droplets. Therefore, the instruments available include sensitive heating elements and humidifiers. The needles or “pins” used are fabricated from inert materials such as stainless steel, tungsten, titanium or, more recently, ceramic. The simplest designs consist of a solid needle with a textured surface at the tip, but split tips that present a narrow opening in the center, useful for loading once and printing several times

(“quills”), are also available. Several pins can be simultaneously attached to a print-head, in order to make the procedure less time consuming. In a high-tech and sophisticated variation of the pin method known as “dip-pen lithography”, nanocantilevers such as those required for atomic force microscopy are utilized.^[122] This high-resolution grafting technique depends on the capillary attraction between the nano tip and the surface to deposit nano amounts of the substance of interest, but is unfortunately prohibitively expensive to use in larger-scale sensor fabrication.

Alternatively, flexible elastomer microstamps made of PDMS are also used for contact printing.^[123] Microstamps are considerably less expensive and better suited for the simultaneous application of several analytes (parallel printing), but they are rather hydrophobic and need to be modified with either a thin aluminum film, a hydrophilic monolayer, or else treated with oxygen plasma, to be rendered capable of adsorbing an aqueous mixture of the analyte. Microstamps can be directly “inked” in solutions, or they can also be custom-modified with microchannels that act as reservoirs for the liquids.

Although popular and relatively accessible, contact printing techniques still present some problems such as cross contamination, droplet inhomogeneity, high costs and low throughput in the arraying process. Furthermore, they are deemed wasteful, since they require considerably more analyte quantities than what is effectively deposited on the sensor surface. Therefore, non-contact printing methods have been developed in an attempt to overcome these difficulties. Ink-jet spraying, electrospray deposition, droplet dispensing and laser writing have all provided examples for substance deposition in the field of array fabrication. They are faster printing methods and require little analyte, but still present shortcomings, particularly regarding printing reproducibility.^[124-126]

2.3 Solid Phase Peptide Synthesis (SPPS)

2.3.1 Generalities and Principle of SPPS

Solid phase peptide synthesis (SPPS) is a heterogeneous synthetic technique used to obtain polypeptide sequences by the sequential addition of amino acids to a growing, linear chain anchored to a solid support, an idea originally conceived by R. B. Merrifield in 1963.^[127-129] Prior to this benchmark development, chemical synthesis and particularly peptide synthesis were carried out exclusively in homogenous solution. The tedious purification steps necessary to produce even short oligopeptides rendered this technique impractical. The birth of SPPS opened the doors to the efficient chemical synthesis of peptides and proteins. Moreover, automated synthesis became a reality, advancement mainly achievable because SPPS technology consistently uses orthogonal protecting strategies and relies on the physical separation of the reaction products from the work solution. For the development of chemical synthesis on a solid support, Merrifield was awarded the Nobel Prize in Chemistry in 1984.

In SPPS, one amino acid is added at a time to a growing peptide chain. Since this peptide chain is separated from the reagent solution by covalently attaching it to a solid support, a significant excess (usually 1 to 5) of reagents can be used to drive the coupling reaction to completion. The building blocks of SPPS consist of N^α-protected amino acids with additional protecting groups for the side chains. The first step in the synthesis anchors the carboxyl group of the first amino acid to a chemically functionalized resin, so that the peptide chain is built in the direction C to N. After the first coupling step has taken place, the amino group of the immobilized amino acid is deprotected. The subsequent step is the C-activation and addition of the next building block to the immobilized conjugate. Sequential steps of N^α-deprotection, C-activation of the next amino acid and peptide bond formation within the growing sequence can easily afford linear polypeptide chains of up to 60 amino acid residues in length.^[130, 131] Figure 11 shows a schematic representation of this sequential process.

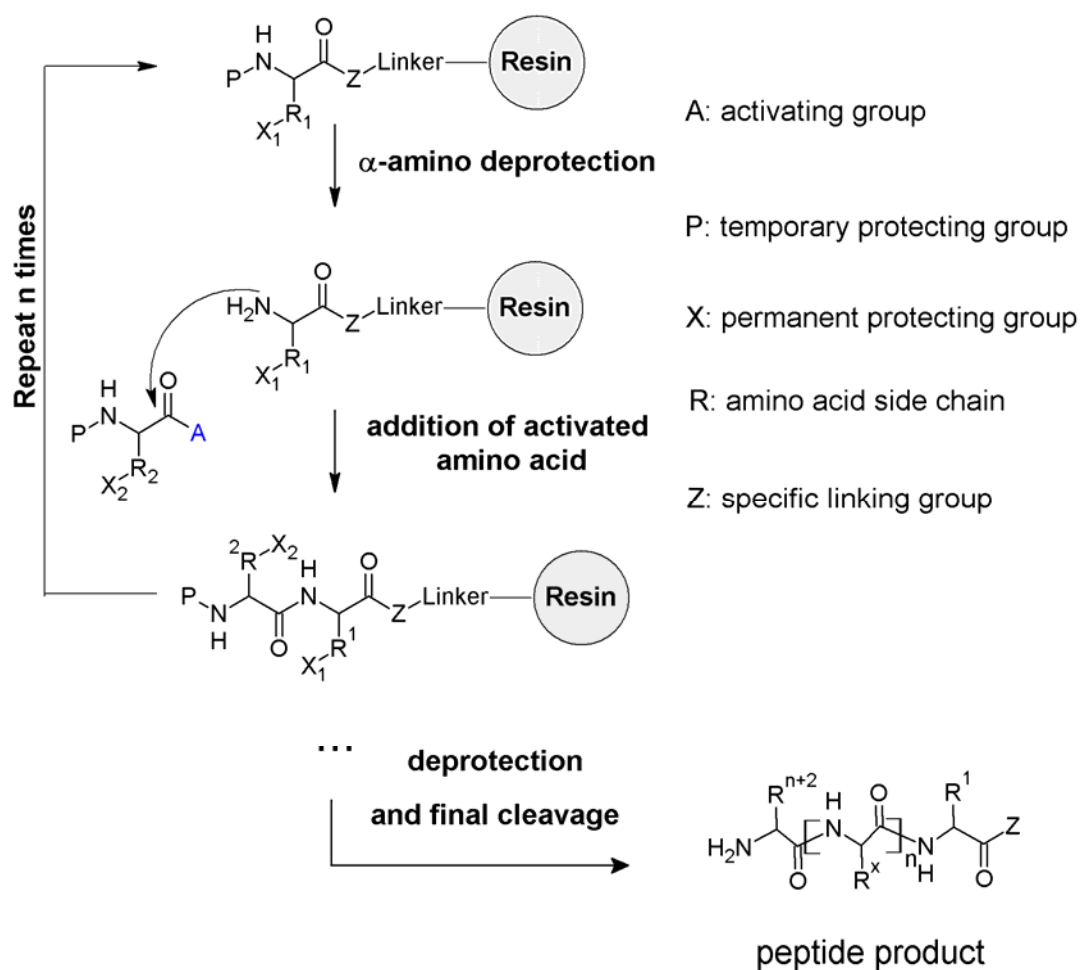


Figure 11 Diagram of the sequential steps involved in SPPS.

There are two types of protecting groups characteristic of the building blocks of SPPS. The temporary protecting groups of the N^α functionality are removed from the resin-bound peptide shortly before carrying out the next coupling reaction. On the other hand, the permanent protecting groups of the amino acid side-chains are used to keep the later intact during peptide chain elongation. Permanent protecting groups are usually removed when the finished peptide sequence is cleaved from the solid support. Because permanent and temporary protecting groups can be detached independently from each other (i.e. their mutually exclusive reactivity allows for selective removal under different chemical conditions, such as pH), they are called *orthogonal* protecting groups.

Two main coupling and deprotecting strategies are widely used for peptide synthesis: the Boc (*tert*-butyloxycarbonyl) strategy and the Fmoc (9-fluorenylmethyloxycarbonyl) strategy. Boc chemistry, or “standard Merrifield” chemistry, was extensively used in the first applications of SPPS and is based in the graduated acid liability of the Boc and benzyl (Bzl) groups.^[131, 132] The temporary Boc protection is removed from N^α by treating the resin with 20 – 30%

trifluoroacetic acid (TFA) in DCM. Because the side-group protection in Boc chemistry involves urethane derivatives of benzyl alcohol, capable of withstanding multiple cycles of TFA deprotection, harsher acidic conditions are required for permanent group removal and final resin cleavage. For this purpose, anhydrous HF at 0°C is generally used, which makes Boc chemistry technically impractical. The toxicity and reactivity of HF requires the use of polytetrafluoroethylene (PTFE) lined storage vessels, stringent security measures and considerable expertise on behalf of the scientist. Moreover, the strongly acidic conditions necessary throughout the synthesis can also cause undesirable side-reaction of sensitive amino acid sequences.

The Fmoc strategy is the most widely used SPPS strategy today. The Fmoc protecting group is depicted in figure 12. During Fmoc-based SPPS, this temporary group is removed from N^α under weak, basic conditions (i.e. 20% piperidine in DMF). The ring proton β to the urethane oxygen is particularly labile towards bases, since the resulting electron density can be stabilized in a cyclopentadienide system. Upon elimination, carbamate salts and the reactive dibenzofulvene solid are formed, which can be easily rinsed off the resin.^[133]

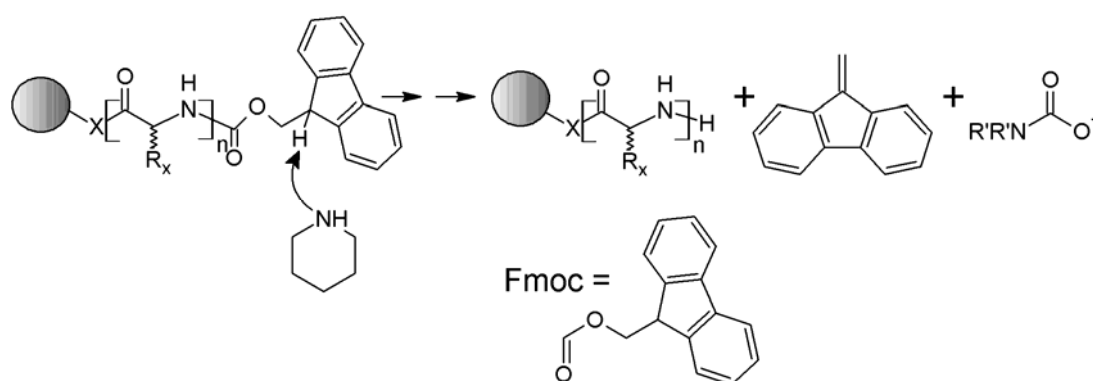


Figure 12 Fmoc deprotection of a resin-anchored peptide.

The side chains of the Fmoc-protected amino acid building blocks are protected with the Boc functionality, or with other acid-labile groups removed simultaneously in the final TFA cleavage of the resin.^[134] After successful synthesis and final cleavage of a peptide, gradient RP-HPLC is the method of choice for purifying the product. Because both acidic and basic functionalities are present in the cleaved peptide, adequate pairing reagents must be used for chromatographic purification. The usual choice of a mobile phase consists of a water ACN or a water methanol mixture. The peptide bond absorbs strongly in the far UV with a maximum at about 190 nm, but in order to avoid difficulties caused by absorption of oxygen, detection

in HPLC is carried out by measuring the absorbance at 205 nm. Additionally, the side-chains in Trp, Phe, Tyr, His, Cys, Met and Arg make contributions to the absorbance at 205 nm as well.^[135] A summary of the most commonly used side chain protecting groups for Fmoc SPPS is presented in figure 13.

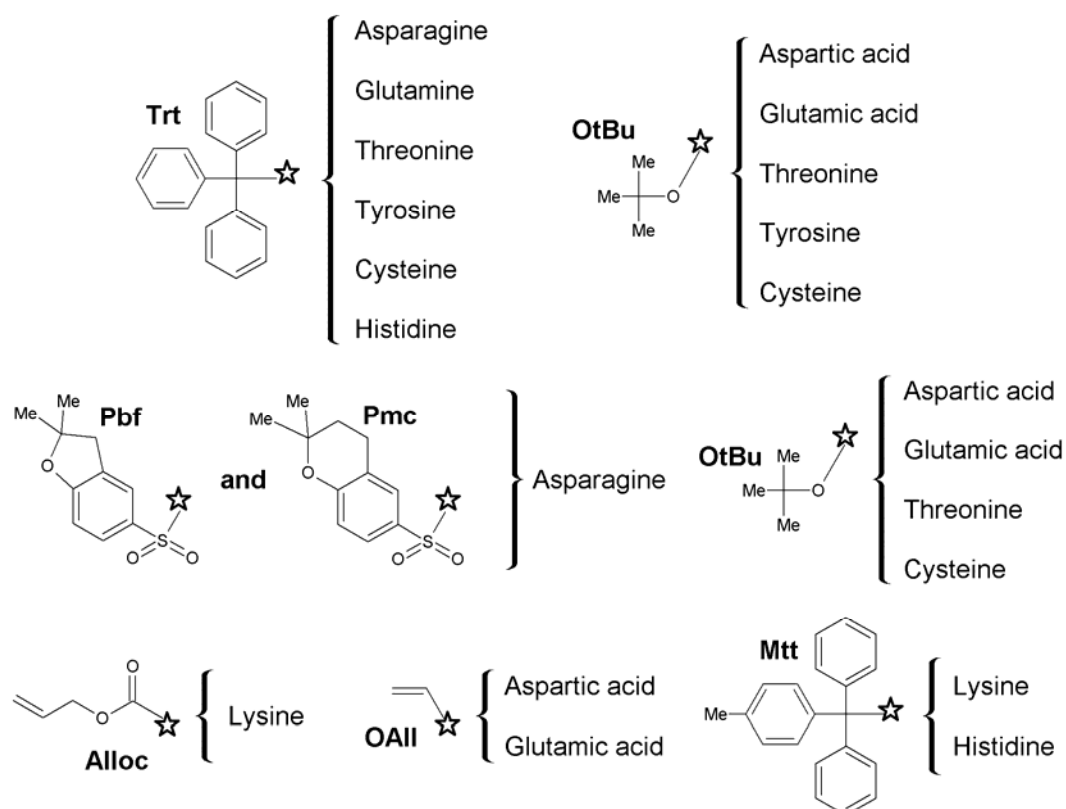


Figure 13 Usual side-chain (permanent) protecting groups in Fmoc-SPPS.

In the Fmoc-approach, permanent and temporary protecting groups are eliminated by truly different mechanisms, but most importantly, secondary base cleavage of temporary protecting groups is absent from side reactions, even with potentially sensitive amino acid derivatives.^[136] For all of the reasons mentioned above, the milder Fmoc chemistry approach is usually preferred over the classical Boc strategy for routine SPPS.

2.3.2 Activating Reagents in Fmoc Chemistry

For efficient, stepwise introduction of the N-protected amino acids in Fmoc-based SPPS, the previous, in-situ activation of the carboxylic functionality is a widely used strategy. Some of the most popular reagents are benzotriazol-1-yl-oxy-tris-(dimethylamino) phosphonium hexafluorophosphate (BOP) or benzotriazol-1-yl-oxytripyrrolidino phosphonium

hexafluorophosphate (PyBOP), for phosphonium-based activation, and *O*-(benzotriazol-1-yl)-1,1,3,3-tetramethyluronium tetrafluoroborate (TBTU) or *O*-(benzotriazol-1-yl)-*N,N,N',N'*-tetramethyluronium hexafluorophosphate (HBTU) for aminium or uronium-based activation. The chemical structure of these compounds, along with the activating mechanism of HBTU/TBTU is presented in figure 14. Several factors need to be taken into consideration when choosing either of these coupling reagents. Phosphonium-based activation is more efficient compared to uronium activation, but the side reaction products are very toxic (particularly hexamethyl phosphoric triamide, HMPA). On the other hand, uronium activation can limit coupling yield if the guanidinium adduct of the N^α deprotected amino acid is formed, since the reaction is irreversible and hinders further coupling of the immobilized amino acid residue. Therefore it is recommended to form the carboxylate of the incoming amino acid before it is added to the resin by dissolving it in the presence of a tertiary amine, such as *N,N*-diisopropylethylamine (DIPEA or Hünig's base). A slight deficiency in the coupling reagent with respect to the free amino acid also prevents this unwanted side reaction.

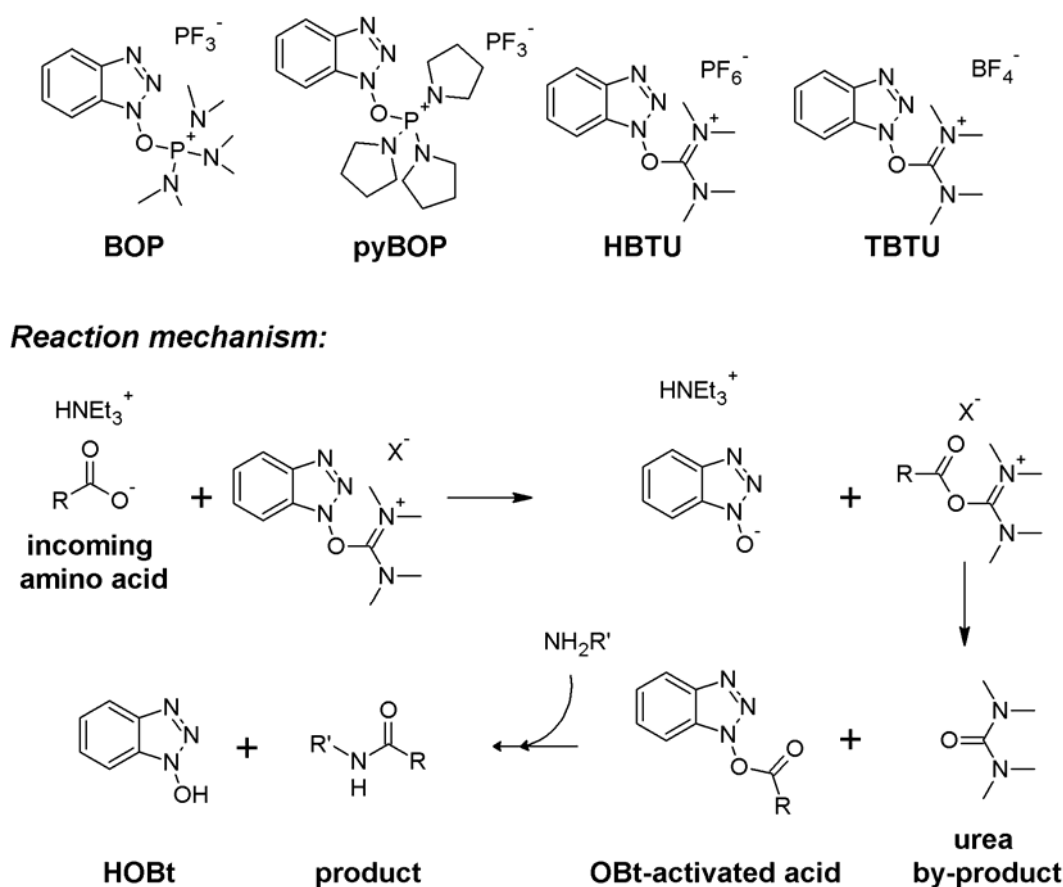


Figure 14 Selected activating reagents for SPPS and activation mechanism.

Depending on the chain sequence and on the number of amino acid residues, coupling of the growing peptide chain may become more troublesome with every new amino acid addition. Especially when synthesizing hydrophobic sequences and/or those consisting of a long peptide chain (which becomes gradually hindered in the polymer matrix), incomplete coupling will diminish the overall yield of the product and will make its purification difficult. Therefore it is recommended to assess the extent of Fmoc deprotection with the aid of a colorimetric method, such as the Kaiser test or the TNBS test, which show a change of color in the resin when free amino groups are present. Equipment for automated SPPS might include a UV detector for quantitative determination of dibenzofulvene, the product of base-catalyzed Fmoc cleavage, which absorbs strongly at 300 nm in the form of a piperidine complex.^[137]

2.3.3 SPPS Solid Supports

The type of material used for anchoring the peptide chain and the particular end functional group in the C-end of the final product are two important aspects that bring diversity to the choice of solid support in SPPS. Hundreds of different resins are commercially available for Fmoc synthesis. Generally, the bulk of the support consists of either cross-linked polystyrene (PS), crosslinked polyamide, or a composite of either of these with polyethylene glycol (PEG). As 99 % of the coupling sites are inside the resin beads^[132], the resin needs to be adequately swelled in a solvent such as DCM, DMF or *N*-Methyl-2-pyrrolidone (NMP) before coupling. The swelling properties of the resin determine also the limiting length of the chain that may be coupled because steric hindrance of closely packed peptide chains will prevent further coupling. The resin linker that serves the purpose of anchoring the first amino acid will determine the C-end functionality of the peptide upon final cleavage. For free acids, Wang, Sasrin, 4-hydroxymethyl-3-methoxyphenoxybutiric acid (HMPB), or trityl chloride resins are used. On the other hand, peptide amides are obtained from cleaving a finished product from a Rink amide, Pal, or Sieber resin. In general, the synthesis of acid-terminated peptides is more laborious, since it requires anhydrous conditions for a first coupling. If a free acid is to be synthesized, the use of pre-loaded resins (e.g. already containing the first amino acid in the sequence) is highly recommended. As can be seen from figure 15, resins for peptide acid synthesis link the first amino acid to the –OH group of the resin and those for peptide amide synthesis do so to the –NH functionality.

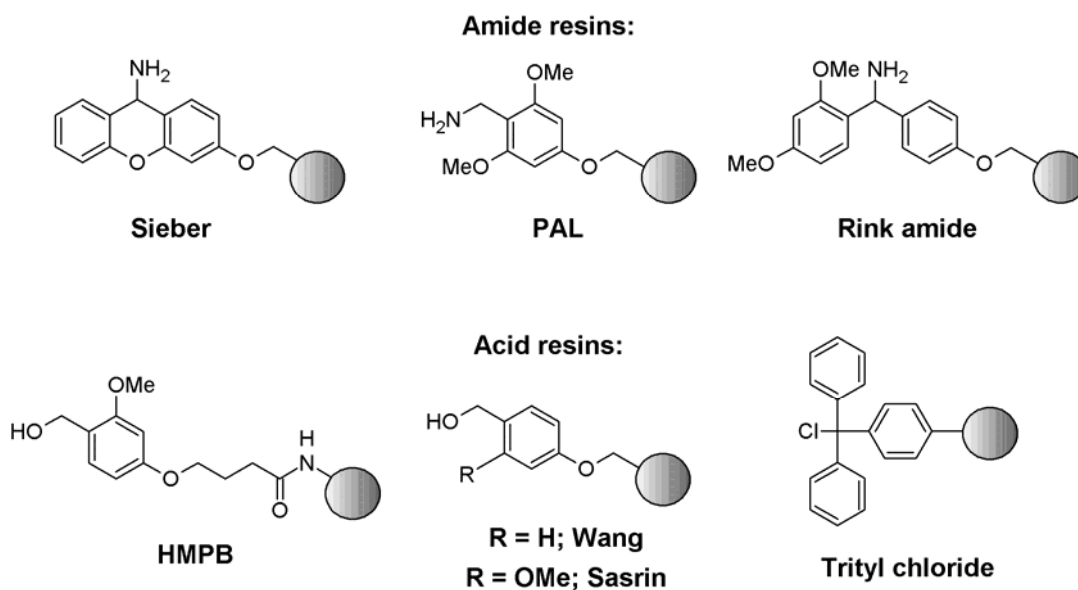


Figure 15 Acid and amide resin supports for SPPS.

2.3.4 Side Reactions in SPPS

Being a chemical method that lacks the fidelity of finely tuned enzyme catalysis that is characteristic of biological systems, Fmoc-SPPS is not free of unwanted side reactions. Difficulties arising from the nature of the peptide bond, the reaction conditions or the type of protecting group used in the building blocks are not unusual and careful characterization of the final products should be exerted. Some documented side reactions include the racemization at the α -carbon, diketopiperazine formation and aspartimide formation. Given their importance, these side reactions will be discussed further.

Racemization at the α -Carbon

Perhaps the most important side reaction in peptide synthesis is the loss of chirality at the C-terminal residue of the peptide. With the exception of glycine, all 20 standard amino acids present a chiral center at the α -carbon. Depending on the side group present, base-catalyzed epimerization of the peptide bond becomes a favored process when the activated ester of the carboxylic acid in the Fmoc-protected amino acid is formed. In an effort to avoid it, the addition of a sterically hindered tertiary base represents an alternative. Figure 16 shows the oxazolone-mediated racemization of the incoming activated amino acid during peptide coupling, a reaction that is especially common when coupling activated Fmoc-derivatives of histidine and cystein (Fmoc-Cys(Trt)-OH and Fmoc-His(Trt)-OH).^[138]

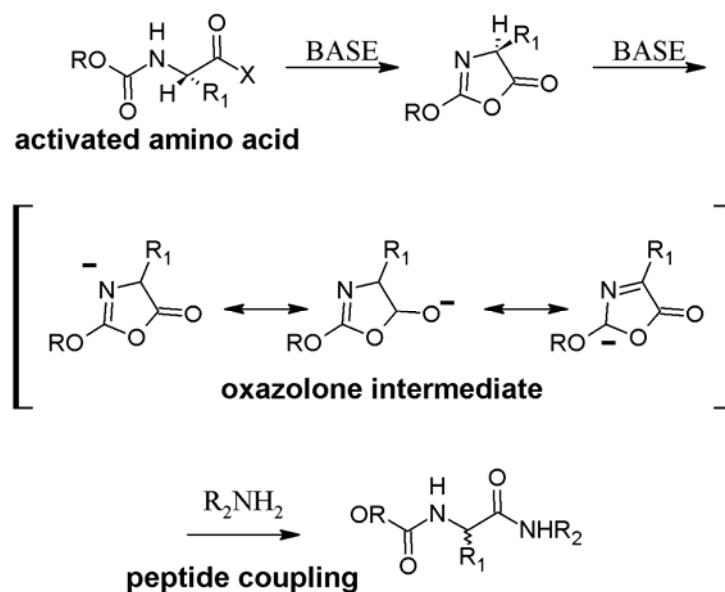


Figure 16 Loss of chirality of incoming peptide through oxazolone formation.

Diketopiperazine Formation

This source of side reaction affects immobilized products at the dipeptide stage, after N^α-deprotection, as shown in figure 17. The extent of this reaction depends greatly on the type of resin being used (i.e. the linker attaching the first amino acid to the resin), and of the amino acids present. In particular, sequences starting with proline or with glycine are susceptible to this side reaction, which is significant because it compromises the total yield of peptide synthesis from the first steps of chain formation. Some measures that can be adopted are the selection of a resin with a sterically hindered linker to the peptide.

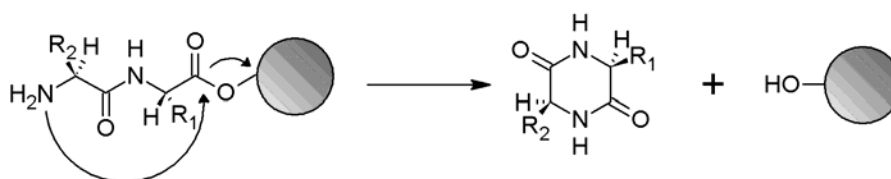


Figure 17 Diketopiperazine formation of a dipeptide linked to the resin during SPPS.

Aspartimide Formation

This reaction is the result of the inclusion of aspartic acid residues in the peptide chain, particularly in sequences containing the “Asp-AA” sequences, where AA = Gly, Asn, Ser, or Ala (figure 18).^[139] In this reaction the β-carboxylic acid side-chain of aspartic acid forms a ring with the nitrogen of the closest α-carboxamide.

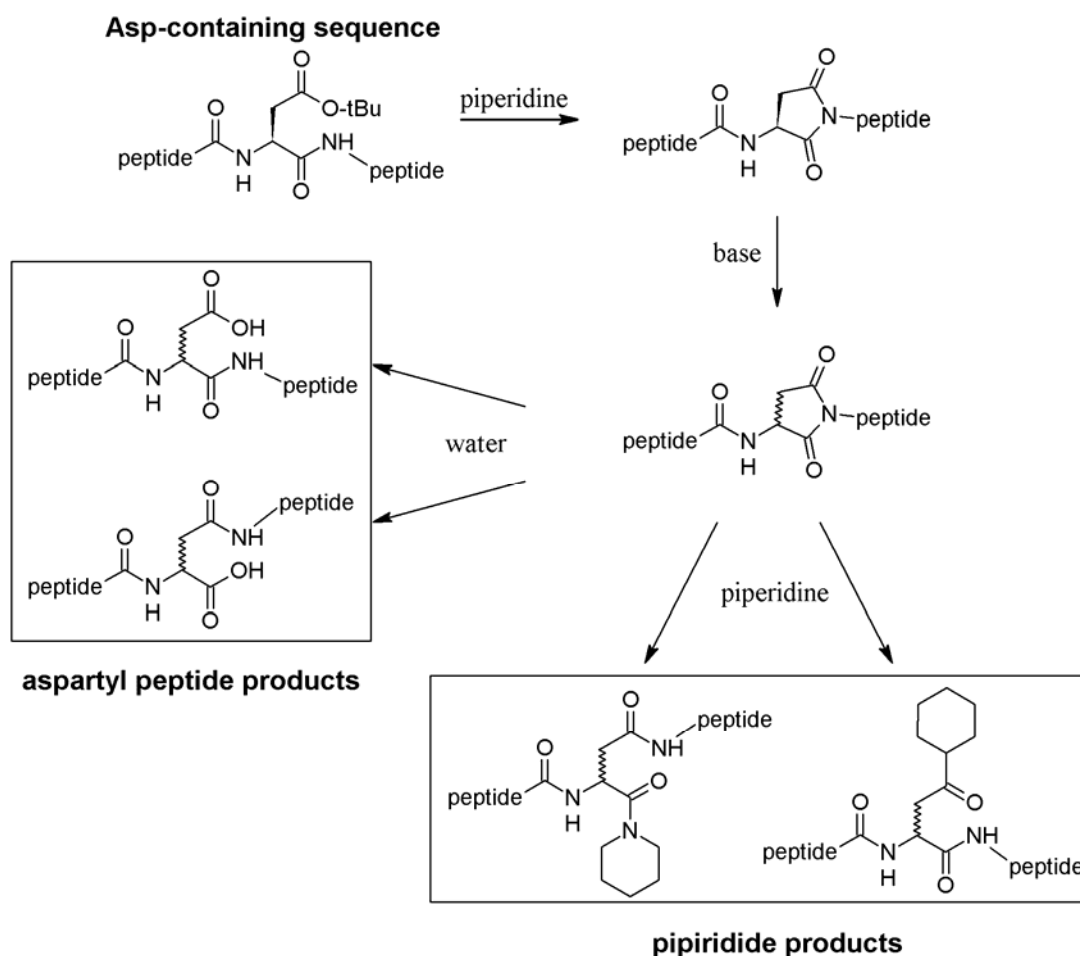


Figure 18 Base-catalyzed aspartimide and piperidide formation in sequences containing Asp.

The reaction is especially favored in the presence of piperidine, which is frequently used for Fmoc-deprotection.^[140] Ring re-opening occurs with loss of chirality and can happen through hydrolysis during final deprotection, or by nucleophilic attack of piperidine itself.^[141] Since this reaction is base-catalyzed, the risk of forming the unwanted derivatives increases with each cycle of deprotection needed in the assembling of the peptide chain. In order to prevent it, the Hmb protecting group is used for the aspartate side-chain^[142]; however, Hmb derivatives are more expensive than their t-Boc counterparts and therefore not suitable for large-scale applications. The use of a milder base such as piperazine instead of piperidine for deprotection also diminishes the risk of forming the α and β piperidines, but longer deprotection times are required in this case.

3 Results and Discussion

3.1 Customization and Characterization of the MCR 3

3.1.1 MCR 3: General Description and Characteristics

The Munich Chip Reader 3 (MCR 3) was used in this work mainly to develop a fast screening method for the quantification of the mycotoxin OTA in green coffee samples. This instrument developed at the IWC consists of a self-contained platform with operating software that responds to the ever-growing need for automation and simultaneous screening of multiple analytes in complex samples. The concept of the MCR 3 is based on the Parallel Assay Sensor Array (PASA), also developed at the IWC and already tested for several applications.^[143-146] In particular, both instruments have been used for the determination of antibiotic residues in raw milk in the past.^[98, 147, 148] Immunoaffinity-based recognition is at the core of the platform's conception and the HRP-catalyzed chemiluminescence of luminol is employed for signal generation, which is recorded by a CCD camera. Reagents for the programmed assays are dispensed in a semi-continuous manner towards the working flow-cell with practically no incubation required. It is for this reason that the MCR 3 has been previously classified as a "flow-through" device. Figure 19 shows a simplified representation of the MCR 3 along with its main components.

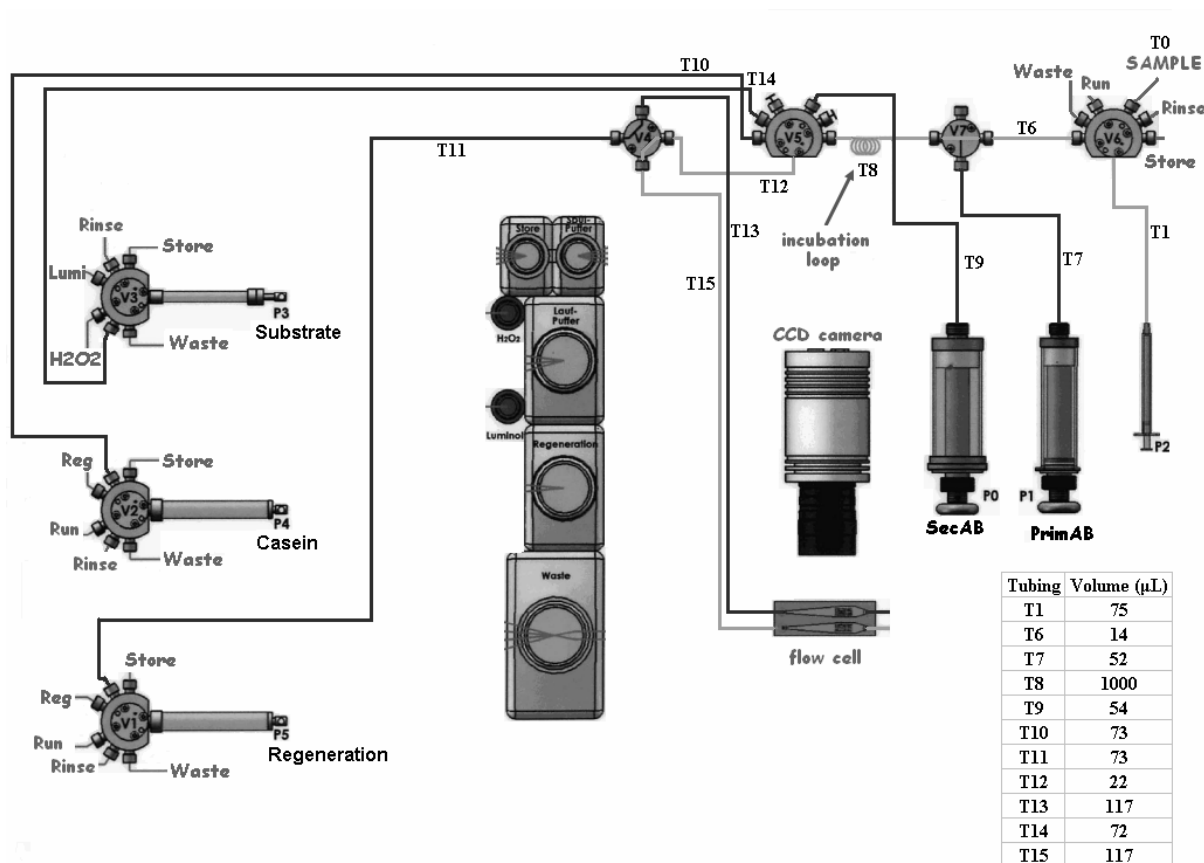


Figure 19 Simplified scheme of the MCR 3: system components and tubing dead volume. Legends: SecAB = secondary HPR-marked antibody solution; PrimAB = primary antibody solution; Lumi = luminol; Reg = regenerating solution; Run = running solution (casein); Rinse = rinsing solution; Store = storage buffer.

The MCR 3 consists of six plunger-type piston pumps that can be operated independently, connected by means of PTFE tubing to individual solution reservoirs. Seven port valves offer further choices for the sequential or simultaneous dispensing of solutions, ultimately driven into a working flow cell. The configuration of the system was planned in such a way that each of the four six-port valves attached to the pumps can connect with four of the seven solution reservoirs, using up to four of the six available ports per valve, thus leaving two ports for the intake and pumping of the solutions (to the waste, for rinsing, or to the tubing network). This feature offers the possibility of pumping different solutions through one particular section of the tubing with the same pump, as well as several options for programming assay sequences. Furthermore, since at least one of the reservoirs contains rinsing solution, and this is available to four of the pumps, washing can be thoroughly carried out in between reagent addition to avoid cross contamination. Such a feature is highly desired when using several chemicals in the same assay. A picture of the actual instrument is presented in figure 20.

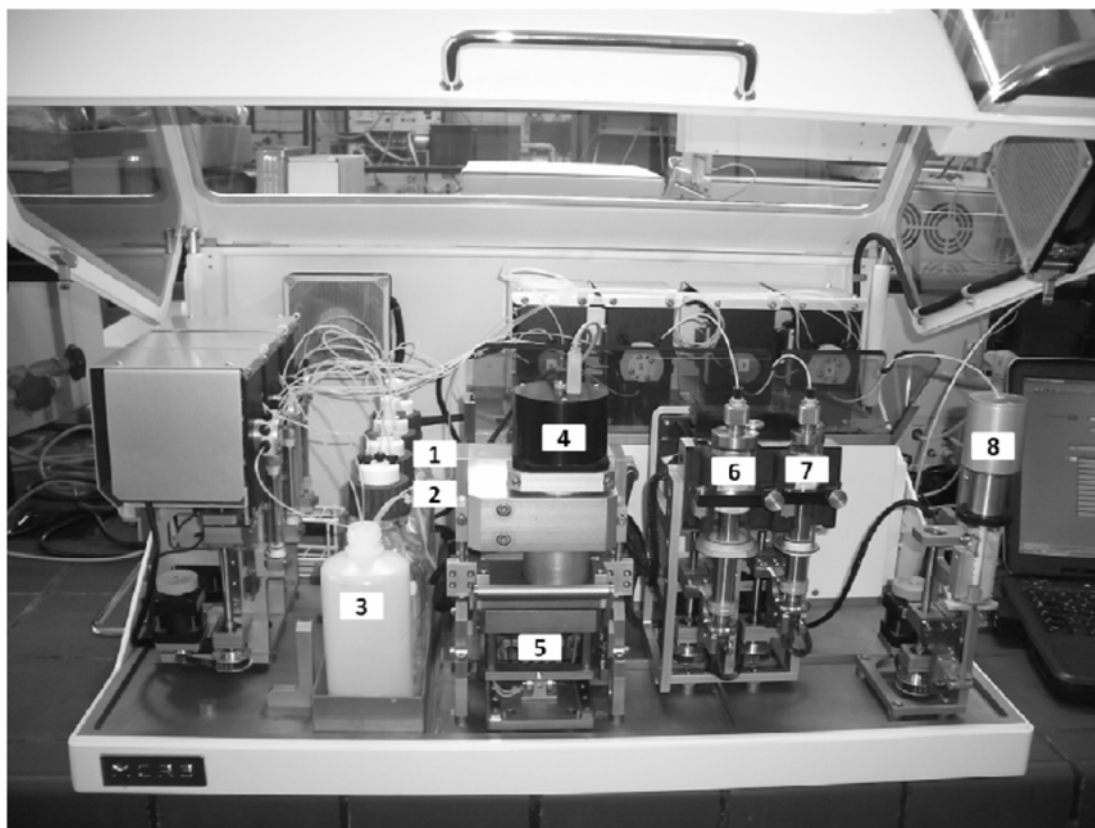


Figure 20 The MCR 3. Labels: 1-2 = solution reservoirs; 3 = waste outlet; 4 = CCD camera; 5 = flow-cell holder; 6 = secondary antibody syringe-pump; 7 = primary antibody syringe-pump; 8 = sample introduction pump.

A typical indirect competitive immunoassay sequence starts by simultaneously pumping the sample and the primary antibody solution (P2 and P1, respectively) into the incubation loop, (“T8” in figure 19), and then closing the input port of V5 for a short waiting period to take place, in order to improve the mixing of the two solutions. Following incubation of the reagents, the sample input syringe is automatically filled with running buffer and pumped to displace the loop contents towards the flow cell, where the toxin receptors have been immobilized. After pumping the mixture to the chosen flow cell chamber and allowing for competition to take place, some toxin-specific antibodies will bind to the immobilized receptors. The remaining solution in the flow cell will be rinsed before secondary HRP-marked antibody is introduced in the flow cell, as a means to detect the binding of the primary, specific antibody to the immobilized receptor. After rinsing again, a mixture of the reagents luminol and hydrogen peroxide are then pumped to the working chamber. The HRP tag of the marked secondary antibody catalyzes the conversion of luminol to a chemiluminescent species and a CCD image that shows bright spots in the places where secondary antibody is present is generated. Finally, the flow cell is washed one more time and “regenerated” by introducing a solution that will disturb the antibody-antigen interaction and

return the surface to the state in which it was before the measuring cycle started. These “regeneration” solutions capable of destroying the antibody-antigen complex usually consist of a tenside, a chaotropic agent like sodium chloride, and a buffering substance that confers an acidic pH. The number of cycles that the sensor is able to withstand is dependent on the nature of the regeneration solution, on the surface properties and on the complexity of the substances that come in contact with the sensor.

As can be seen from the fluidic scheme presented in figure 19, the access to the flow cell is controlled by means of valve 4 (V4), which consists of a 4-port T-distribution valve. It can be positioned so that the outlet of valve 5 (V5) or the contents of pump 5 (P5, or the “regeneration” pump) are directed either to the back chamber or to the front chamber, the diamond-shaped carvings shown in figure 21, either in a sequential or in a simultaneous manner. This makes the simultaneous dispensing of reagents to the two flow cell chambers possible, a feature that simplifies the rinsing needed in-between assay steps. Another important feature of the MCR 3 is the flow cell construct and its holder, pictured in figure 21.

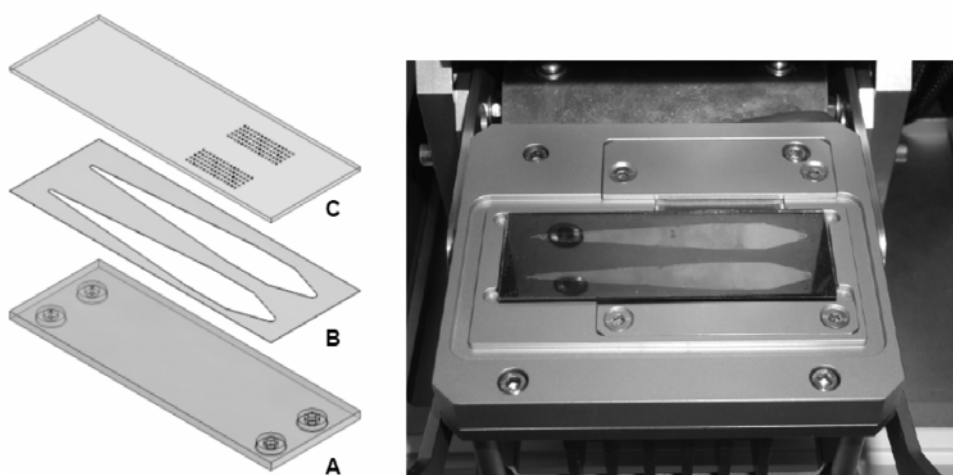


Figure 21 Left: flow cell construct forming two diamond-shaped chambers, consisting of opaque synthetic slide (A), double-sided sticky film (B) and microscope glass slide (C). Right: MCR 3 flow cell holder.

The flow cell support consists of a movable drawer encasing two tubing inlets and their corresponding outlets, with a carving where the flow cell is placed horizontally. The flow cell itself is constructed of an opaque slide made of black poly(methyl methacrylate) (PMMA, figure 21-A), a double-sided sticky film cut out with two parallel diamond shapes (figure 21-B), and a commercially available glass microscopic slide (figure 21-C). The receptor molecules are immobilized to the chemically modified glass slide along the broader region of

the diamond shape, so that they become exposed to a lateral flow of reagents, orthogonal to the plane of immobilization. Immunoaffinity-based lateral flow devices such as the MCR 3 considerably reduce assay time and equilibration periods, otherwise required in traditional microtiter plate ELISA because the transport of the analyte to the receptor molecule on the surface of the flow cell is much faster through the thinner and more constant diffusion layer (ca. 142 μm).^[149, 150]

The antibody solutions needed for the immunoassay are stored in the two removable syringes of the MCR 3, P0 and P1 (figure 19 and 20). These syringes can only be pumped in one direction, thus they cannot be automatically filled with reagents by sucking up solution from a reservoir and must be loaded manually before the assay starts. Nevertheless, the amount of antibody solution required for each assay is generally small (between 0.5 and 1 mL) and one load of the system is usually sufficient to run at least 30 independent assays without the need for re-filling the antibody syringes. The syringe holder of these two components is also temperature-controlled in order to avoid antibody denaturation and to enhance signal reproducibility. However, this feature was not used in this work because at the time, the materials for the construction of the removable syringes would significantly change their volume upon cooling, making the syringe pistons leaky. One difference of the present system compared to the previous MCR 3 version used for antibiotic analysis in milk is the casing of the syringe used for sample introduction, P2. In the “milk system”, the P2 syringe unit is built so that a 1 mL, one-time-use polypropylene syringe must be loaded by hand with the milk sample and placed in the syringe holder at the beginning of each measurement. The syringe is further used for the remaining of the assay (for example, for pumping rinsing solution through the tubing and the flow cell), and then removed and disposed after each cycle. This is by all means adequate when handling harmless substances, but it is certainly not practical for mycotoxin contaminated food extracts, or when handling the calibrant solutions, which can reach toxin concentrations as high as 1000 ppb and may contain MeOH or other organic solvents. In this case, the original P2 unit was replaced with a fixed 1 mL glass syringe. Sample introduction was carried out by reprogramming the sample input routine and by drawing the extract connected to port 4 of valve 6 (V6, figure 19). Glass also has the advantage of being more adequate for handling mycotoxins, as it can be more easily cleaned than synthetic materials. The differences between the two P2 units are shown in figure 22.

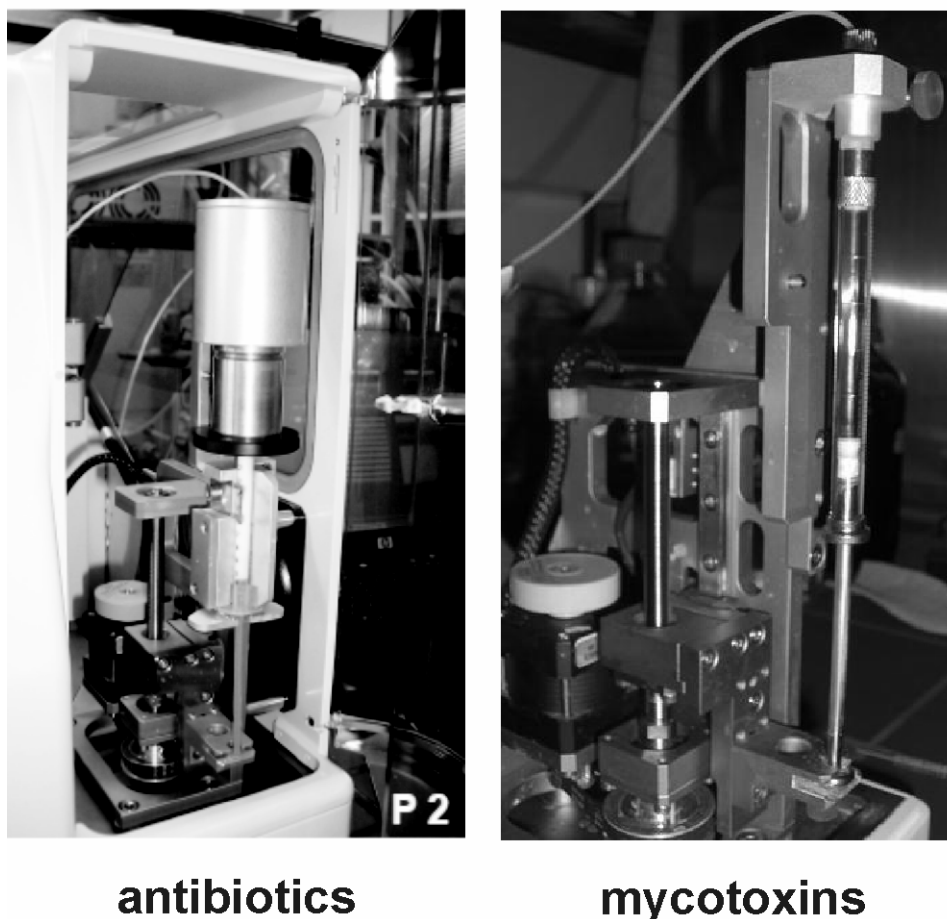


Figure 22 Sample input unit, P2, for antibiotic determination in milk (left) and modified unit for mycotoxin determination in food extracts (right).

3.1.2 The Flow-Cell Work Surface

As a base surface for the immobilization of the capture analytes in the biosensor fabrication process, chemically derivatized microscope glass slides were used. The chemical process for surface derivatization is schematized in figure 23. First, the surface was modified with an epoxy-silane (GOPTS) and then reacted with polyethylene glycol diamine (DAPEG), with the purpose of diminishing unspecific interactions of the sensor with the sample components. As shown in figure 23, one of two surface activation strategies for analyte coupling were possible from this point on: either the introduction of epoxy groups (by reacting with the homobifunctional linker diepoxy-PEG), or the activation of the available end amino groups by means of a succinimidyl carbamate (by reacting with the homobifunctional linker disuccinimidyl carbonate, DCC).

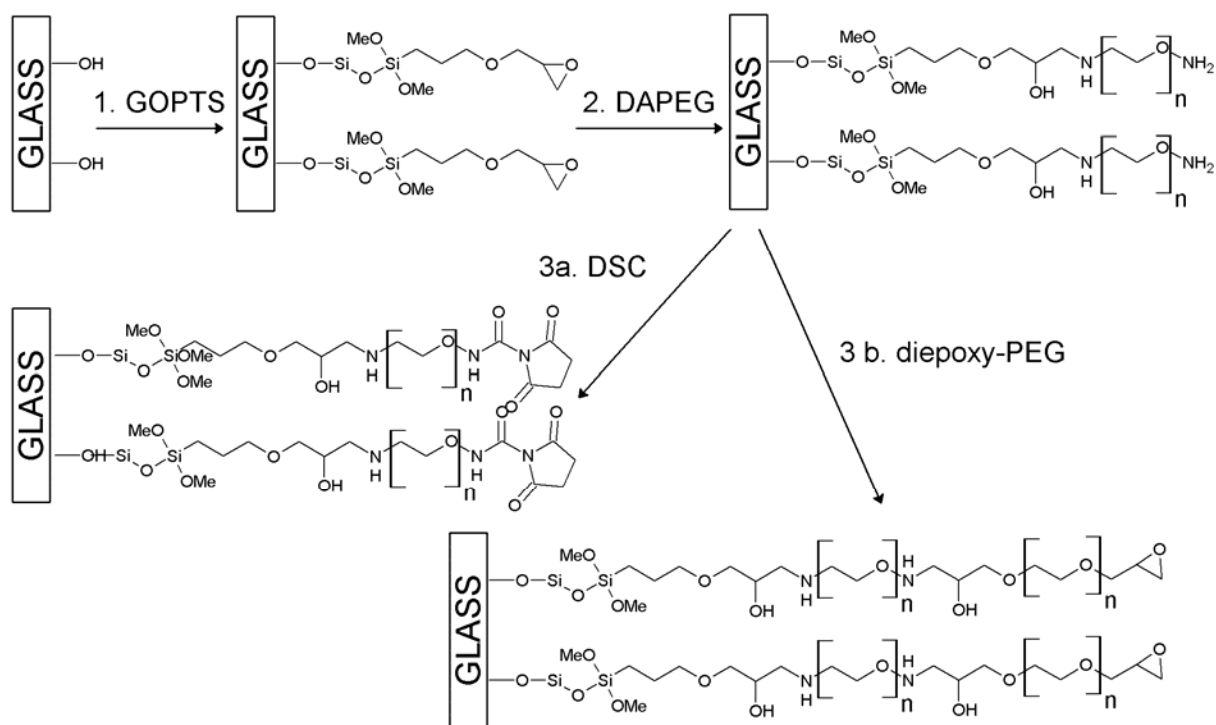


Figure 23 Two possible strategies for the introduction of end reactive groups: glass chip surface derivatization for further receptor immobilization.

This surface-modification strategy was developed at the IWC and has already been tested for a variety of applications. Some of these applications include the fabrication of antibody microarrays^[151] and the immobilization of other small molecules, as in the case of antibiotic immobilization for milk screening already mentioned.^[148] Polyethylene glycol (PEG) coatings not only offer the advantage of reduced unspecific interaction when dealing with complex samples, but they also represent a simple way to introduce useful “anchor” groups for further surface derivatization. PEG chains are highly hydrophilic as well, an important feature necessary for the diffusion of the key analytes in the interface region of flow-through biosensors.

Epoxy groups and succinimidyl carbamates are good electrophiles capable of reacting with amino groups and other common nucleophiles. Moreover, they also react slowly with moisture, so that coupling to the analyte of interest can still take place under humid conditions. In this work, all the immobilized receptor analytes contained one primary amino group (either originally or chemically introduced).

3.1.3 Analyte Chemical Modification for Immobilization

Immunoassays aimed at detecting and quantifying small molecules are only possible under a competitive assay format, as pointed out previously. Of the two versions available for competition (antibody immobilization or hapten immobilization), this work relied exclusively on hapten immobilization in the shape of peptide-derivatized toxins for several reasons. First of all, it was the goal to develop an OTA microchip that could be used and regenerated multiple times. Finding conditions in which an immobilized capture antibody releases the bound analyte, yet maintains its functional 3D structure for further assay cycles, is in general difficult to achieve, especially when working with monoclonal antibodies that already present high affinity to their target. On the other hand, if a small receptor (such as OTA) is directly immobilized as a capture molecule, it is not relevant whether antibody removal damages the antibody structure at all, and there is more liberty to use harsher conditions as antibodies bound to them are washed away under a flow of denaturing buffer and the surface may be used again. This fact alone is the decisive factor in designing a regenerable assay, as in our case. Another point to take into consideration is the reporter, particularly if more than one analyte is to be detected in one single assay. Competitive formats with antibody immobilization inevitably require the generation of as many analyte-label conjugates as there are analytes to be detected. In comparison, small molecule immobilization would only require a *single* type of labeled, secondary antibody for detection, one that is capable of binding to the constant region of *every* primary detection antibody used, in the step that follows competition. Regarding the linker that would allow attachment of a small mycotoxin to the surface of our modified glass chip, we decided in favor of the short amino acid sequence Gly-Ser-Gly-Lys, and a second linker for OTA with the sequence Gly-Ser-Gly-Lys-Gly-Lys, was tested as well. OTA presents a carboxylic acid group of its own that can be easily reacted to the amino end of a peptide with a uronium activation strategy, a method that is frequently used in SPPS as well. On the other hand, AFB₂, also tested for immobilization in this work, presents no chemical functionality that can be directly coupled to a peptide chain. Therefore, AFB₂ was first modified by adding a carboxymethyloxime functionality, which introduces an additional carboxylic acid, in order to make the attachment to the peptide linker possible. This modification of the aflatoxin allowed the standard activation and coupling through this reactive group, in a similar way to OTA.^[152-154] Figure 24 presents a scheme of the toxin modification strategy with the mentioned peptide linker.

The peptide sequence chosen as toxin linker not only transforms the relatively hydrophobic mycotoxins into more water soluble analogues, but it also quantitatively introduces a single, nucleophilic group –the ϵ -amino group of the C-terminus lysin– needed for the covalent attachment of the toxin to either of the two derivatized glass surfaces (figure 23). Moreover, peptide modification of both toxins is carried out entirely on the solid phase, minimizing the risk posed to the chemist when handling the poisonous analytes. The toxin is to be added in the final synthetic step and the protected linker can be stored attached to the solid resin for relatively long periods of time. As discussed in the theoretical background of this work, solid phase synthesis is advantageous in comparison to homogeneous phase synthetic methods because excess and unreacted reagents can be easily removed by rinsing the solid resin. This affords a cleaner product.

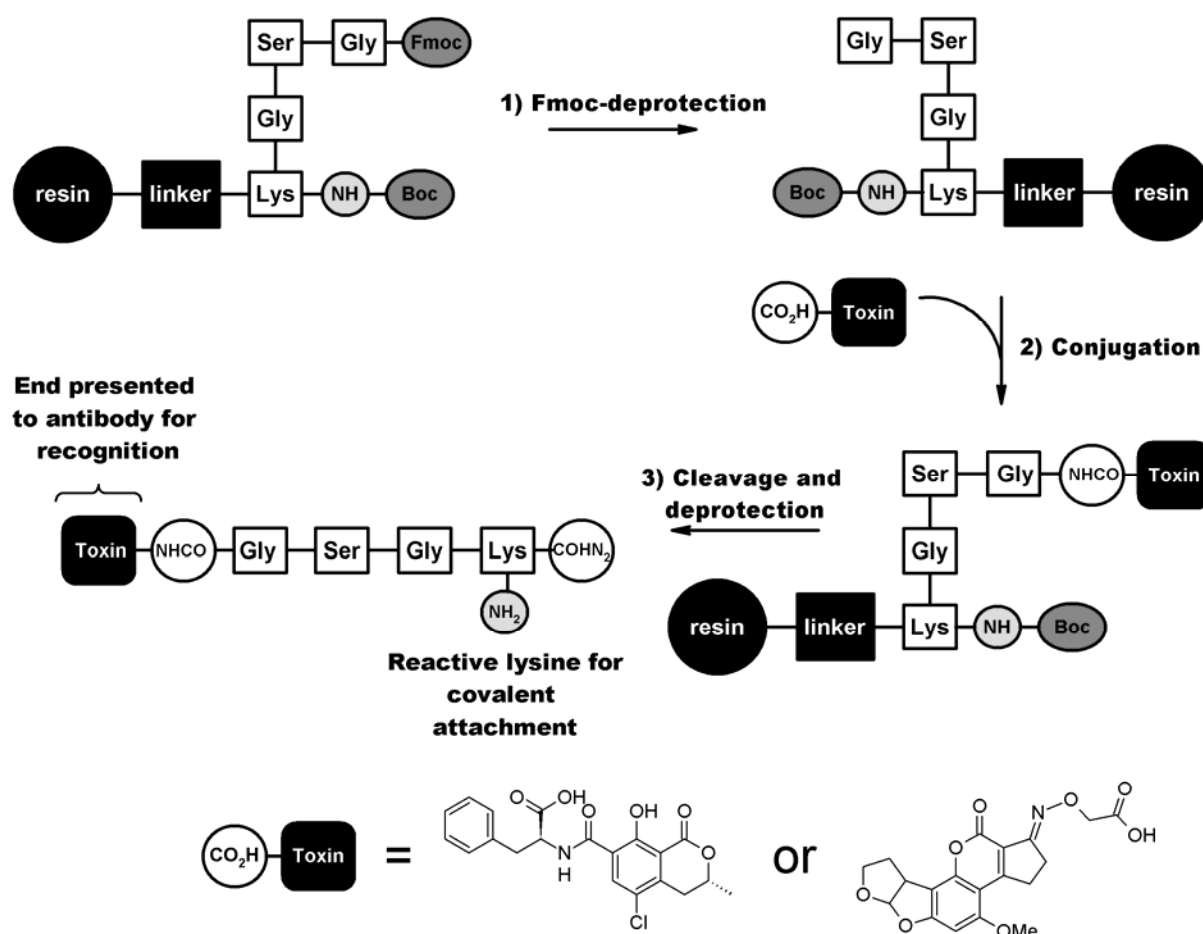


Figure 24 General strategy for toxin modification by SPPS. In this case, analytes containing carboxylic acid groups can be easily coupled to a previously synthesized peptide linker.

The modified analytes were synthesized and cleaved from the resin. Cleanup was performed by semi-preparative HPLC and characterization followed with mass spectrometry. The

products obtained, as well as the expected and experimental masses, are presented in figure 25 and table 3.

Table 3 Characterization of modified toxins and biotin by ESI-MS

Analyte	m/z measured	m/z calculated (monoisotopic)	Error (ppm)
OTA-peptide-I	732.276 [M+H] ⁺	732.275	1.36
OTA-peptide-II	917.4 [M+H] ⁺	917.392	8.72
AFB ₂ -CMO-peptide	738.268 [M+H] ⁺	738.271	4.06
Biotin-peptide	743.389 [M+H] ⁺	743.387	2.28

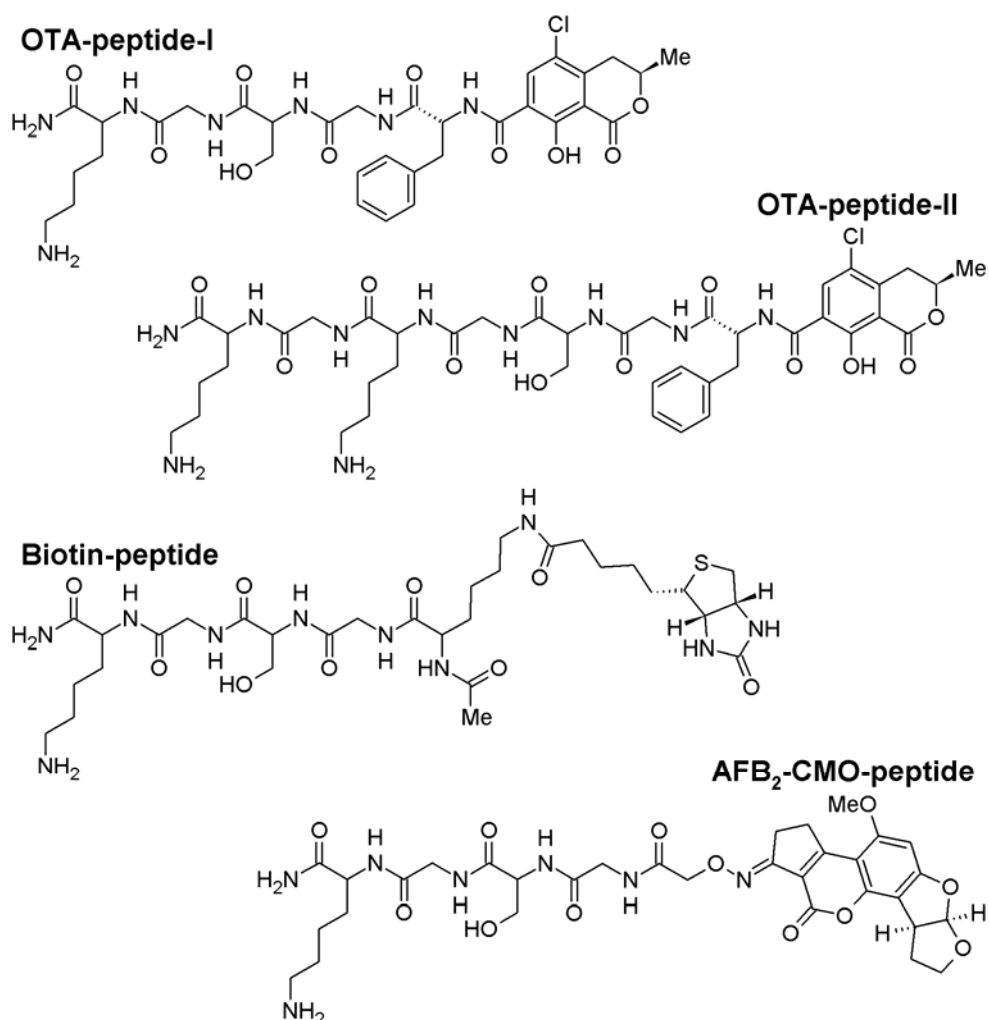


Figure 25 Chemical structures of the synthesized toxin-peptide and biotin-peptide receptors.

The synthesized receptors were further used for immobilization on the previously described special glass surface.

3.1.4 Reactive Surface Characterization: Contact Spotting

The deposition technique chosen in this work to transfer the receptors of interest to the biosensor surface was contact spotting. In essence, the instrument used consists of a very precise robotic arm with a needle holder that can move along the three coordinates inside a closed chamber, where the glass substrates are placed. For the purpose of optimizing reagent spot characteristics and morphology, different printing conditions were tested. There are several parameters capable of exerting an influence on microarray fabrication, among them the hydrophilicity (or hydrophobicity) of the interface, the spotting humidity and temperature, the composition of the spotting solution and the “tapping” of the needle, e.g. the distance that the robotic arm is lowered so that the reagent drop is completely transferred to the surface. By maintaining the temperature and humidity constant, it was possible to record observable differences when varying both spotting buffer composition and “z” distance traveled by the robotic arm. Figure 26 shows pictures of the spotted droplets taken with light microscopy, 30 min after spotting had taken place. Panel A shows an almost dried-up droplet, where the salts contained in the buffer have crystallized. Panel B shows a figure of a similar droplet, only this time the solution had been supplemented with a small amount of glycerol to avoid the fast evaporation of the spotting buffer. Finally, panel C and C.1 shows what happens when the needle is “tapped” too close to the glass slide surface, namely that the droplet breaks and generates what is referred to as “satellite” drops. These inhomogeneous droplets have a negative impact on the quality of the chemiluminescence (CL) signal.

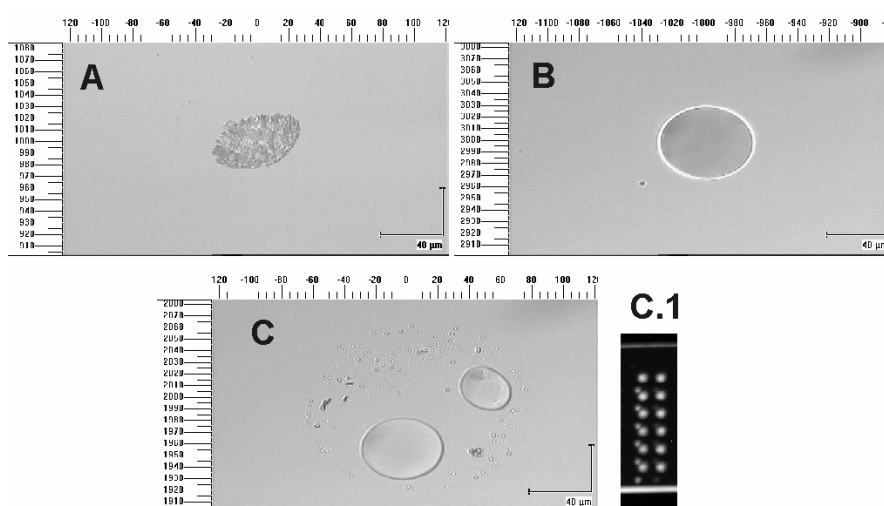


Figure 26 A: droplets spotted on derivatized glass chips. A: carbonate buffer and DMSO (30% v/v), “z” down 18.78 mm. B: same as A, but spotting solution supplemented with 2.5% glycerol. C: same as B, but “z” down 18.80 mm. C.1: chemiluminescence picture of a glass chip where “satellite” drops occurred (on DAPEG modified with DSC). Individual pictures representative of six replicates, after 0.5 h of contact spotting.

The microscopy pictures show the importance of choosing adequate spotting conditions for microarray fabrication. The use of a small percent of glycerol in the spotting solutions (2.5% v/v) greatly improves the shape of the drop on the surface. The function of glycerol is also to prevent spot evaporation, a factor that is important to enhance reactivity of the analyte to the chemically modified glass surface. Adding glycerol to the spotting solution increases its surface tension and prevents droplet evaporation. It is of general knowledge that when spotting small amounts of antibodies on a microarray, droplet evaporation can be prevented by adding trehalose to the buffer solution. We also tried trehalose in this work, but the shape of the spots was not optimal in our experiments (pictures not shown). Finally, a small difference in the distance traveled downwards by the pin needle (in this case 0.02 mm) also exerted an influence on the shape of the drop. Frequent fine-tuning of this distance may be required when spotting sensors on different days. It was our experience that sometimes “satellite” signals were present in the CL picture of a particular chip, although the spotting parameters were exactly the same that produced neat droplets some days before.

3.1.5 Optimization of Surface Regeneration Conditions

The spotted glass chips were tested for signal generation in a non-competitive assay format. In this type of assay, the immobilized receptors are exposed to a lateral flow of primary antibody solution, followed by a secondary anti-mouse HRP-marked antibody solution, and finally by a chemiluminescent substrate (washing is carried out in-between steps, to remove remaining reagents). Because the input solution contains no free analyte that competes for the limited antibody-binding sites, the maximum number of antibodies binds to the immobilized receptor and therefore maximum signal intensity is detected. As one of our main objectives in the biosensor production was to be able to reuse the sensor surface for several assay cycles, it was necessary to show that the bound antibodies could be completely eliminated from the surface in a so-called regeneration step after CL signal recording. In a first approach, the suitability of the regeneration solution was tested: the objective consisted in determining whether antibody removal from the immobilized receptor had been indeed complete. Figure 27 schematizes the original, non-competitive binding assay followed by a regeneration step. The experiment consists of running one cycle of the non-competitive binding assay and recording the CL, then applying the regeneration solution, and finally providing the working surface with chemiluminescent reagent one more time, to check for the presence of HRP. As can be noticed, four outcomes of this experiment are possible depending on the strength of the

antibody-binding interactions, on the tolerance of the HRP towards the components of the regeneration solution, and on the effectivity of the regeneration solution. These are:

- 4 a) the entire removal of the antibody complex (wished outcome, optimum regeneration);
- 4 b) failure to remove both primary and secondary antibodies from receptor and preservation of HRP catalytic activity (insufficient regeneration);
- 4 c) the removal of the secondary, HRP-marked antibody, but failure to remove the primary antibody bound to the receptor (insufficient regeneration), and
- 4 d) failure to remove both antibodies from the receptor and loss of HRP catalytic activity (insufficient regeneration).

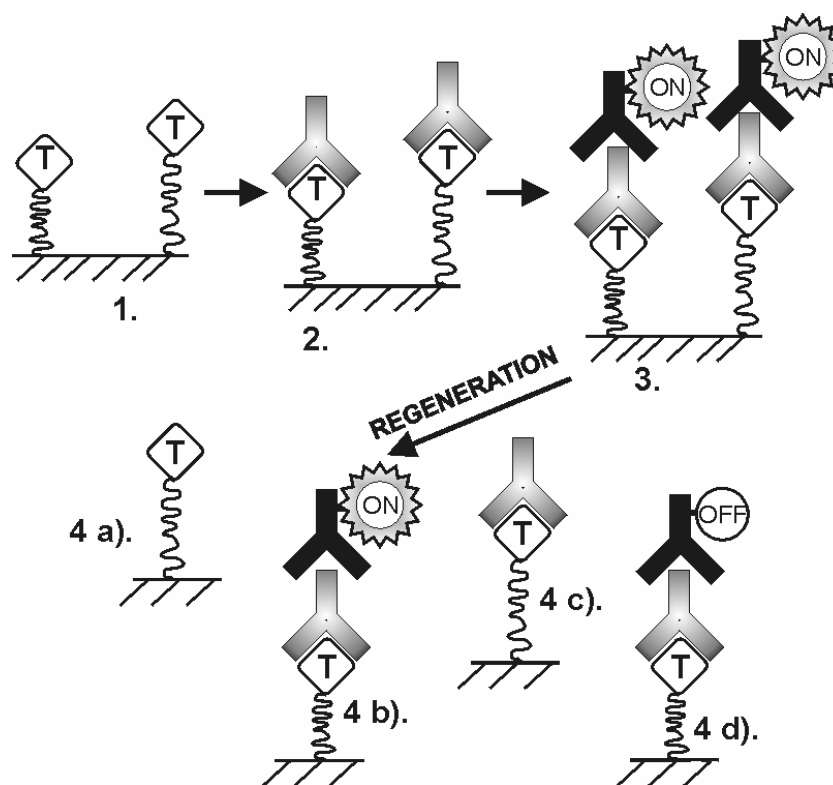


Figure 27 Assay 1: non-competitive binding assay, original format. Regeneration takes place at the end of the assay cycle: different outcomes depending on regeneration efficiency. Each assay step is followed by a neutral washing step.

Assuming that regeneration is insufficient, only situation 4 b) can be unambiguously detected under this experiment type since CL is still triggered after attempted antibody removal, which confirms the presence of HRP on the chip surface. If, on the other hand, substrate solution is supplemented to the chip after regeneration and CL is not to be detected, there is no possible way of distinguishing between outcomes 4 a), 4 c) or 4 d). It is not possible to distinguish

between sufficient regeneration (situation 4 a), or inactivation of the HRP by any of the components of the regeneration buffer (situation 4 d). In order to shed light on the different effects of a particular regeneration buffer, the assay format was slightly modified according to the scheme presented in figure 28.

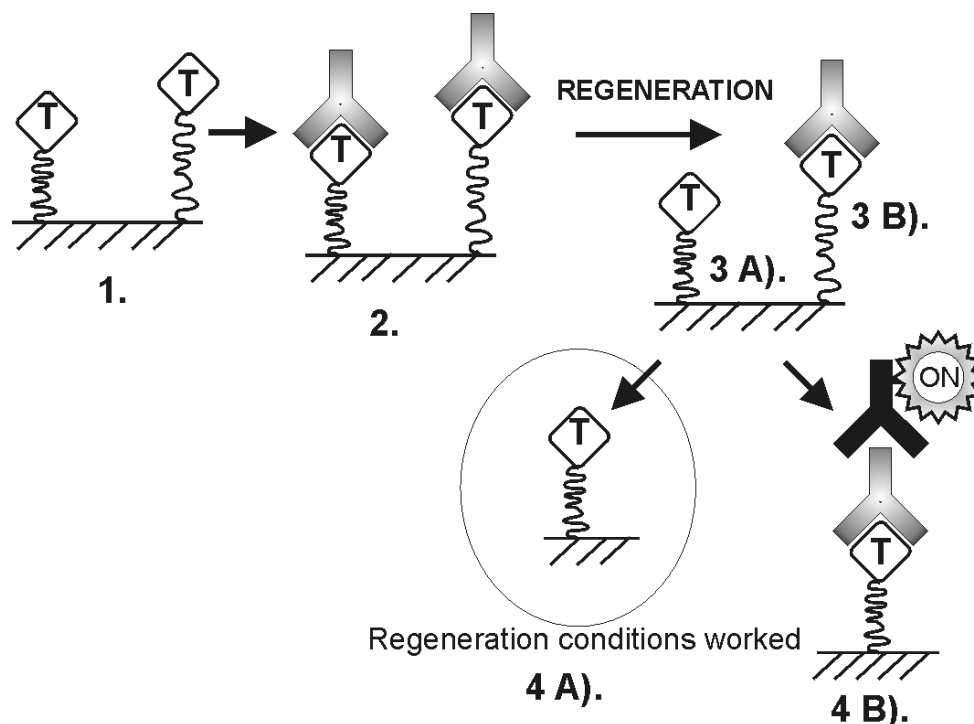


Figure 28 Assay 2: non-competitive binding assay, modified format. Regeneration takes place before adding the HRP-marked, secondary antibody. Different outcomes depending on regeneration efficiency. Every assay step is followed by a neutral washing step.

In the modified assay format (Assay 2), the interaction to be examined is the binding of the primary antibody to the immobilized receptor. Removal of the primary antibody is attempted before the secondary antibody is added, in order to avoid damage to the HRP when too harsh regeneration conditions are used. If the primary antibody was not entirely removed in the regeneration step, chemiluminescence will nevertheless be recorded upon addition of the chemiluminescent substrate, after the secondary, HRP-marked antibody has been supplemented to the system. On the other hand, signal absence unequivocally points to a successful recovery of the surface binding activity. Even if the regeneration step is insufficient to disrupt the binding of the primary antibody to the secondary, HRP-marked antibody, it should be kept in mind that the goal is to remove the *antibody complex*, whose interaction is ultimately determined by the binding affinity of the primary antibody to the immobilized receptor itself. The effect of 6 different regeneration solutions was tested under assay format 2 and Table 4 summarizes the outcomes obtained.

Table 4 Antibody removal efficiency of different regeneration buffers. Results are applicable to the two immobilized analytes (OTA-peptide and AFB₂-CMO-peptide).

Solution No.	Components	Outcome Assay 1 (original)	Outcome Assay 2 (modified)
1	100 mM glycine 100 mM NaCl 0.1% SDS (w/v) pH 3.0	absence of CL	absence of CL (sufficient removal of antibody)
2	same as solution 1; pH 2.0	absence of CL	absence of CL (sufficient removal of antibody)
3	100 mM glycine 100 mM NaCl 0.2 % Tween (v/v) pH 2.0	absence of CL	absence of CL (sufficient removal of antibody)
4	100 mM TRIS 100 mM NaCl 0.1% SDS (w/v) pH 8.5	presence of CL (regeneration conditions insufficient)	N/A
5	100 mM glycine 100 mM NaCl 1% DMSO (v/v) 0.1% SDS (w/v)	absence of CL	absence of CL (sufficient removal of antibody)
6	PBS:MeOH, 1:1 solution (v/v)	absence of CL	presence of CL (regeneration conditions insufficient)

Adding DMSO to the regeneration buffer has been proven a suitable choice for the removal of small analytes from immobilized specific monoclonal antibodies.^[155] Glycine buffer at low pH (between 1.5 and 3.0) has also been shown to deliver good efficiencies, for example in the desorption of parathion from polyclonal antibodies^[156], and gave good results here, as well. Other commonly used regeneration solutions include chaotropic agents such as concentrated guanidine hydrochloride (6 M, pH 2.0, 50 mM glycine)^[71], lower pH (30 mM HCl in water)^[157], or other organic solvents in basic solution (20% ACN in NaOH).^[158] In this case, solution No. 1 (see table 4) was preferred for further assays because it had also shown suitability for other applications,^[148] because of its milder pH in comparison to other buffers tested, and because of its relative ease in preparation and use. Although proven to deliver good results in the removal of antibodies from an immobilized analyte, solutions with a pH > 8 or < 2 could cause hydrolysis in the Si-O bond and cleave the immobilized receptors from the sensor surface.^[159] Concentrated guanidine hydrochloride (6 M), such as that used by Ngundi et al. for the regeneration of an OTA microchip immunoassay,^[71] was not deemed a

suitable choice in this case because due to the high salt concentration, it could cause obstruction of the tubing in the MCR 3.

3.1.6 Signal Decrease with Surface Regeneration

The choice of an adequate regeneration buffer was followed by system assessment for signal variation along multiple assay cycles. This type of experiment consists in sequential, non-competitive binding and regeneration assays. In this case, the original assay depicted in figure 27 was carried out: the sequential steps were 1) pumping a mixture of the primary antibodies to the measuring flow cell (anti-OTA and anti-AFB), 2) pumping the secondary, HRP-coupled anti-mouse antibody and detecting this maximum CL signal with the CCD camera, and 3) regenerating the glass chip surface. At the end of these steps, the measuring sequence was started all over again for 27 remaining times. Washing of the sensor surface was always carried out in between steps. Figure 29 shows the absolute and relative CL signal intensity (right and left of the “y” axis respectively), recorded for both the AFB₂-CMO-peptide and the OTA-peptide-I (one lysine in the peptide linker).

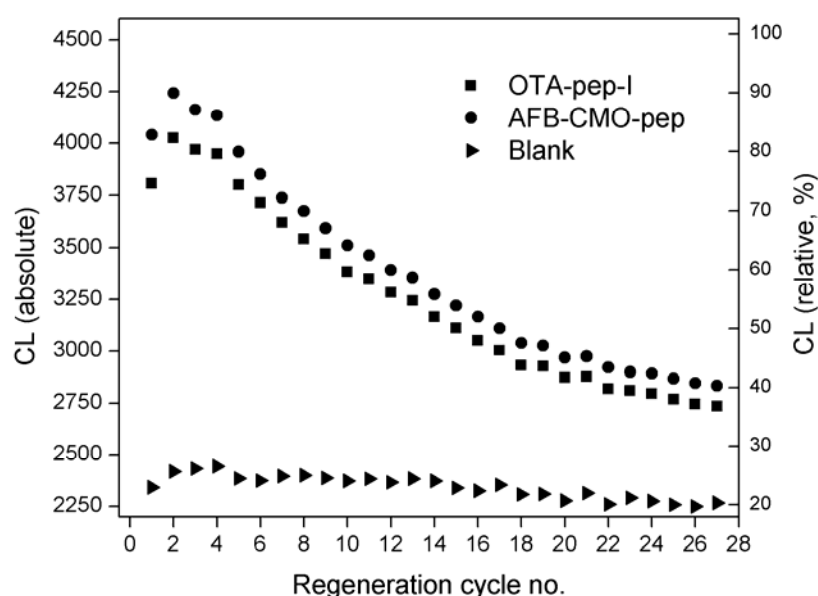


Figure 29 Non-competitive, regeneration assay. Signal intensity loss along 28 regeneration cycles for OTA-peptide-I and for AFB₂-CMO-peptide. Individual points average of 6 spot intensities. Standard deviation for each determination was always within 6 – 2% of signal intensity (not depicted since it overlaps for the two immobilized molecules). Absolute background signal intensity: 1690 ± 60 (0% relative CL). Spotted blank solution signal (buffer) also depicted.

For both immobilized receptors, signal intensity constantly decreased with increasing number of regeneration cycles. Although sufficient surface regeneration was achieved with the chosen regeneration solution as demonstrated in the previous section, signal decrease for both analytes still took place after multiple cycles of non-competitive binding. The cause of signal loss must lie elsewhere, as it was not due to insufficient analyte removal; it was suspected that a permanent change in the surface prevents the access of the free antibodies to the binding sites of the immobilized receptor. This effect increases with increasing number of sensor regeneration steps. The literature attributes PEG's "shielding" effect to its ability of forming dense layers with high exclusion volume, to the thick and highly organized water interface between the PEG layer and the solution, and to the high entropic cost of adhering proteins to the PEG chains.^[85, 100, 160] Therefore, it would be reasonable to suppose that adhering proteins were causing this type of sensor behaviour. In the regeneration experiments, the only source of protein was the running buffer, a solution prepared from 0.5% casein (w/v) in PBS. This solution is used along the assay before the antibodies are pumped to the flow cell, in order to further enhance the protecting effect of the PEG layer. Nevertheless, casein in the running buffer could not be altogether avoided. It was noticed that background signal was greatly increased when no casein was used, making it difficult to identify and analyze the chemiluminescent spots. Therefore, it was not possible to test the effect on signal intensity along successive regeneration cycles without the influence of the casein solution. On the other hand, it has also been reported that amino-PEG coatings are stable in 50 mM sodium phosphate solutions at pH 4 – 9 for at least 3 weeks^[161]. In general, the PEG-derivatized surfaces described in the literature have been tested after an incubation period in water solution, since this is usually a part of the manufacturing process. Consequently, pre-incubating the derivatized glass chips overnight in PBS buffer before performing the regeneration experiments was carried out to see if the signal would improve. Figure 30 shows the results obtained for the OTA-peptides and the AFB₂-CMO-peptide (background included).

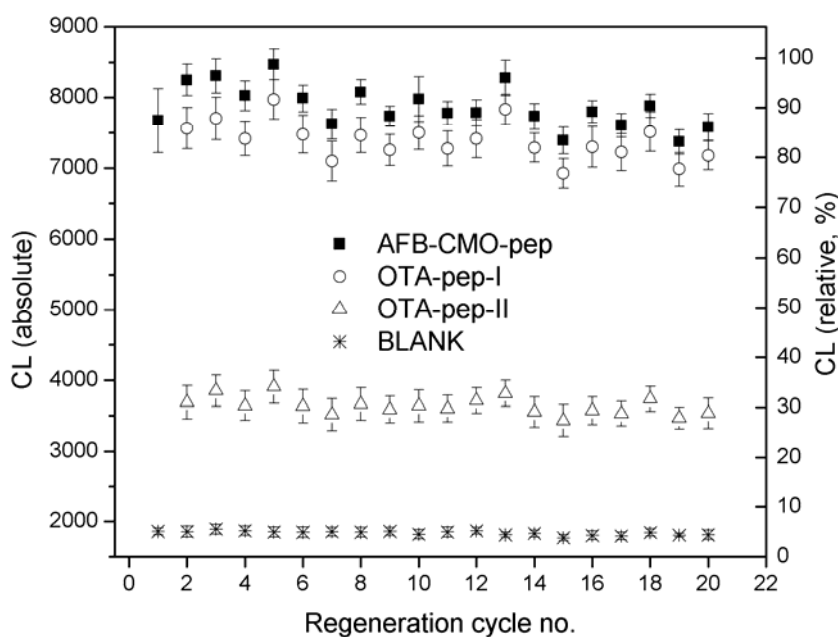


Figure 30 Non-competitive, regeneration assay. Chip incubated overnight in PBS. Signal intensity along 20 regeneration cycles for OTA-peptide-I (one lysine), OTA-peptide-II (two lysines) and AFB₂-CMO-peptide. Individual points average of 5 spot intensities. Absolute background signal intensity: 1690 ± 60 (0% relative CL). Spotted blank solution signal (buffer) also depicted.

Clearly, incubating the biochip in solution before measuring considerably improves its regeneration properties and its reusability. The reason for this could be that the PEG interface slowly hydrates, which increases its resistance towards unspecific protein adsorption. Nevertheless, the CL signal still showed a decrease after regeneration cycle no. 21, especially the signal for AFB₂-CMO-peptide. The reason for this is not clear, but the effect was evident in more than one experiment and the cycle number at which the signal started going down was slightly variable. Overall, incubation of the chip in solution before use was considered a suitable option for improving signal stability of the biosensor surface.

Figure 30 also shows the signal intensity associated to the OTA-peptide-II receptor that presents two lysine residues as part of its linker structure (see figure 25). It was hypothesized that an additional lysine would cause the receptor to bind more strongly to the derivatized glass surface. At an equimolar spotted concentration, the CL signal of the OTA-peptide-II receptor was nevertheless weaker than for the OTA-peptide-I in an experiment carried out on the same chip surface. Regardless of its absolute value, the signal intensity stays constant for all receptors, which excludes the possibility of the receptors being washed away and points towards a stable, covalent binding between the receptors and the chemically modified glass

surface of the biochip. Nevertheless, the weaker signal from the receptor modified with two lysines, which can be assumed to bind by more than one functional group in comparison to its single-functionalized counterpart to the chemically derivatized glass surface, could be a consequence of how the peptide linker structure folds upon itself, negatively influencing antibody accessibility, or of its particular interaction with the underlying PEG surface.

A more detailed comparison between the absolute CL intensities in figure 29 and figure 30 also shows differences in experiments carried out independently: for OTA-peptide-I in figure 29 the maximum value is 4026, whereas in figure 30, the same receptor gives an average signal of 7387, an signal 94% higher. In the case of AFB₂-CMO-peptide, the signal is 85% higher as well. This disparity in signal intensity could also be a consequence of the better solvated PEG chains, but could also have its source in the differences in composition of the glass slides used for immobilization, effect that has been recently reported in the literature.^[90]

3.1.7 Additional Surface Modifications: Star-PEG

The new coating material “Star-PEG” was also tested for receptor immobilization and CL signal consistency in a non-competitive regeneration assay format, with the objective of comparing to the surface modified with the linear PEG chains. For this purpose, the star-PEG pre-polymers were reacted to the end amino-groups of amino-PEGylated glass chips, and the slides were subsequently spotted with the receptors OTA-peptide-I and AFB₂-CMO-peptide. This time, chip incubation was carried out in demineralized water instead of PBS.^a Figures 31 and 32 show the comparison between the two modified surfaces:

^a Suggestion of Dr. Jürgen Groll, who kindly donated the star-PEG pre-polymers.

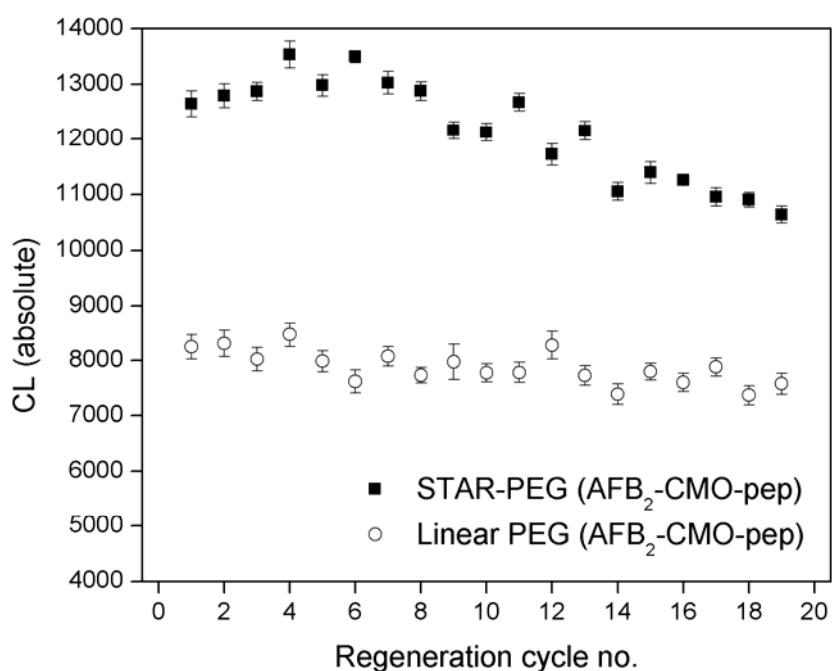


Figure 31 Non-competitive regeneration assay. Comparison of two active surfaces with protein-repelling properties for the immobilization of AFB₂-CMO-peptide: linear-PEG (epoxy-terminated) and star-PEG (isocyanate terminated).

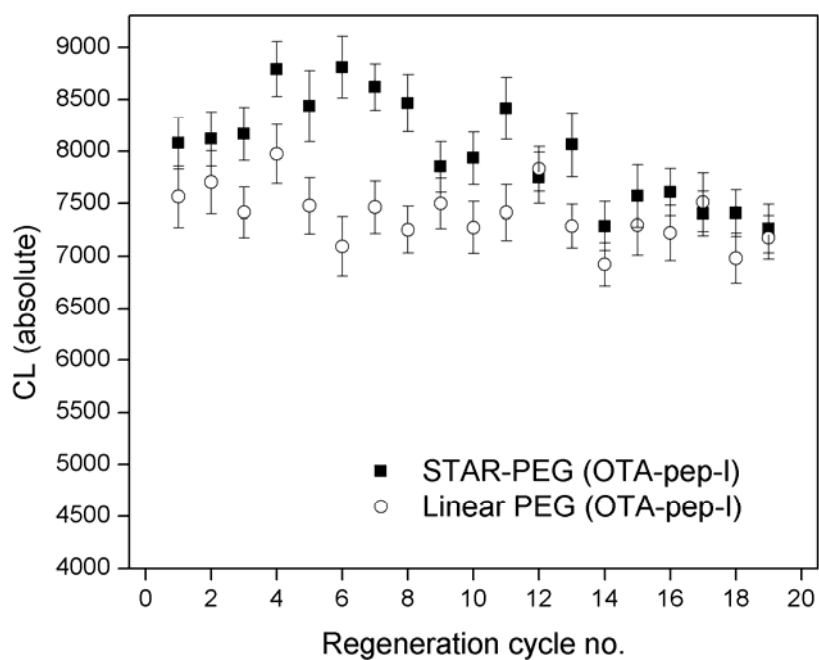


Figure 32 Non-competitive regeneration assay. Comparison of two active surfaces with protein-repelling properties for the immobilization of OTA-peptide-I: linear-PEG (epoxy-terminated) and star-PEG (isocyanate terminated).

In the case of the AFB₂-CMO-peptide receptor, it is clear that the signal is more stable in the linear PEG-coated sensor. Although the signal is approx. 50% higher for the star-PEG immobilized receptor in the first regeneration cycles, a decreasing tendency is clearly noticeable after regeneration cycle no. 9. The coupling density (e.g. the density of the isocyanate groups available for receptor immobilization) might be higher in the star-PEG coated sensor, but this does not necessarily mean a more stable signal. The case of the OTA-peptide-I is not so straight-forward. The absolute signal intensities are comparable in both surfaces. Nevertheless, the signal distribution along the sequential regeneration cycles seems to be broader for the star-PEG surface. The details of the analysis are summarized in table 5, as follows.

Table 5 Statistical parameters of CL signals for OTA-peptide-I immobilized on two different surfaces. All signal intensities (5 individual spots per regeneration cycle) were taken into consideration.

(n = 95)	Star-PEG	Linear PEG
CL average	8000	7387
St. Dev.	541	348
St. Dev., %	6.8%	4.7%
Dispersion range (max. CL - min. CL)	9140 – 7013	8291 – 6784

Since the CL signal is stable for both spotted receptors on the linear-PEG surface, this particular surface was chosen for further assay development.

3.1.8 Instrumentation: Flow Cell Characteristics

The flow cell construction of the MCR 3 consists of two independent chambers, originally integrated to carry out individual steps of two different assays simultaneously with the objective of reducing the analysis time. The present flow cell design was conceived so that while the upper chamber is being used for measurement, the lower chamber can be regenerated and vice versa. This assumption presupposes that the individual measurements carried out in the two chambers are equivalent, or more clearly stated, that the CL signal intensity should be the same for two identical assays. In order to test this hypothesis, an amino-PEG modified glass chip was activated with end epoxy functional groups and completely derivatized with the receptor biotin-peptide. The resulting surface was then

exposed to a solution of the conjugate streptavidin-HRP, followed by the luminol / hydrogen peroxide mixture, and CL was induced to produce a full-coverage signal. Because the amount of OTA-peptide-I receptor was very limited, it was not possible to carry out this experiment with our immobilized molecule, the OTA-peptide-I. Nevertheless, the biotin receptor used instead binds to the glass chip surface with the same peptide linker and it was considered adequate for testing total coverage of the surface. Figure 33 shows a picture of the CL signal distributed along the upper chamber and the actual chip magnitudes for orientation. Worthy of attention is the zone where receptor immobilization takes place, a rectangle with an area of 96 mm^2 .

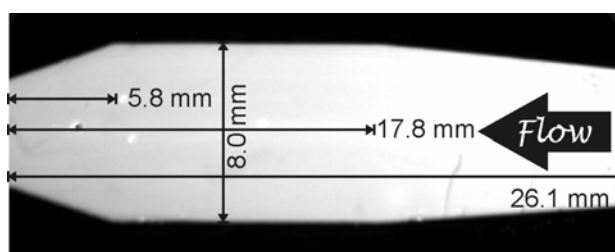


Figure 33 Chamber dimensions in the flow cell (to scale, upper chamber). The spotting area enclosed along $5.8 \text{ mm} \leq x \leq 17.8 \text{ mm}$ and $0 \leq y \leq 8.0 \text{ mm}$ (96 mm^2).

The following plots (figures 34 and 35) give a visual representation of the signal intensity distribution along the two chambers for comparison. The profiles in the horizontal and vertical axes are representative of the CL signal distribution along the spotting area.

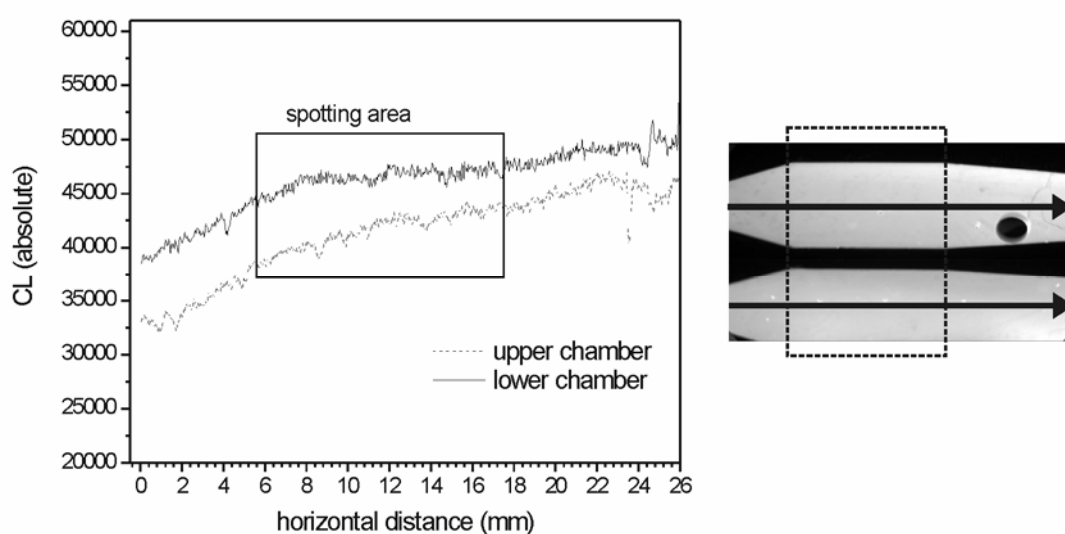


Figure 34 Comparison of the two flow cell chambers. Signal intensity profile of flow cell along the horizontal axis. Maximum measurable signal: 65 000. Area suitable for spotting indicated inside the square.

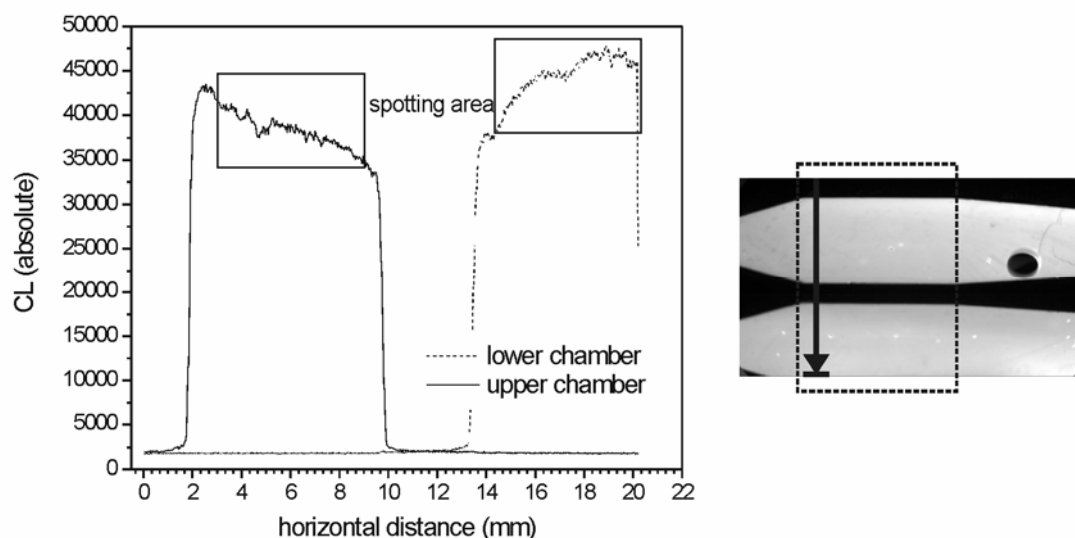


Figure 35 Comparison of the two flow cell chambers. Signal intensity profile of flow cell along the vertical axis. Maximum measurable signal: 65 000. Area suitable for spotting indicated inside the square.

As can be seen from the figures above, the absolute signal intensity in the upper chamber of the flow cell is in general lower than in the lower chamber. Also, the signal intensity distribution along the surface of each chamber is not constant. This effect can be appreciated with even more detail in the following 3-D rendering of the full measuring area from both chambers.

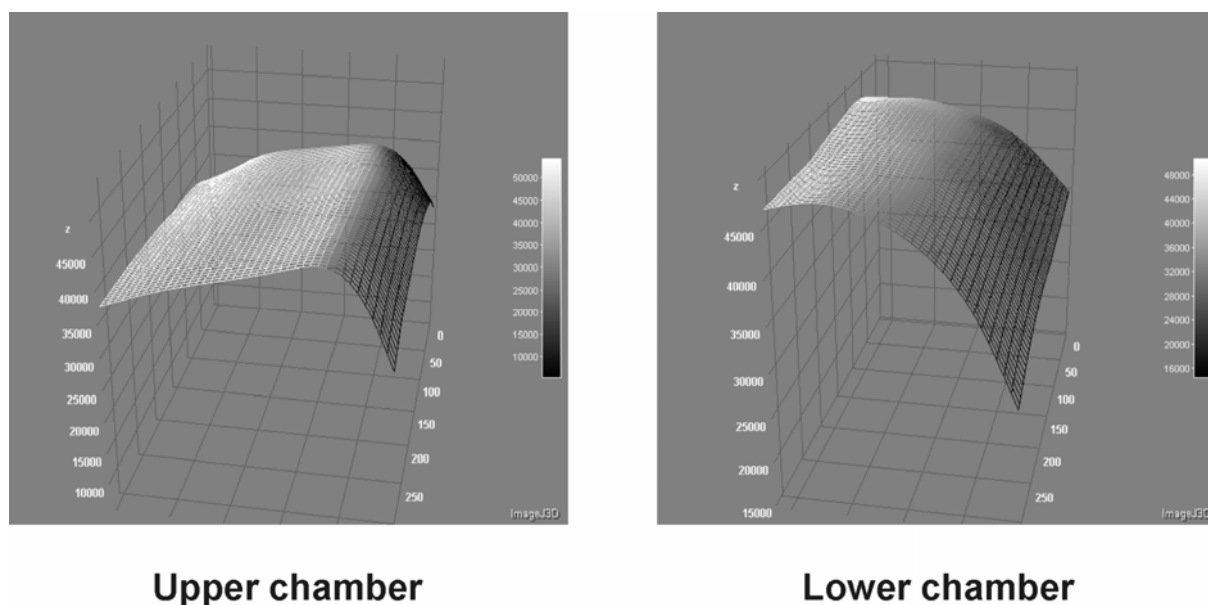


Figure 36 Absolute signal intensity for upper and lower chamber surface area, 3-D representation.

Because the signal intensity varies depending on the location of the immobilized receptor along the measuring chambers, it was judged important to always immobilize the analytes on the same physical spot. Also, due to signal differences in the two chambers, it was considered that using both chambers for performing measurements in the same calibration sequence would not provide reliable results, i.e. calibration should be carried out in one single measuring chamber and the subsequent measurement of unknowns should also be performed in the same chamber used for calibration. This result differs from the statement of Cervino ^[153], who mentions that the two measuring chambers could potentially be used in an alternating manner, in one set of measurements. It must be kept in mind, though, that this assumption was made for a prototype. The results shown here should of course be considered in further developments of the MCR 3. The unequal signal distribution along the two chambers was discussed with the company GWK. Nevertheless, the CCD camera holder was fixed physically to the MCR 3 and made any adjustment difficult. The shape of the flow cell could also be a factor in the unequal signal distribution along one chamber and should therefore be optimized in upcoming instrumental development.

An alternative function for one of the chambers was nonetheless suggested in order to minimize assay time. This consists in using one chamber to extensively rinse the fluidic path from P2 to the flow cell at the same time as regeneration is taking place in the parallel (measuring) chamber. It has been shown that in order to remove analyte residues in subsequent assay cycles the tubing leading to the flow cell needs to be systematically cleaned, otherwise carry-over occurs.^[162] The time used for regeneration can therefore be efficiently utilized for simultaneous instrument rinsing.

3.1.9 Instrumentation: Optimized Assay Conditions

The programming of the assay sequence was also accordingly optimized in order to avoid carry-over of the substances within assay cycles, and to minimize the measuring time needed for one complete cycle.^b The sequence of the optimized assay is summarized in table 6 with the time and the amount of reagents required for each step.

^b For complete programming sequence see the experimental section in this work

Table 6 MCR 3 steps in assay version optimized for flow-immunoassay

Step	Volume	Time
“PRIMING” Load sample	800 μ L sample	46 s
“MIXING” Mix sample with primary antibody	700 μ L sample 500 μ L primary antibody 1000 μ L casein	18 s
“LOOP INCUBATION” Incubate AB mixture, pump it to flow cell, wash tubing and wash flow cell	2000 μ L of store 1000 μ L of rinse, 4000 μ L of casein	86 s
“TRACKING” Add secondary antibody)	1000 μ L of secondary antibody	83 s
“WASHING” Wash tubing and flow cell	2000 μ L of casein	10 s
“SUBSTRATE” Add substrate solution	400 μ L of substrate	6 s
“RECORDING” Detect with CCD	N/A	60 s
“REGENERATION” Wash tubing and regenerate chip surface	8500 μ L of rinse 8500 μ L of store 3000 μ L of casein 3960 μ L regeneration	346 s
	Solution total:	10.0 mL casein 10.5 mL store 9.5 mL rinse 0.4 mL substrate 1.0 mL primary AB 0.5 mL secondary AB 3.96 mL regeneration
	Time total:	11 min (655 s)

From table 6, it is worth noticing that although the final washing and regeneration steps run parallel to each other, they take up more than 50% of the total assay time. It is therefore legitimate to ask whether the long washing/regeneration sequence can be shortened. However, the extensive washing step is crucial because a typical assay battery consisting of calibration and subsequent sample measurement uses calibrant solutions in a concentration range spanning roughly 5 orders of magnitude (generally within $0.001\text{-}100 \mu\text{g L}^{-1}$). The 20 mL of different washing solutions used for flushing the complete tubing is 11 times the total volume

of the path that starts at the sample input and ends in the waste. This measure was adapted from a common practice in HPLC procedures which suggests column flushing with at least 10 column volumes within measurements, in order to avoid cross contamination and carry-over.^[159] Washing of the tubing with this large amount of solution is necessary to guarantee the removal of all substances that could cause interference in the following assays. By measuring enzymatic activity of glucose oxidase on the out-flow of the MCR 3, Wutz was able to demonstrate that thorough rinsing of the tubing is an important factor to avoid carry-over in MCR 3-based procedures.^[162] In order to reduce the flushing time, one option not explored in this work due to instrument limitations is the reduction of the dead volume contributed by the tubing , for example by bringing all instrument components (pumps and valves) closer to each other.

3.2 MCR 3-Based OTA Determination in Green Coffee

3.2.1 HPLC Testing of Blank Green Coffee

The development of immunoanalytical tests to be applied in food and raw stuff analysis requires the detailed consideration of the particular matrix effect on the specific antibody or antibodies chosen for the methods. Therefore and for calibration purposes, a blank sample as closely related to the unknown has to be found, preferably without contaminant traces. Contamination of the blank sample should be assessed by an orthogonal method to the method being developed, one that uses a different measuring principle. HPLC-based techniques are generally a good choice for this purpose. Such was the method of choice to determine whether store-bought green coffee beans were indeed free of OTA and ideal for further method implementation. Once that the absence of OTA contamination in the green coffee beans was demonstrated, these were further used for spiking in the immunoanalytical methods (both microtiter plate and MCR 3-based).

Two different HPLC based methods for the detection of OTA in green coffee were examined. Method 1 was based on the DIN EN 14132 (2003)^[33] and method 2 was based on a procedure previously reported in the literature.^[163] LODs for both methods were calculated according to the definition given by the IUPAC for spectrochemical analysis, also adequate for LC.^[164]

$$LOD = \frac{3s_B}{S}$$

where s_B is the standard deviation of the blank signal

and S is the linear slope of the calibration curve

The LOQs associated to each method were estimated as the concentration necessary to produce a signal ten times larger than the signal-to-noise ratio of a blank solution injected:

$$S/N = \frac{A}{a} \qquad LOQ = \frac{10S/N - b}{S}$$

where S/N is the signal-to-noise ratio,

A is the area under the peak specific to the analyte of interest,

a is the absolute value of the largest noise fluctuation of a blank solution,

b is the “y” intercept of the calibration curve,

and S is the linear slope of the calibration curve.

The analytical parameters associated to each tested method are summarized in table 7:

Table 7 Comparison of two chromatographic methods for the determination of OTA in green coffee extract.

	Method 1	Method 2
separation type	isocratic	isocratic
detection	FD 330 nm ex 470 nm em	FD 330 nm ex 460 nm em
mobile phase	45% acetate buffer 55% ACN	51% water 48% ACN 1% acetic acid (V/V)
flow rate	1 mL min ⁻¹	1 mL min ⁻¹
Injection volume	20 µL	100 µL
OTA retention time	14.3 min	13.3 min (approx.)
running time	20 min	20 min
linear range	0.2 – 25.0 µg kg ⁻¹	0.3 – 30 µg kg ⁻¹
LOD	0.08 µg kg ⁻¹	0.07 µg kg ⁻¹
LOQ	0.20 µg kg ⁻¹	0.30 µg kg ⁻¹
column temperature	27 °C	45 °C
remarks	Standards prepared in mobile phase	Standards prepared in MeOH

As can be noticed from table 7, the two standardized methods tested are fairly comparable in their LODs and their LOQ, showing no significant differences. The methodologies differ slightly in the injection volume chosen, the mobile phase composition, the column temperature and the sample injection solvent. Regarding method differences it must be mentioned that generally, larger injection volumes afford better precision, i.e. reproducibility, in trace analysis, but in this case we were not aware of such an effect, even when using five times less calibration solution in method 1 (20 µL in method 1 vs. 100 µL in method 2). On

the other hand, mobile phase composition did show a significant influence in the assay performance. In the case of method 2, changes in the retention time of OTA were noticed for three independent determinations of the calibration curve. This solvent composition in HPLC-based OTA analysis was originally reported by Baumann and Zimmerli^[9] and optimized further for roasted coffee by Pittet, who modified the method by buffering with acetate instead of using an ACN acetic acid mixture.^[163] The effect described by Pittet, namely better reproducibility in the OTA retention times when using a buffered mobile phase, was also recognized in our method comparison. The pH of the aqueous component in the mobile phase is known for exerting a dramatic effect on the reproducibility of ionizable analytes in trace analysis, as is the case with OTA. Also worthy of attention is the fact that the composition of the injection solvent used in method 2 is different from that of the mobile phase. The reason for this is that MeOH, a weaker solvent than ACN in RP-HPLC, improves analyte retention to the column according to theory, although we were not aware of significant differences when injection took place in the same mobile phase instead. Finally, constant column temperature was achieved in both methods with the aid of a column oven. This should be at least 5 °C above room temperature to allow for reproducible retention times. Theory states that increasing column temperature generally reduces retention time and can have some effects on selectivity. In this case, as testing of the methods was only carried out with standard calibrating solutions, selectivity was not evaluated. Nevertheless, a significant difference of approximately one minute in OTA retention time was noticed when the column temperature was increased from 27 to 45 °C (14.3 vs. 13.3 min).

The attributes of the two methods were weighed against each other, but the decisive factor was the more reproducible OTA retention time in method 1. This feature was deemed more important as the reduction in retention time afforded by method 2. Therefore, method 1 was further used for independent determination of OTA in green coffee.

The two calibration curves corresponding to the methods tested are presented as follows.

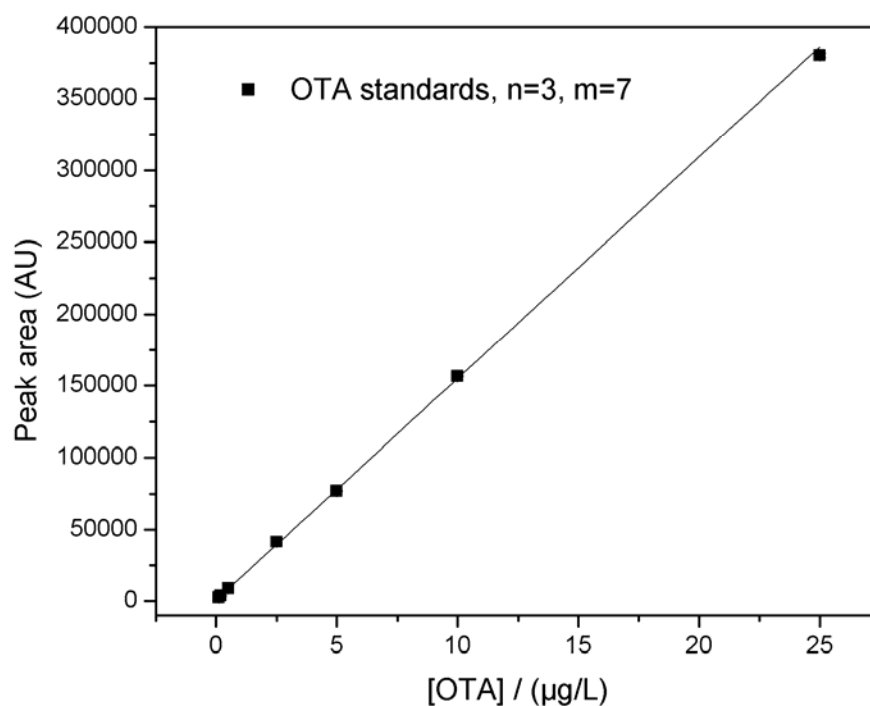


Figure 37 Calibration curve for ochratoxin A in acetate buffer/ACN mobile phase.

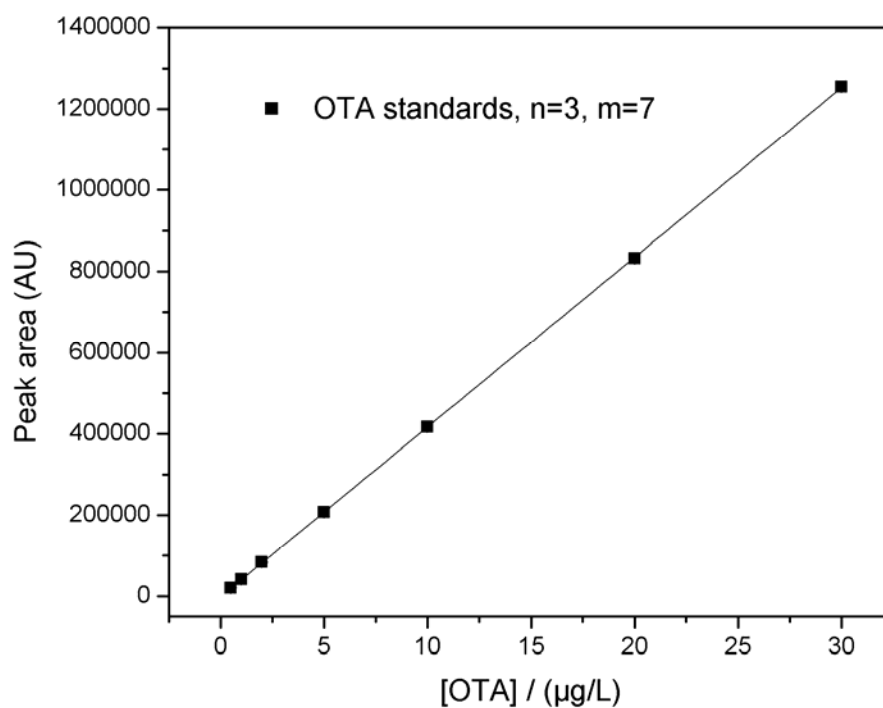


Figure 38 Calibration curve for ochratoxin A in acetic acid/ACN mobile phase.

The OTA content of a store-bought green coffee sample consisting of the whole raw coffee beans was further determined with the HPLC procedure described in method 1. For this purpose, previous immunoaffinity chromatography clean-up and enrichment of the extracted sample was carried out preceding HPLC determination. The sample was ground to a fine powder and extracted for 30 min under magnetic stirring with a mixture of MeOH/aqueous sodium hydrogen carbonate (50:50, v/v; NaHCO₃ 3% w/v). Although some methods employ fast blending of the slurry with a homogenizer, we opted for longer, gentler stirring because this is the standardized procedure reported in the DIN.^[33] Before application of the filtered extract to the immunoaffinity column, care has to be taken to dilute the sample with PBS for two reasons: first, the high MeOH content of the original raw extract could potentially damage the immobilized antibodies on the column, and second, OTA binding to the antibodies is optimal at physiological pH (the pH of extraction being 8.4). Elution, on the other hand, takes place at 100% MeOH and is reported to be quantitative when the solvent is left in contact with the column for longer periods of time (3 min), such as those recommended by most column manufacturers.^[163, 165] HPLC analysis of the cleaned-up extract showed no detectable trace of OTA, therefore guaranteeing the use of this coffee lot for further immunoaffinity-based analysis.

3.2.2 Comparison of Four Available Anti-OTA Antibodies

The selection of an adequate antibody against OTA for further use in the MCR 3 method development was carried out by applying a modified version of the standard strategy used at the IWC to screen for specific monoclonal antibodies in cell supernatants.^[166] An assay format consisting of a 96-well MTP indirect competitive ELISA (ic-ELISA) was chosen because of its effectiveness in simultaneously estimating the measurable OTA concentration ranges of four different anti-OTA antibodies and their respective IC₅₀ parameters. These assays were first carried out in buffer solution (PBS) to choose the antibody with the lowest IC₅₀ value, and then the chosen antibody was further tested in the presence of blank green coffee matrix.

Three of the antibodies tested were obtained from two commercial sources (LCTech, one available clone, and Soft Flow, clones 5G9 and 5E2) and one antibody was received as a donation from Prof. Erwin Märtlbauer (LMU). First, non-competitive, “checkerboard”-type ELISA plates were run for each antibody in order to determine the adequate starting values for the coating conjugate and the antibody concentrations to be further used under competitive

conditions. Such a “checkerboard” assay decreases the coating conjugate concentration and the antibody along the horizontal and the vertical directions of the microtiter plate. The intensity of the signal can be judged to obtain an optimal starting antibody concentration in a subsequent competitive immunoassay (results not shown).

Next, a so-called 2-D competitive assay was carried out.^[153] In this format, the microtiter plate is divided into column sections, each of them with independent concentrations of coating conjugate and detection antibody, and the competing analyte (in this case OTA) is given in increasing concentrations along the plate rows. Two further negative controls are also evaluated: one consisting of coated wells to which no specific antibody has been added, and the other consisting of untreated wells to which the specific antibody and the competing analyte have been added. Both of these control rows are to be supplemented with the competing analyte and should afford as little signal as possible, in order for the assay to be valid and to guarantee that no cross-contamination has taken place. The positive control is the first well in each row, to which no competing analyte has been added.

The reagent distribution in 2-D competitive assay used to determine the characteristics of the four different antibodies tested is presented in table 8:

Table 8 96-well plate configuration for the estimation of the anti-OTA antibodies’ binding properties. Two types of negative controls are also performed in plate rows 11 and 12 (not included).

Column	1	2	3	4	5	6	7	8	9	10
Dilution of coating conjugate (haptene)	1:x	1:nx	1:x	1:nx	1:n ² x	1:nx	1:n ² x	1:n ³ x	1:n ² x	1:n ³ x
Dilution of primary AB	1:y	1:y	1:my	1:my	1:my	1:m ² y	1:m ² y	1:m ² y	1:m ³ y	1:m ³ y
Row	A	B	C	D	E	F	G	H		
[OTA]µg L ⁻¹	0	p	pz	pz ²	pz ³	pz ⁴	pz ⁵	pz ⁶		

For the specific anti-OTA assays, values of “n” and “x” were 10 000 and 2. Values of “m” and “y” were either 5000 or 10 000, and 2. For OTA concentrations, “p” (not to be confused with the fitting parameter p of the logistic equation) was 10⁴ and “z” was 10.

The most useful information provided by this type of experiment is the competing analyte concentration at half maximum signal, or the IC₅₀ value. The maximum sensitivity in an

antibody series correlates well with the lowest possible IC_{50} value. In choosing assay parameters for an ic-ELISA (indirect competitive ELISA), there are two primary ways for improving the sensitivity, not altogether independent from each other: 1) decreasing the amount of hapten used for coating the plates, and 2) decreasing the concentration of added reporter (the specific antibody), so that appreciable reduction in the signal occurs at a lower concentration of the competing analyte.^[167, 168] In theory, infinite reporter antibody dilution should afford an IC_{50} value very close to the true affinity of the antibody. Also, it is important to notice that the competing analyte concentrations should be spaced evenly along the concentration range because in this way the systematic error associated to each concentration is constant, and because a constant dilution factor guarantees ease in the preparation.^[169] Figure 39 presents the plot of one of the examined antibodies (Märtlbauer's), at 10 different coating and antibody concentrations in a 2-D type titration. It can be seen that as the coating conjugate and antibody concentrations decrease, the IC_{50} value also moves toward lower values. The maximum signal intensity also decreases with these two parameters, so that the optimum set of conditions will nevertheless be constrained by an adequate signal response (e.g. sufficient measurable intensity). The same plate format was used for the other remaining three antibodies affording similar plots, but with significantly lower IC_{50} values.

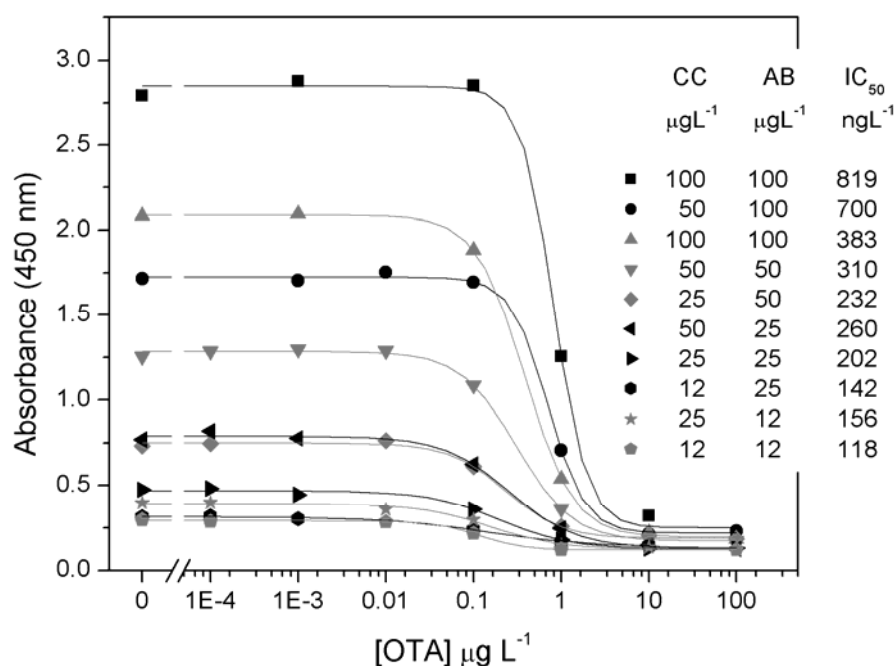


Figure 39 ELISA calibration curves for 10 sets of assay conditions to determine limiting IC_{50} value for the Märtlbauer anti-OTA antibody. Each experimental point consists of a single determination. OTA-BSA coating conjugate was used. CC = coating conjugate; AB = specific antibody.

At limiting dilutions of $25 \mu\text{g L}^{-1}$ of coating conjugate and either 50 or $25 \mu\text{g L}^{-1}$ of antibody, the three commercially available antibodies showed comparable IC_{50} values between 54 and 73 ng OTA L^{-1} , whereas the donated antibody showed an IC_{50} value three times larger. Selected values are presented in table 9. Therefore, it was concluded that the three commercial antibodies were comparable in their affinity to OTA, and the remaining antibody had a lower affinity. The antibody clone 5G9 was chosen for further optimization because of its guaranteed commercial availability.

Table 9 Selected values of limiting IC_{50} for four different anti-OTA antibodies at limiting hapten and reporter antibody concentrations. CC = coating conjugate; AB = specific antibody.

antibody	CC ($\mu\text{g L}^{-1}$)	AB ($\mu\text{g L}^{-1}$)	IC_{50} (ng L^{-1})
Märtlbauer	50	50	310
	25	25	202
	12.5	25	142
	12.5	12.5	118
LCTech	50	100	64
	25	100	59
	25	25	65
	12.5	25	63
SoftFlow-5G9	50	50	151
	50	25	63
	25	25	69
	25	12.5	61
SoftFlow-5E2	25	100	126
	50	50	73
	25	50	71
	12.5	50	54

3.2.3 Optimization of Assay Conditions with Coffee Extract

Conditions for ic-ELISA assays were also optimized for green coffee. The purpose of this experiment was to explore viable assay conditions as a starting point for the MCR 3-based flow assay and to provide an independent method of comparison for the results obtained. The

microtiter plate-based optimization procedure in this case was very similar to the one used previously for determining the efficiency of the four available anti-OTA antibodies. It is important to point out that due to unspecific matrix effects of the raw coffee extract, the working concentrations for the sensing antibody turned out to be much higher than in the buffer-based assays. To produce measurable absorption signals, the coffee assays worked better when a concentration of $200 \mu\text{g L}^{-1}$ of the primary (the detection) antibody was used, four times more as in the assays conducted in PBS, reported in the previous section. Additionally, the optimized coating conjugate concentration was $50 \mu\text{g L}^{-1}$. After extraction, the coffee is to be processed as soon as possible, but if stored undiluted (at 50% MeOH v/v), it could be kept overnight and tightly closed at $6 \text{ }^\circ\text{C}$, to be analyzed after undergoing adequate dilution the following day. The final sample-to-solution ratio was 1 g green coffee to 26.66 mL solution, at 10% MeOH (v/v). The IC_{50} value of the ic-ELISA of $\sim 0.2 \mu\text{g L}^{-1}$ corresponds to $5.3 \mu\text{g}$ OTA per kg coffee, which is within the EU maximum permissible contamination value of $5 \mu\text{g}$ OTA per kg roasted coffee, or $10 \mu\text{g}$ OTA per kg soluble (instant) coffee, as a point of comparison (see table 2). Further dilution of the extract would therefore not be recommended because by doing so, the EU limits would not be reached, even if it would mean diminishing the matrix effects. Since the methanol component of the extract is detrimental to the antibodies, incubation time for competition was also kept to a maximum of 30 min. The following table shows a summary of the plate parameters obtained for the 2-D titration in green coffee extract:

Table 10 2-D indirect competitive ELISA titration of OTA in green coffee extract. CC = coating conjugate; AB = specific antibody.

	CC ($\mu\text{g L}^{-1}$):	100	CC ($\mu\text{g L}^{-1}$):	50	CC ($\mu\text{g L}^{-1}$):	100	CC ($\mu\text{g L}^{-1}$):	50	CC ($\mu\text{g L}^{-1}$):	50
	AB ($\mu\text{g L}^{-1}$):	400	AB ($\mu\text{g L}^{-1}$):	400	AB ($\mu\text{g L}^{-1}$):	200	AB ($\mu\text{g L}^{-1}$):	200	AB ($\mu\text{g L}^{-1}$):	100
para- meter	value	\pm	value	\pm	value	\pm	value	\pm	value	\pm
A1	1.575	0.028	0.912	0.029	0.939	0.015	0.510	0.016	0.311	0.004
A2	0.106	0.049	0.108	0.059	0.071	0.026	0.106	0.032	0.106	0.005
IC_{50} (OTA, $\mu\text{g L}^{-1}$)	0.487	0.058	0.413	0.105	0.248	0.022	0.281	0.065	0.079	0.008
p	2.512	0.361	2.303	0.857	1.609	0.268	1.528	0.576	1.753	0.239

The best assay conditions (namely a coating conjugate concentration of $50 \mu\text{g L}^{-1}$ and an antibody concentration of $200 \mu\text{g L}^{-1}$) were further used to measure real green coffee samples. This ic-ELISA procedure was deemed adequate for measurement of coffee samples to compare against MCR 3 results.

3.2.4 MCR 3 OTA Measurements in Green Coffee Extract: Search for an Adequate Positive Control

In an ic-immunoassay, the dose-dependent signal intensity decreases with increasing target analyte and signal maximum takes place when no target in the sample is present. This characteristic presents some difficulties when analyzing unknown samples, especially those that could be contaminated at levels significantly larger than the IC_{50} value. In this case, a complete lack of signal in the assay might raise concerns whether this was carried out properly. Some assurance is indeed needed in the form of a control signal that, regardless of the outcome of competition, always provides a constant guideline to indicate that all steps in the assay have been successfully executed. In the plate-based ELISA assays, respective rows for a positive control (coated wells, no competing analyte) and a negative control (not-coated wells, no competing analyte) serve this purpose. In the case of the MCR 3, where reagents are given in an automated way, this type of control becomes crucial, but the matter is more complicated because the negative control must be included in each independent, single measurement. If controls are to be supplemented during the competitive step, they also need to be selected keeping in mind unspecific matrix effects. For example, the use of a highly selective anti-TNT antibody in combination with glass immobilized DNT was proven an adequate positive control in the MCR 3-based screening of antibacterial residues in milk.^[148] This same strategy was tested for OTA-contaminated green coffee samples without success; a signal could not be detected. The reason for this effect is not clear, nevertheless it can be speculated that the abundant phenols, polyphenols and chlorogenic acids present in green coffee (figure 40) may easily cross-react with the anti-TNT antibody, depleting the number of molecules available to bind to the immobilized DNP.^[170, 171] The manufacturing company of the monoclonal anti-TNT antibody that was tested did not give further details regarding its cross-reactivity when we asked for the information.

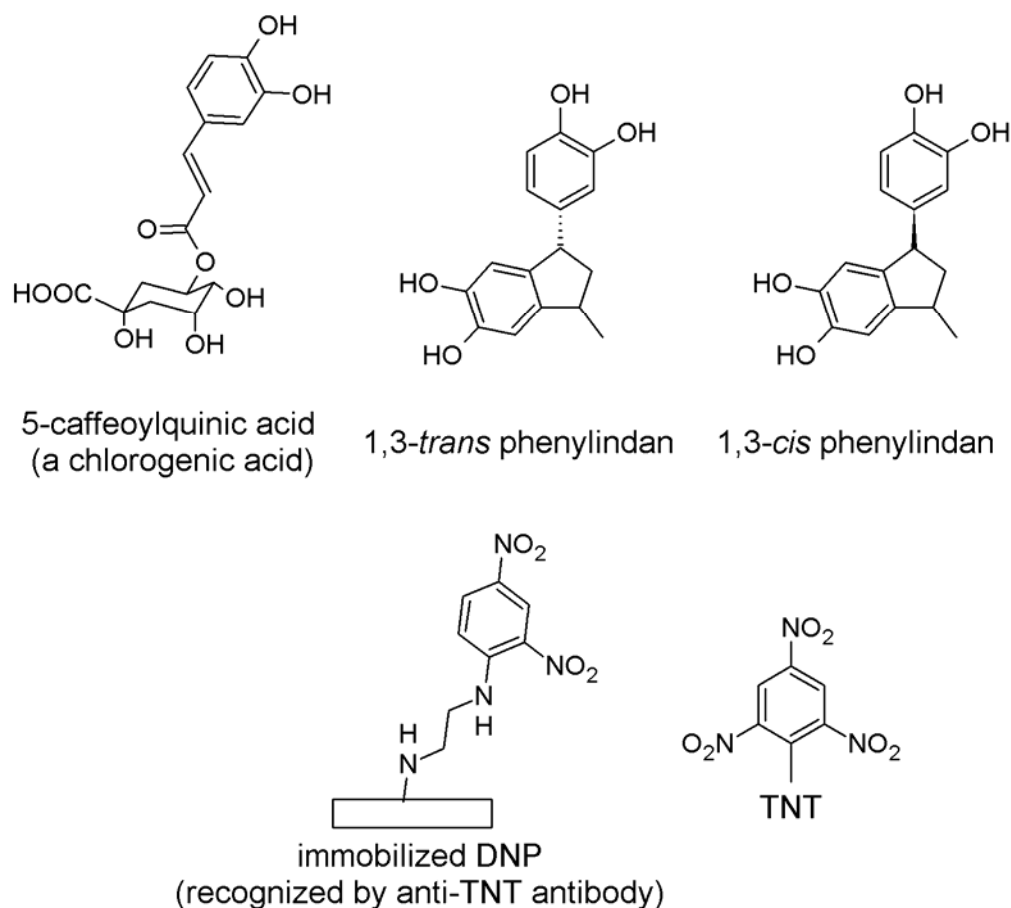


Figure 40 Compounds present in coffee that may react with anti-TNT antibody, immobilized DNP used as negative control and trinitrotoluene (TNT) molecule.

Therefore, a new positive control had to be chosen. Because of its robustness, another good candidate for a positive control is the specific and high-affinity interaction between biotin and streptavidin. This second strategy was also tried out: our synthesized biotin-peptide was immobilized to the modified glass surface. Detection followed with an HRP-modified streptavidin conjugate during the tracing step of the assay. Nevertheless, this strategy was not altogether free from difficulties. Although a high signal was observed along multiple non-competitive assay cycles, also in the presence of a blank green coffee extract, the signal inevitably decreased with increasing regeneration of the chip. This strategy only meets the requirements of a good positive control half-way: it provides an independent signal that is, however, not constant. The reason for abrupt signal decrease is most likely the incomplete disruption of the biotin-streptavidin complex, which is known to be one of the strongest, non-covalent interactions in nature at femtomolar affinity.^[108, 172] HRP is also irreversibly inactivated at low pH, which explains why the chemiluminescence intensity decreases with increasing number of cycles. Under this scheme, repeated addition of the streptavidin-HRP

complex will progressively block growing fractions of the total immobilized biotin, hence causing an exponential decrease in the CL signal.

The problem being too strong an interaction between receptor and reporter molecule, it was decided to maintain the immobilized biotin-peptide on the chip surface, but change the reporter and opt for a weaker, HRP-labeled binding partner that could be completely removed under the regeneration conditions already optimized for the recognition of the immobilized OTA by the anti-OTA antibody. Therefore, an HRP-labeled, anti-biotin antibody was chosen and mixed in the secondary HRP-labeled antibody solution that is supplemented to the assay during the “tracing” step (see table 4). It is important to point out that adding the control tracer *after* competition also prevents possible unspecific matrix interactions because at this point in the assay, the washing off of the raw sample from the chip flow cell has already taken place. The condition for using this kind of receptor, though, is of course that it needs to be available in its HRP-labeled form. This strategy might also have worked with the anti-TNT antibody and the DNT receptor described previously, but an adequate HRP-labeled anti-TNT antibody was not commercially available. The signal intensities of the three different positive controls tested can be seen in figure 41.

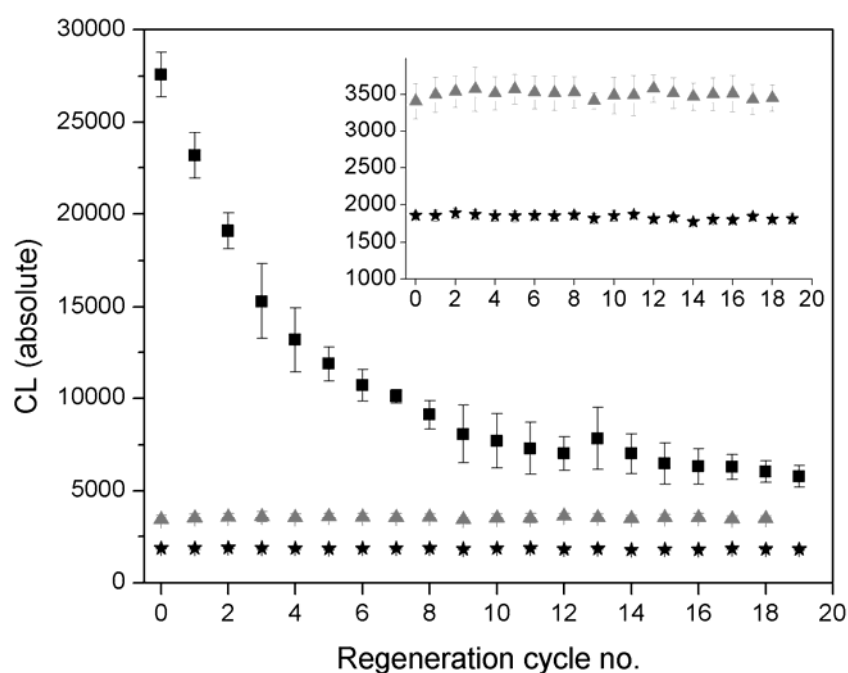


Figure 41 Positive control signal intensity along multiple regeneration cycles. Biotin detected with HRP-streptavidin (■); biotin detected with HRP-anti-biotin (▲); blank (★). Graph inset: zoom-up of blank and biotin detected with HRP-anti-biotin. Each experimental point is the average of 6 spots, uncertainty is the standard deviation.

In summary, a good positive control for an MCR 3-based indirect competitive immunoassay fulfills these two characteristics:

- constant signal along multiple, sequential assay cycles, and
- either tolerance for the sample matrix, or the availability of the tracking antibody in its HRP-coupled form.

3.2.5 Dose-Response Curves in Buffer and in Green Coffee Extract

In order to achieve a fast OTA screening method with the aid of the MCR 3 it was important to reduce sample processing to a minimum. The most straight-forward sample extraction includes the mixing or vortexing of a so-called “slurry” that contains a set amount of organic solvent, for example MeOH or ACN. In this case, MeOH was preferred since antibodies tolerate it better than ACN, and the project partner’s standardized method included extracting the samples in a MeOH-water mixture. Both the organic solvent content and the co-extracted matrix of the sample usually play a detrimental role in the antibody sensitivity; therefore these effects had to be tested individually.

Figure 42 shows the MCR 3 generated dose-response curve for OTA (buffered solution, 20% methanol), as an initial estimate of how solvent content influences curve parameters, and for further reference when comparing with real coffee extract. It can be noticed that the IC_{50} value of $0.48 \mu\text{g L}^{-1}$ free OTA in the MeOH-containing solution is larger than for the ELISA-plate-based assay, which delivers a value of 0.24 to $0.28 \mu\text{g L}^{-1}$ at a comparable antibody concentration of $200 \mu\text{g L}^{-1}$. At comparable receptor densities, shorter incubation times during competition usually lead to increased sensitivity in the assay (lower IC_{50} values). In the MCR 3 based assay the effective time of exposure of the immobilized receptor to the antibody-analyte solution is small compared to the time required for the microtiter plate version (~ 1 min vs. 30 min). Nevertheless, sensitivity is better in the ELISA-based assay than in the MCR 3. The only possible explanation is that the receptor densities are not comparable, i.e. they are larger in the glass chip than in the polymer microtiter plate. Increased sensitivity in the MCR 3 assay can only be reached by either diminishing the spot size or by decreasing the receptor density of the spot. Unfortunately this strategy did not generate the desired results, since both of these alternatives effectively lead to decreased CL intensity and high background signals.

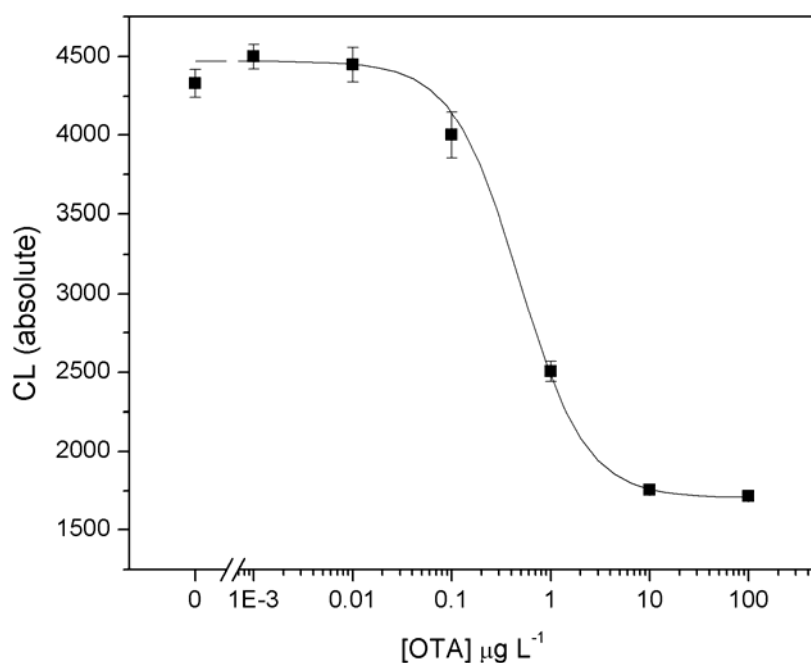


Figure 42 MCR 3-generated dose-response curve for OTA spiked in a MeOH-buffer mixture (20% MeOH, 80% PBS v/v). Each experimental point plotted is the average of 3 CL signals recorded, error bars are the standard deviation associated. $A_1 = 4471 \pm 63$; $A_2 = 1707 \pm 13$; $IC_{50} = 0.48 \pm 0.06 \mu\text{g L}^{-1}$; and $p = 1.29 \pm 0.13$ ($m = 3$; $n = 7$; $R^2 = 0.9992$).

For the next step in the optimization process, regenerability of the chip was measured in a non-competitive immunoassay format, but this time carried out with blank green coffee, in order to assess matrix effects in the MCR 3. For this purpose, a green coffee slurry (blank, OTA contamination $\leq 0.2 \mu\text{g kg}^{-1}$) provided by our working partner was also tested independently at our facilities, extracted according to the partner's standardized procedure and diluted to a final MeOH content of 20% (v/v, final sample-to-extract ratio 1 g in 26.666 mL extract). The signal intensity along 20 regeneration cycles can be seen in figure 43.

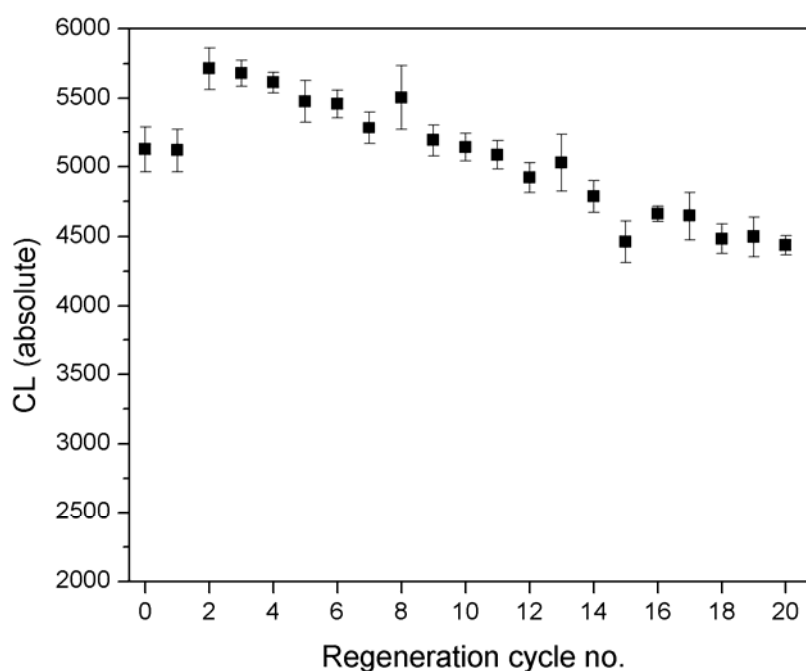


Figure 43 Non-competitive regeneration assay in blank green coffee matrix. Signal decrease along 20 cycles. Each experimental point plotted is the average of 6 CL signals recorded, error bars are the standard deviation associated.

As opposed to the regeneration experiment conducted in buffer, it can be appreciated from figure 43 that the diluted green coffee extract does have an influence on the stability of the signal. In buffered MeOH solution, the signal associated to OTA remains relatively constant, showing no visible tendency, with a relative standard deviation of 4% from the average along 20 repetitions (see figure 32). Nevertheless, as shown in figure 43, in the presence of matrix a clear decrease in the signal can be appreciated. Without taking into account the first two experimental points in the graph, the signal range spans from 5126 (2nd regeneration cycle) to 4437 (final regeneration cycle, absolute CL signal). In other words, the final CL intensity is only 86% of its initial value. Since the regeneration works adequately in buffered MeOH solution, it is clear that the green coffee matrix has a detrimental influence on the regenerability of the assay and possibly on the chip surface. However, the question of whether calibration and sample measurement may be carried out still remains open. Consequently, OTA calibration in green coffee matrix and recovery rate experiments were carried out. The resulting dose-response curve is shown in figure 44.

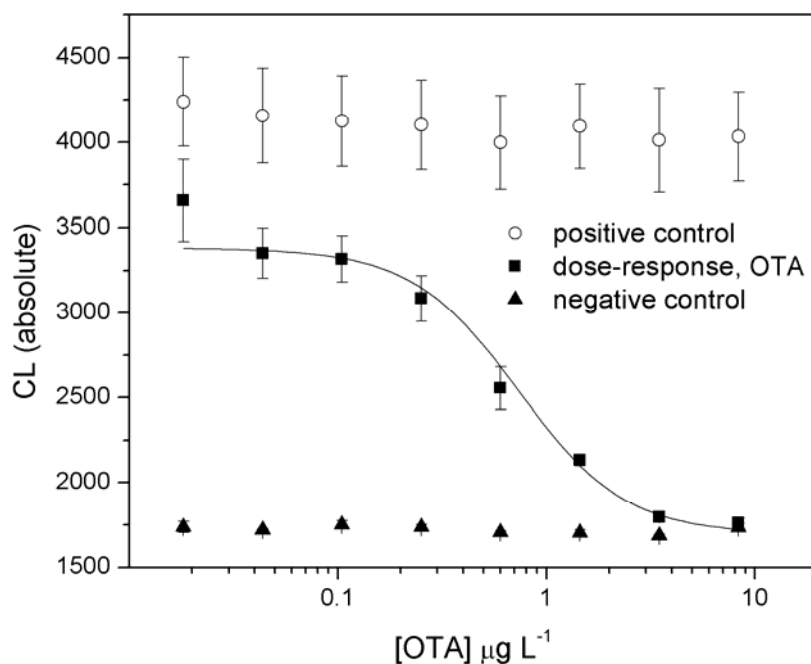


Figure 44 MCR 3-generated dose-response curve for OTA spiked in blank green coffee extract (20% MeOH, 80% buffer, NaHCO_3 v/v). Each experimental point plotted is the average of 6 CL signals recorded, error bars are the standard deviation associated. For the dose-response curve, $A_1 = 3381 \pm 102$; $A_2 = 1697 \pm 39$; $\text{IC}_{50} = 0.74 \pm 0.09$; and $p = 1.71 \pm 0.30$ ($m = 6$; $n = 7$; $R^2 = 0.9875$). Positive control: biotin detected with anti-biotin-HRP; negative control: average intensity of blank spotted buffer.

Once again, in figure 44 it is interesting to notice that the absolute CL intensity at very low OTA concentrations is only a fraction of the signal in the preceding figure (figure 43, non-competitive regeneration assay with green coffee extract), but a comparable coffee extract was used. Again, the reason eludes us, since the only difference among the two experiments was that they were carried out on different days, on different glass chips. It could well be that differences in the glass composition already discussed indeed play a role in the immobilized receptor density.^[90] Nevertheless, the fact that the negative and positive controls remain constant, at least during the cycles required to calibrate the system, is a good indicator that there are no sources of systematic errors during this part of the procedure. To better appreciate the system behavior, the CL signal as a function of the regeneration cycle for sequential measurements (whether they be blank extract measurements, calibrant measurements, or sample measurements) is shown in figure 45. Table 11 includes the obtained values for each cycle as well.

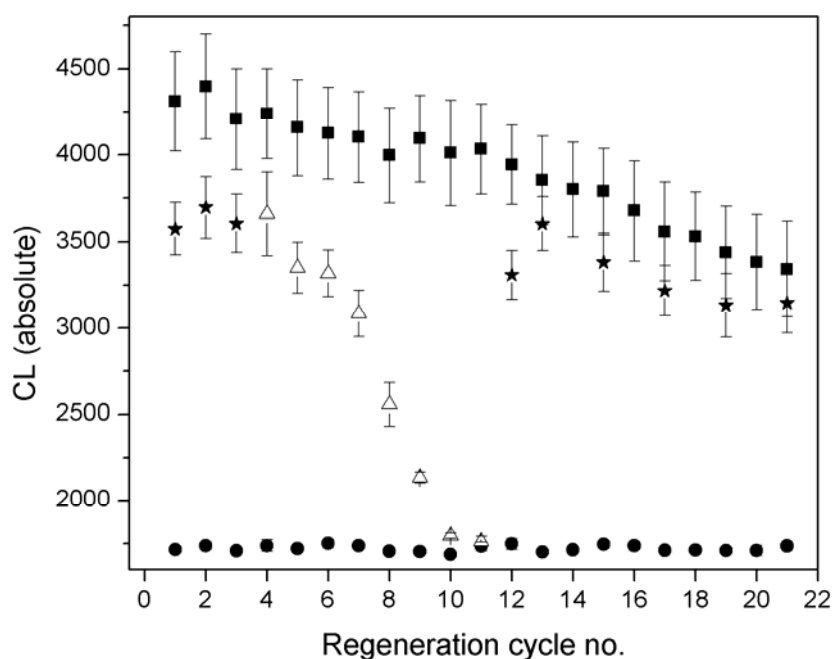


Figure 45 Detailed sequence of individual MCR 3 measurements in green coffee samples. Positive control, all cycles biotin-related signal (■); blank coffee, OTA-related signal, cycles 1-3, 12, 13, 15, 17, 19, 21 (★); spiked green coffee for calibration, OTA-related signal cycles 4-11 (△); negative control, spotted buffer, all cycles (●). Cycles 14, 16, 18 and 20 used to measure samples for calculating recovery rate (CL value not shown on graph).

Table 11 Absolute CL values for blank green coffee: OTA signal at maximum CL and positive control along 21 regeneration cycles (as depicted in figure 45)

	Positive control (■, n=6)	Error, ± St.Dev.	OTA max. signal (★, n=6)	Error, ± St.Dev.
Reg Cycle				
1	4310	289	3575	151
2	4398	306	3696	176
3	4208	293	3605	166
4	4239	262	N/A	N/A
5	4157	280	N/A	N/A
6	4125	266	N/A	N/A
7	4103	264	N/A	N/A
8	3998	275	N/A	N/A
9	4094	251	N/A	N/A
10	4012	306	N/A	N/A

11	4033	262	N/A	N/A
12	3943	229	3309	141
13	3853	255	3604	155
14	3799	272	N/A	N/A
15	3788	248	3383	168
16	3677	288	N/A	N/A
17	3558	284	3218	147
18	3530	252		
19	3438	266	3133	185
20	3382	274		
21	3343	276	3147	175
Signal decrease (absolute) ^{a)} :	22.4%		12.0%	
Signal decrease (relative) ^{b)} :	35.7%		21.7%	

Note: the total decrease in signal is a) absolute, if the blank is not subtracted; and b) relative, if the blank value of 1600 is subtracted from the original value.

Figure 45 shows the sequential CL signals obtained for the step-by-step experimental measurements that are part of the routine needed to analyze unknown coffee samples. First, an OTA-free green coffee extract is to be measured (in this case, three times sequentially), to get an accurate starting value for the maximum signal intensity in the competitive immunoassay. Then, the calibrants that consist of OTA-spiked green coffee extract are measured from lower to higher free OTA concentration. Between the last calibrant (highest OTA concentration, in this case $8.3 \mu\text{g L}^{-1}$) and an unknown sample, at least two green coffee blanks must be measured, in order ensure adequate rinsing of the tubing and to avoid cross contamination that would introduce an overestimation in the actual OTA content of an unknown sample. Finally, coffee blanks are also run in between measurements of unknowns, as a further means of control. In this pilot sequence it is noticeable that the absolute CL signal intensity, both for the OTA-related signal and for the positive control, is still slowly going down with increasing number of chip regeneration cycles. It is interesting to mention that this effect was not noticeable when focusing only on the signal behavior during calibration, as depicted in figure 44. Because signal decrease is slow, the positive control recorded along the 8

regeneration cycles needed for system calibration does not show a marked tendency to go down. Nevertheless, this is an important factor, as it will inevitably introduce an overestimation in the OTA content of an unknown sample measured after calibration.

The following table gives a summary of the calibration parameters obtained for three independent assays with the developed procedure.

Table 12 Summary of parameters for IC-immunoaffinity OTA determination via the MCR 3 in green coffee samples. Independent experiments.

Parameter	Exp 1	Exp 2	Exp 3
A1 (absolute CL)	2698 ± 47	3196 ± 178	2021 ± 40
A2 (absolute CL)	1669 ± 17	1637 ± 54	1730 ± 3
IC50 ($\mu\text{g L}^{-1}$)	0.763 ± 0.085	0.824 ± 0.218	0.575 ± 0.207
IC50 ($\mu\text{g kg}^{-1}$)	15.3	16.5	11.5
p	1.202 ± 0.137	1.239 ± 0.287	2.032 ± 0.788
R ² (n = 3; m = 7))	0.99771	0.99663	0.97167
80% LOQ signal ($\mu\text{g kg}^{-1}$)	4.8	5.4	5.8
20% LOQ signal ($\mu\text{g kg}^{-1}$)	48.4	50.5	22.8
LOD ($\mu\text{g L}^{-1}$)	0.164	0.487	0.487
LOD ($\mu\text{g kg}^{-1}$)	3.3	9.7	9.7

As can be appreciated, the results are slightly variable among different days, but within an expected margin usual for indirect competitive immunoassays. At 80% maximum signal intensity, the inferior limit of quantification values (lowest LOQ) vary from 4.8 to 5.8 μg OTA per kg green coffee. Although legal maximum residual limits for OTA in green coffee beans have not been unambiguously adopted, values within 5 – 10 $\mu\text{g kg}^{-1}$ have been suggested, and given that contamination in roasted or instant coffee obviously stems from the raw stuff, it is meaningful to determine OTA content in green beans. In this regard, the experimental limits of the developed assay are considered to be adequate for the screening procedures. The one inconsistency evidenced by the table 12 is the high LOQs calculated for two of the three assays. These values are even higher than the lower LODs (calculated from

the 80% maximum signal intensity of the calibration curves), which does not make sense. The values arise from the high standard deviation in the CL signal when measuring blanks or minimally contaminated samples. Nevertheless, the high deviations actually decrease when moving towards higher OTA concentration, as can be appreciated from figure 44. In the dose-response curves for indirect competitive immunoaffinity assays the standard deviation associated to the dependent variable does not remain constant along the concentration range, but tends to be greater at lower competing analyte concentrations.^[169, 173]

Furthermore, recovery rate experiments where blank solid green coffee was extracted and measured after spiking of the solid material with OTA were also carried out in this work. The following table presents a summary of the obtained data.

Table 13 OTA calculated content of spiked green coffee samples. Values are the average of independent experiments. The OTA content range was calculated by taking into account the error (i.e. the standard deviation) associated to the average CL of three spots.

[OTA], spiked in solid, $\mu\text{g kg}^{-1}$	[OTA], calculated, $\mu\text{g kg}^{-1}$	Recovery rate
2	CL > 80% LOQ	N/A
4	7.9 ± 0.5	185 – 210 %
8	9.2 ± 1.2	100 – 130 %
10	11.2 ± 1.0	102 – 122 %
20	28.7 ± 2.3	132 – 155 %

In general, the recovery rate experiments show that the OTA values obtained for the spiked samples tend to be overestimated, sometimes by a factor larger than two. This could be expected on the basis of signal decrease by multiple regeneration cycles on a single chip biosensor. Nevertheless, the fact that samples spiked at low OTA levels of $2 \mu\text{g kg}^{-1}$ were always detected as negative (the signal recorded being in every case higher than the LOQ), is welcome and makes the developed strategy an efficient, moderately expensive screening procedure. Moreover, the possibility of an automatized sensor calibration that runs overnight, before the actual screening takes place, could be a reality if an autosampler was included, a possibility contemplated in the MCR 3 design. In our present version of the assay, the effective measuring time for each sample is of 12 minutes, plus time needed for extraction. In the final section of this chapter, comparison of the developed method against other available, novel procedures to screen OTA in coffee will be discussed.

3.2.6 Real Sample Measurements

Green coffee samples from different origins were received from our project partner, Eurofins WEJ Contaminants, Hamburg, in order to test the developed method for OTA screening in the MCR 3 platform. These samples were originally prepared by our project partner by extracting a green coffee-water slurry (sample-to-water ratio of 1:3 w/w) with MeOH. The final composition of the delivered samples consisted of 80% MeOH (v/v), 20% water (v/v), 1.6% NaHCO₃ (w/v), and had a solid coffee-to-solution ratio of 1 to 8.333. Before measurement (either ELISA plate-based or MCR 3 based), samples were further diluted in our labs to a final MeOH content of 20% (v/v) with a 2.5% NaHCO₃ solution (w/v), to prevent antibody damage due to the original high MeOH content. The exact composition is to be noted, since final OTA determination must be carried out by multiplying the obtained OTA concentration times the total dilution factor. In this case, the final solutions for the indirect competitive immunoaffinity assays had a total MeOH content of 20% (v/v) and an overall sample-to-extract ratio of 26.66.

Blank samples, as well as samples contaminated at original values of 0.3 to 5.4 µg OTA per kg green coffee were all screened by MTP-based ic-ELISA upon arrival. The curves obtained for the calibration are depicted in figure 46 and were obtained by spiking blank coffee extract of identical composition and ratio as in the delivered samples. They show varying absorbances within different, individual assays (conducted along two days), but the crucial parameter, the IC₅₀ value, remains fairly constant.

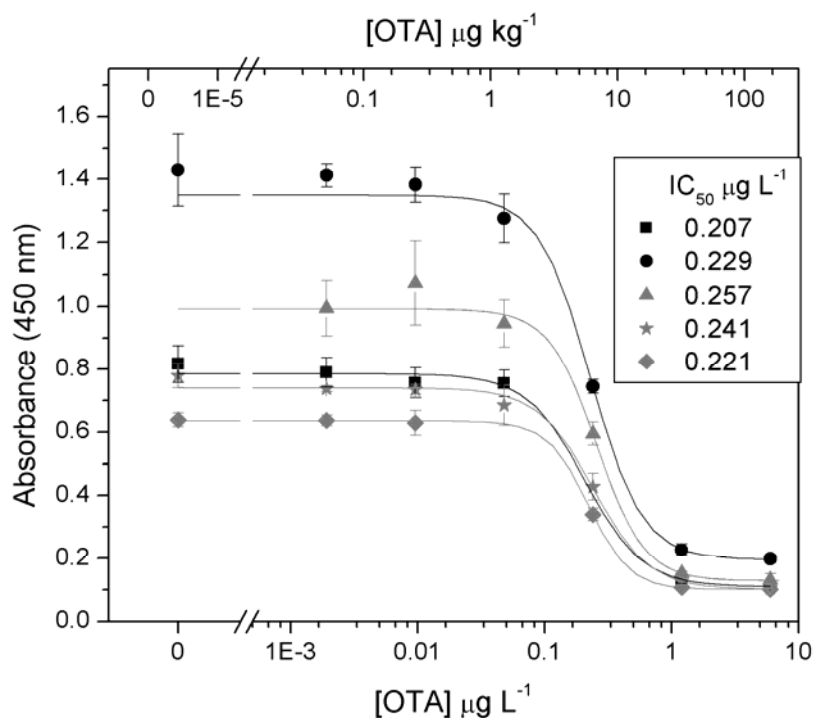


Figure 46 MTP ic-ELISA calibration curves for green coffee extract, MeOH content 20% (v/v). Each set of data measured independently ($n = 6$; $m = 3$). Upper “x” axis indicates contamination in μg OTA per kg of raw coffee; lower “x” axis gives contamination values in final extract solution. IC_{50} average = $0.231 \mu\text{g L}^{-1}$; standard deviation = $0.019 \mu\text{g L}^{-1}$.

The results obtained for the 30 different real samples delivered for the screening of OTA with the developed MTP-based ELISA procedure are shown in the following pie diagram, figure 47.

The results obtained for ELISA screening of the real samples are consistent with comparable published procedures. Zheng et al. validated their commercially available ic-ELISA for OTA detection and reported a ratio of ELISA/HPLC-detection of 1.1 to 2.5, as well as an LOQ of $3.8 \mu\text{g kg}^{-1}$, values in accordance to our own.^[174] In summary, the plate-based ic-ELISA for OTA screening in green coffee extract afforded adequate results in 73% of the total samples screened. Of the 6 blank samples received, 2 were detected as false positive (33%). Notably, no false negatives were detected.

Real sample analysis outcome: green coffee extract,
screened with ic-ELISA (MTP) for OTA determination

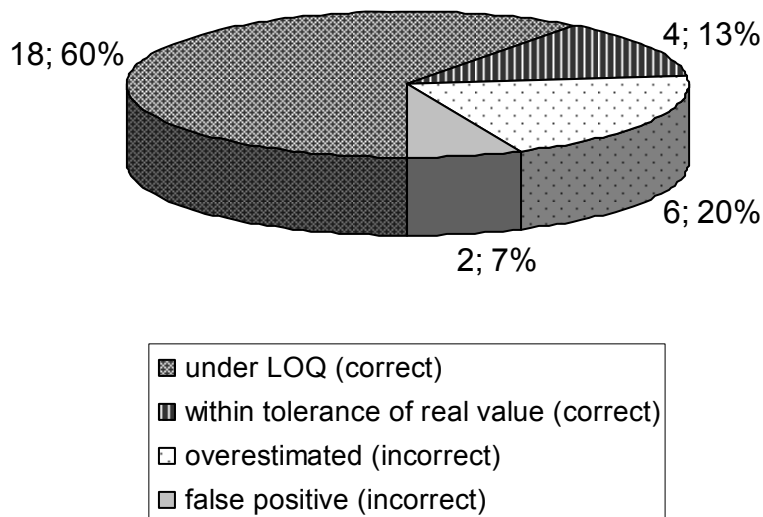


Figure 47 Results of MTP-based ic-ELISA for OTA determination in green coffee (real samples). 30 samples screened. Pie labels: number of samples that delivered a particular outcome followed by percent of total samples screened. Criteria: sample was correctly determined if a) real contamination value delivered an absorbance below LOQ of assay, or b) determined contamination value fell within 70 – 130% of real value given. Samples were considered incorrectly determined if a) determined contamination value was lower than 70% or higher than 130% of the real value given, or b) false positive samples were detected.

Furthermore, 18 samples chosen randomly from the original 30 were measured with the developed method using the MCR 3, along 7 days of experimental work. Some of the real samples were measured more than once (see table below). Figure 48 and table 14 summarize the outcome of the determinations.

Table 14 OTA determination in real samples (green coffee extracts). Details of measurement with MCR 3

Sample No.	Real value $\mu\text{g kg}^{-1}$	Measured value $\mu\text{g kg}^{-1}$	Factor (measured over real)	Times measured	Outcome	Identified as:
693997	blank	< LOD	N/A	4	correct	negative
692692	1.7	16.5	9.7	2	incorrect	false positive
694000	3.8	12.8	3.4	4	incorrect	false positive
692707	3.4	13.5	4.0	1	incorrect	false positive
692688	2.6	< LOQ	N/A	1	correct	negative
694183	4.9	20.4	4.2	1	incorrect	false positive
692706	2.2	17.6	8.0	3	incorrect	false positive
693740	2.8	< LOQ	N/A	3	correct	positive
694184 (1st)	5.4	4.7	0.9	2	ambiguous	ambiguous
694184 (2nd)	5.4	25.0	4.6			ambiguous
692693	1.8	23.4	13.0	2	incorrect	false positive
693748	2.7	30.4	11.3	2	incorrect	false positive
693889	4.1	19.5	4.8	2	incorrect	false positive
692690	blank	< LOD	N/A	1	correct	negative
692692	1.7	15.6	9.2	1	incorrect	false positive
694814	5.4	9.6	1.8	1	correct	positive
692809 (1st)	0.3	5.4	18.0	2	ambiguous	ambiguous
692809 (2nd)	0.3	< LOD	N/A			ambiguous
693742 (1st)	0.5	4.5	9.0	2	ambiguous	ambiguous
693742 (2nd)	0.5	< LOD	N/A			ambiguous
692694	0.8	23.6	29.5	2	incorrect	false positive

Real sample analysis outcome: green coffee extract,
screened with MCR 3 for OTA determination

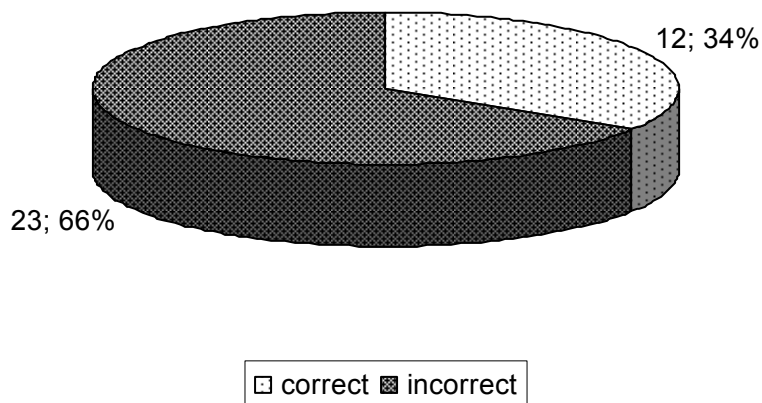


Figure 48 Summarized results of MCR 3-based measurements for OTA determination in real green coffee samples. 18 samples screened, 35 independent measures carried out. Pie labels: number of samples that delivered a particular outcome followed by percent of total samples screened. Determination criteria same as for ic-ELISA (MTP, see figure 47). LOQs and LODs varied slightly among days ($4\text{--}8 \mu\text{g kg}^{-1}$ and $2\text{--}3 \mu\text{g kg}^{-1}$ respectively).

The results generated from the MCR 3 measurements of the naturally contaminated green coffee samples show that in the majority of the incorrectly determined samples, the OTA content estimated was between 2 and 30 times higher than the true value (considered as the value reported by the work partner). In particular, no false negative samples were detected, as in the case of the ic-ELISA assays previously carried out. The reason for this systematic overestimation in the OTA content is unclear, but it can be pointed out that the samples had been stored for at least one month before measuring took place, and that between thawing and air exposure, a notable change in the color of the liquids was noticed (the solutions changed from a light green to a deep, almost black tone).

Other attempts to overcome this bias in the OTA content determination were carried out. Assuming that matrix interferences were the cause of the overestimation, solid phase extraction of the raw extract was tried as a pre-cleanup step in order to determine if the interferences could be removed. Two types of solid support were tested: 1) phenyl-derivatized silica, and 2) isopropylamino-derivatized silica. In the case of phenyl-derivatized silica, recovery rates of OTA-spiked samples were measured via RP-HPLC. The detailed procedure used for cleanup is described by Hinkel et al.^[39] Unfortunately, the OTA recovery rates were very poor at values not greater than 25%. After personal communication with the research

group that had published the procedure, it was brought to our knowledge that the efficiency of phenyl silica SPE columns for cleanup in the OTA determination of coffee samples is strongly dependent on the SPE cartridge lot and not to be relied upon. Due to time constraints, it was not possible to test more than two SPE column lots, unfortunately with unsatisfying results.

On the other hand, the literature states that good OTA recovery rates for roasted coffee samples have been achieved by including an aminopropyl SPE clean-up step in either an HPLC-based or a flow-through immunoaffinity-based screening procedure.^[40, 175, 176] We tested the method described in the literature by means of ic-ELISA, but no differences in the recovery rate with or without the SPE cleanup step were observed for green coffee. Even if this procedure had been successful, the inclusion of such a step would have significantly increased the time needed for single sample measurement and for calibration in the MCR 3. It is estimated that this would take at least 12 additional minutes per sample, but as stated before, our experiments were not conclusive.

In summary, we can further speculate on the reasons of a systematic overestimation in the OTA content of the real samples. The reasons may be varied, but we do not discard the fact that storage time, repeated thawing and cooling of the extracts, repeated exposure to air as well as small variations in the MeOH content of the individual samples could have lead to uncertainty in the OTA estimation, or to an intensifying of the matrix effects that effectively lower the signal intensity and modify the 50% dose response (IC₅₀ value) in IC-immunoassays. This hypothesis is supported by the observation that the provided samples changed color upon thawing and air exposure. Remarkably, our own MCR 3 experiments with spiked samples showed good enough recovery rates. This gives us reason to believe that the developed procedure might still prove efficient as a screening technique. One way of bringing clarity to the point is carrying out real sample measurement shortly after extraction and on the spot. In this way, more information on the assay performance would be collected.

3.2.7 Comparison of the Developed MCR 3 Method with Other Available Methods for OTA Screening in Coffee

In this section, five methods for OTA determination reported in the literature are critically assessed and compared to the MCR 3-based procedure. We base our comparison in the results obtained for in-house, OTA-spiked green coffee, since the results obtained for the delivered,

naturally contaminated samples are inconclusive. In particular, specific reference is made to applications developed for coffee. The published processes being compared are based on diverse principles: classical quantification *via* IAC-HPLC, classical MTP-based ic-ELISA, immunoaffinity screening with a tandem flow-through column, solid-phase microextraction followed by HPLC, and a microarray technology-based procedure. On a side note, it is understood that the fast paced development of LC-MS applications has made it possible in the last decade to simultaneously detect several mycotoxins in one sample, including complex food extracts. The extremely low limits of detection of modern MS equipments and the separating efficiency of HPLC allows for toxin determination in extremely diluted real samples, even without the need of IAC enrichment.^[55, 177, 178] Nevertheless, mass spectrometers capable of doing this are prohibitively expensive for the majority of the users, require special facilities for their housing and are not ideal for on-site screening. Therefore, these developments will not be considered in this section, although they certainly provide the gold standard in terms of analytical efficiency. The objective of the assessment sketched here is to provide the reader with a broader scope of the recently developed methods for OTA determination in coffee samples and a reference comparison for our developed method.

The first method to be discussed, published by Pittet in 1996,^[163] is considered representative of other published procedures and is given as reference by the AOAC.^[53, 179, 180] The sample preparation includes the removal of most of the matrix interferences in the coffee extract by means of an IAC enrichment clean-up step, previous to RP-HPLC separation and fluorescence detection. Unambiguous identification of OTA can be achieved by reacting the cleaned and concentrated extract with BF₃ to form the OTA-methyl ester that causes the original OTA peak to disappear in the chromatogram. HPLC calibration and measurement of an unknown sample can be carried out automatically with the aid of an autosampler. Depending on the size of the column used and the pump capabilities, a reported single-run time of 28 min may be significantly reduced. Since the final sample-to-solution ratio is 1 g coffee to 0.75 mL solution thanks to sample enrichment, the LOD and LOQ of this method are low, with reported values of 0.2 and 0.3 µg toxin kg⁻¹ coffee respectively. In general, methods that include enrichment steps after sample extraction (IAC, solvent evaporation), such as this one, deliver better LODs and LOQ than methods that do not, but render the procedure longer and rather user-intensive. Another point to be taken into consideration is that adequate laboratory settings are also necessary, since HPLC is at the heart of the method. Following the cost of the chromatograph and column, immunoaffinity enrichment is the factor that contributes most to

consumable expenses, running at about €12 per sample, and the IAC cartridges are only suitable for single-use.

The next method to be analyzed in detail also has chromatography at its core. It was developed by Rosa Vattino et al., who coupled the resolving power of HPLC with solid phase micro extraction (SPME). SPME consists of an enrichment procedure that relies on reusable components, avoiding the cost of immunoaffinity enrichment.^[181-183] In this fairly new technique, a thin polymeric film of polydimethylsiloxane and divinylbenzene (PDMS/DVB) is coated on a support fiber and regularly immersed in the liquid extract. Equilibrium transfer of OTA to the thin film slowly takes place without being exhaustive, since the bulk of the extracting phase is very small in comparison to the total sample volume. Desorption of OTA is then achieved by introducing the fiber into an appropriate solvent. At this point, OTA transferred to the solvent may be injected into the HPLC. The technique has also been optimized for OTA detection in beer, wine and cornflakes.^[184-186] Similar to several immunoaffinity-based procedures, calibration must be carried out by spiking the raw samples with known amounts of OTA. Assay limits are highly influenced by matrix components and in this case the values reported in the literature are 0.3 and 2 $\mu\text{g toxin kg}^{-1}$ coffee for the LOD and for the lower LOQ respectively. In this procedure the sample-to-solution ratio before injection is 1 g coffee to 20 mL. Since the total dilution factor is large, it is surprising that the LOD of the method is not so different from the IAC-HPLC-FD method described before. The obvious advantage of SPME over regular IAC-HPLC is that the extracting phase is reusable. Still, the technique proceeds slowly, since the adsorption of the analyte to the membrane is equilibrium-determined. Extraction of the raw solid and the time required for calibration and sample measurement add up to the microextraction step, which takes approximately 1 h per sample, added altogether.

The third published method to be reviewed, the MTP ic-ELISA, is widely used because of its simplicity and affordability. For this example, Fuji et al. have relied on a sensitive monoclonal anti-OTA antibody as tracer and validated their procedure against HPLC, to detect the toxin in green and roasted coffee samples.^[67, 68] Extraction in a water-ACN mixture, back-extraction in chloroform, evaporation and further dilution previous to the 20 h long ELISA contributed a significant amount of time to the already lengthy procedure, but were considered necessary in order to avoid matrix effects. The LOD and LOQ reported for the method were 75 pg OTA (no relation to the original sample amount was given) and 3.75 $\mu\text{g kg}^{-1}$ respectively, at a final sample-to-solution ratio of 1 g coffee to 12.5 mL. Advantages of this method include the

minimal costs involved, but the multiple work-up steps of the samples and the long incubation needed for the microtiter plate assay do not allow for this procedure to be implemented as a fast screening technique.

One good example of a method specifically designed to be used outside the laboratory is the “tandem assay column”.^[175] As with most rapid screening procedures, the detection principle is immunoaffinity recognition of the OTA. Since instrumentation is not at all required and the detection is visual, the method is well-suited to carry out field analysis and is true to the “on the spot” philosophy. The “tandem” columns consist of two individually packed layers of solid phase: one that partially removes interfering matrix components from the raw coffee extract and another one that contains the immobilized anti-OTA antibodies. After an initial application of the extract to the column on the gel-like phase, the addition of an OTA-HRP conjugate for direct competition takes place. Finally, color development is induced by adding an adequate HRP substrate. Response calibration of the system at known OTA concentration needs to be run parallel to the real sample measurement, but only 6 calibrants are needed. The cut-off value for OTA detection reported is $6 \mu\text{g kg}^{-1}$. Although this method is not quantitative, it allows for a fast screening of roasted coffee samples at a value that is certainly useful and under the defined MRL of soluble coffee in the EU. At a sample-to-solution ratio of 1 g coffee to 4.2 mL solution, this method is also economical regarding solvent consumption. Moreover, total analysis time is 35 min for 7 samples, easily carried out by a single user. Nevertheless, one important disadvantage of the method is the strong variability of antibody immobilization efficiency from individual batches of columns.

A last example that shares many similarities with the MCR 3 developed at the IWC is the array biosensor from the Naval Research Laboratory (NRL, Washington, DC).^[187] The device was briefly described in the “Theoretical Background” section of this work. The format of the immunoassay used is indirect competitive and signal tracing is carried out via fluorescence emission of a tagged primary antibody. Indeed, the glass microarray is similar to a “mini” microtiter plate, with individual microchannels able to hold small volumes of samples, where toxin haptens have been immobilized.^[70] Receptor binding is equilibrium-determined, meaning that there are significant incubation steps along the measuring procedure. From the published information, it is not clear whether the sensor has been automatized to load the multiple samples needed for calibration and for the measurement of unknowns. Nevertheless, as with the case of the glass biochips needed for the MCR 3, calibration must be carried out for every wave sensor used. Once the samples are loaded, the complete measurement is run in

parallel, a feature that makes this application time-saving. Regeneration of the sensor would be desirable, but strictly speaking, it is not necessary. Successful attempts for reusing the sensor surface have already been carried out for OTA detection, but with matrices other than coffee. Whether regeneration is total or only partial is also not clear, since the anchoring of the biotin-OTA conjugate is achieved by immobilizing the conjugate on an avidin pattern.^[71] If this conjugate must be removed and patterned again, regeneration would only be partial. On the other hand, if regeneration is so finely tuned that only the antibody-hapten interaction is broken, this would be a true regenerable sensor. As for matrix effects, no additional treatment steps for the removal of interfering compounds in the coffee extract are necessary, since the inventors state that evanescent-wave technology enables fluorescence measurement of inhomogeneous and turbid samples. At a final sample-to-solution ratio of 1 g coffee to 12 mL solution and a total assay running time of approximately 50 min, (non-automated version, with sample preparation) the method is certainly efficient. The reported LOD is 7 $\mu\text{g kg}^{-1}$. Another key feature of this technology has been recently explored: the array biosensor from the NRL is able to simultaneously detect a second mycotoxin contaminant (OTA and deoxynivalenol) in wheat samples.^[71]

Finally, the MCR 3-based method for detecting OTA in green coffee shares some common characteristics with each of the previously described systems. Compared to classical HPLC, our system is also highly automatable. At the present, sample injection is performed manually, but a relatively simple addition of an autosampler unit would make calibration and sample measurement available in one easy step after loading all the reagents. Similar to the SPME-HPLC technology and the NRL array biosensor, the sensing unit, our “biochip”, is regenerable and reusable. This characteristic lowers the cost of single sample determinations. Nevertheless, more efforts are needed to reach the goal of increased number of regeneration steps that a single biochip may undergo. One factor that limits the time efficiency of our system is that sample input may only be carried out sequentially. In that respect, the “tandem column”, the NRL array biosensor and the MTP ic-ELISA are more time-saving, since different samples can be run in parallel (both calibration and measurement of unknowns). Regarding the LOD and LOQ of OTA in coffee, our system is at least comparable to the immunoaffinity-based systems discussed and fares poorly compared to IAC-HPLC. Nevertheless, IAC-HPLC is not suitable for on-the-spot measurement. Systems of detection for all the methods described are also diverse, making use of fluorescence emission, absorption, chemiluminescence, and even color change detected visually. Finally, at a weight of approximately 20 kg, our system may evolve to a more portable device in the future, where

at the time being, tandem columns and the 7 kg weight NRL device are better suited, at a fraction of the bulk. Table 15 summarizing these points of comparison among the different systems discussed.

Table 15 Comparison of different methodologies to detect and/or measure OTA in green coffee. Applications that make use of novel techniques.

HPLC, classic	HPLC, micro	ic-ELISA	NRL Array Biosensor	“tandem” column	MCR 3
IAC cleanup	SPME cleanup	NO cleanup	NO cleanup	Cleanup coupled	NO cleanup
Part-online	online	offline	Stand-alone, parallel	Stand-alone, parallel	Stand-alone, sequential
30 min per sample	60 min per sample	One plate, 2 h	One “plate”, 40 min	35 min per column	12 min per sample
5 calibrants	5 calibrants	8 calibrants	9 calibrants	6 calibrants	8 calibrants
not reusable	reusable	not reusable	reusable	not reusable	reusable
LOQ 0.3 µg/kg (FD)	LOQ 2.0 µg/kg (FD)	LOQ 4.0 µg/kg (UV abs)	LOQ 7 µg/kg (FD)	LOD 6 µg/kg (visual)	LOQ 5-6 µg/kg (CL)
Mobile? NO	Mobile? NO	Mobile? NO	Mobile? YES	Mobile? YES	Mobile? ALMOST
Pittet A., 1996 ^[163]	Vatinno R., 2008 ^[181]	Fujii S., 2006 ^[68]	Ngundi M., 2004 ^[70] (Ligler group)	Sibanda L., 2002 ^[176] (De Saeger group)	Sauceda-Friebe J., 2011 ^[188] (Niessner group)

3.3 Towards Multiple Toxin Screening and Shorter Measuring Times with the MCR 3

Besides sensor miniaturization, one of the major advantages of microarray technology for biochip fabrication is the possibility to immobilize different receptors on the same surface. In order to pave the way towards simultaneous multitoxin determination, this work also explored the possibility of simultaneous detection of AFB₁ and OTA on the sensor chip. Multitoxin detection is meaningful because several agricultural crops may be contaminated with more than one toxin. In the case of aflatoxin contamination, particularly in peanuts, the four types of aflatoxins, as well as OTA, may be present in one sample. The most toxic of these contaminants is AFB₁, with a reported LD₅₀ of 1.7 mg per kg BW in mice.^[189] Therefore, experiments were carried out in this section to judge the viability of a multitoxin-determination in peanut samples, but some difficulties regarding matrix interferences were encountered. It is important to point out that the immobilized receptor AFB₂-CMO-peptide is suitable for carrying out ic-immunoassays with either AFB₂ or AFB₁ as the competing analyte (e.g. the analyte to be detected in a sample), because the in-house produced monoclonal antibody tracer raised against AFB₁ is also cross-reactive with AFB₂ to a 98% extent. The set-up may also be used to determine the total amount of AFB₂ + AFB₁ in a sample, but because of the high antibody cross-reactivity, determining the individual concentration in samples containing both of the toxins is not possible.

Alternative assay variations were also tried in order to shorten assay measuring times in the future. For this last type of experiment, an HRP-labeled antibody against AFB₂ was used to provide proof-of-principle, but we expect that similar results can be achieved for AFB₁ or for OTA.

3.3.1 Simultaneous Detection of AFB₁ and OTA, Proof of Principle

For the detection of aflatoxins of the “B” family (AFB₁ and AFB₂) in food samples a monoclonal antibody of high affinity was produced and characterized by means of ic-ELISA at the IWC. The detailed description has been reported elsewhere and it shall not be further discussed in this work.^[153] For the MCR 3 applications, two anti-AFB antibodies were chosen for the following experiments: 1F2 and 3A7. Under optimized conditions, (MTP-ic-ELISA) the antibody 1F2 presented a minimum IC₅₀ value of $2.7 \pm 0.2 \text{ ng L}^{-1}$ against AFB₁ and had a

cross-reactivity of 98% with AFB₂. The displayed cross-reactivity makes this antibody suitable for total aflatoxin B detection. The same receptor, the AFB₂-CMO-peptide, is also adequate to be used in ic-immunoassays for the determination of either AFB₁, AFB₂ or the total amount of “B”-type aflatoxins. It should be pointed out that before attempting multiple toxin experiments, the optimal conditions for the individual AFB₁ assay in 20% MeOH-buffer solutions were inspected for MTP-based ELISA, in the same way that this was done for OTA (results not shown).

Figure 49 shows the dose-response curve for the simultaneous calibration of the MCR 3 with standards containing known amounts of OTA and AFB₁. For this purpose, the two receptors OTA-peptide-I and AFB₂-CMO-peptide were immobilized on an activated glass chip. Liquid samples supplemented with 20% MeOH (v/v) were used for simulating real extracts.

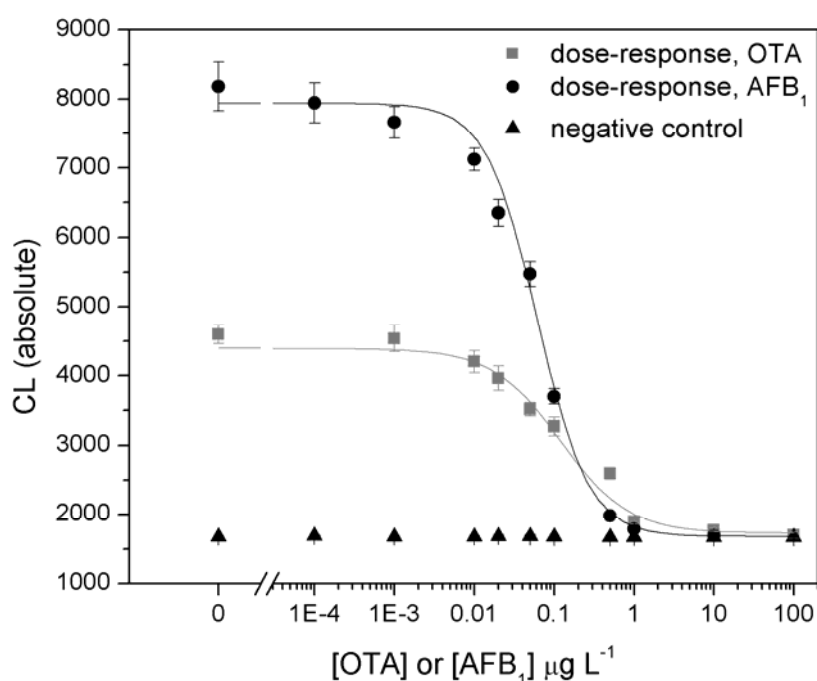


Figure 49 MCR 3-generated dose-response curve for OTA (■) and AFB₁ (●) on the same biochip, calibrants prepared in MeOH-buffer (20% MeOH, 80% PBS v/v). Negative control (▲): blank spotting buffer. Experimental points average of 5 CL signals, error bars standard deviation associated. For OTA, A₁ = 4393 ± 152; A₂ = 1727 ± 18; IC₅₀ = 0.12 ± 0.02 µg L⁻¹; and p = 1.02 ± 0.09 (n = 10; m = 5; R² = 0.96981). For AFB₁, A₁ = 7941 ± 14; A₂ = 1680 ± 14; IC₅₀ = 0.06 ± 0.00; and p = 1.35 ± 0.06 (n = 10; m = 5; R² = 0.998).

This experiment shows that it is indeed possible to simultaneously determine the two toxins with the MCR 3 platform. As a first estimation, it can be said that the IC₅₀ values of 0.12 and 0.06 µg L⁻¹ for OTA and AFB₁ respectively are also adequate for detecting these toxins in real

samples. If a raw food sample is extracted with 80% MeOH, for example (usual for peanut samples^[190]), the extract would need to be further diluted by a factor of 4-3 to reach a final MeOH concentration of 20-25% (v/v), so that the antibodies used for detection remain functional. Depending on the original sample-to-solution ratio, a total dilution factor of 20 to 30 would be needed. For OTA and for AFB₁ or total AFB content, this would imply IC₅₀ values of 3.6 and 1.8 µg kg⁻¹ respectively at the maximum dilution, values which are under the MRLs of several food commodities. Nevertheless, matrix effects are usually detrimental to the assay performance and the IC₅₀ values found in spiked solution are often lower than when testing real samples, a point that should always be taken into consideration. Finally, the LODs and the two working concentration ranges for the toxins of interest in the buffer-based models are shown in table 16.

Table 16 Parameters for OTA and AFB₁ determination, simultaneous measurements

	OTA signal	[OTA] µg L ⁻¹	AFB ₁ signal	[AFB ₁] µg L ⁻¹
80% signal intensity	3860	0.03	6689	0.02
20% signal intensity	2260	0.47	2932	0.17
LOD	3935	0.03	7899	0.002

3.3.2 Dual Signal Stability with Peanut Extract

For the next step in multiple toxin detection, a foodstuff susceptible to contamination with the two toxins AFB₁ (or AFB₁+AFB₂) and OTA was chosen. Nuts and nut products are foods that usually fall into this category. In our experiments, peanuts were chosen as a “pilot matrix” and as a representative of the nut products. It is well-known that the poisonous aflatoxins of the class B and G typically contaminate peanuts and other types of nuts such as hazelnuts, pistachio and almonds.^[191] Although simultaneous OTA contamination is not frequent, cases have been documented in the literature since 1985^[192], and the need for multimycotoxin screening in these commodities has been recently recognized.^[193-195]

Regeneration non-competitive immunoassays were conducted on a chip spotted with the two receptors of interest on the MCR 3. Figure 50 records the signal intensity along sequential assay cycles, as well as the negative control. As can be seen, signal decrease is evident and does not plateau at any point. The absolute CL signal intensity decreases to 38% (OTA-

peptide) and 50% (AFB₂-CMO-peptide) of its starting value by regeneration cycle no. 20, which makes the assay unsuitable for toxin detection. The conditions used in this assay were very similar to those optimized for green coffee, the only difference being that the primary antibody solution (1F2 and 5G9) was pumped simultaneously with the blank peanut extract, instead of the coffee extract (20% MeOH, v/v) into the incubation loop. Therefore, the steep signal decrease can only be attributed to the matrix effect on the biochip surface. Based on our previous experiments, the possibility of insufficient surface regeneration and/or inadequate analyte immobilization may be excluded.

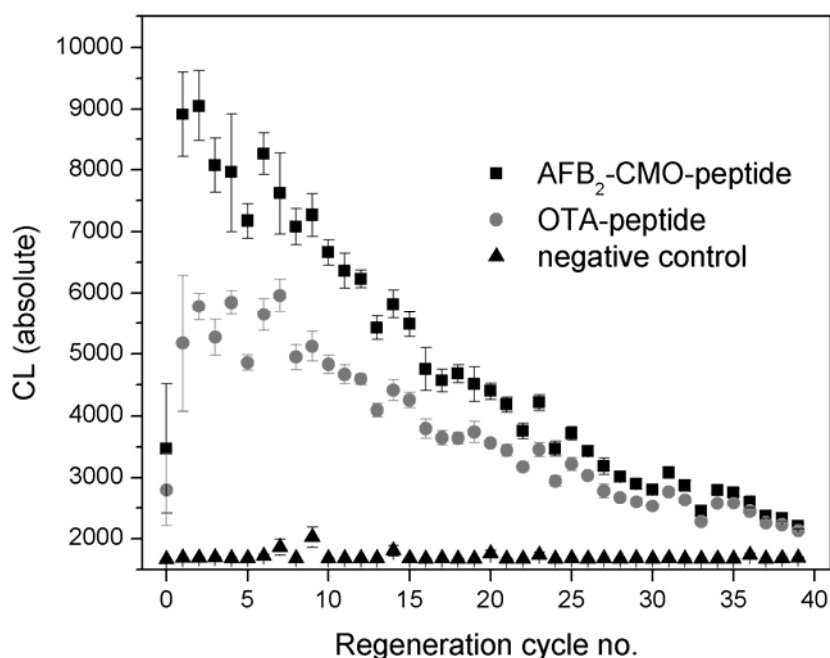


Figure 50 Non-competitive, regeneration assay in blank peanut matrix for the simultaneous detection of OTA and AFB. Signal decrease along 40 cycles.

In order to tackle the signal decrease, attention was again directed to the regeneration step. As mentioned before, sufficient regeneration had already been evidenced with the glycine buffer, pH 3.5, so the question was not if antibody removal had been complete at the end of the assay cycle, but rather whether the matrix components present in the peanut extract had been thoroughly eliminated. The fat and the diverse proteins present in peanuts may be hard to remove from both MCR 3 components (tubing, input syringe and valve openings) and from the PEG-coated surface of the biochip. Therefore, a commercial enzyme-anionic tenside mixture (Tergazyme[®]) was tested to this end. According to the manufacturer, the use of this powder detergent is recommended for cleaning proteinaceous soils and fat from glass and

plastics, among other applications. For the specific requirements of the MCR 3 it was also important that the substance be corrosion-inhibited so that contact with the few metal components of the instrument (valve head joints, flow cell drawer) would not be counterproductive. Figure 51 shows again a multiple cycle, non-competitive assay, this time using the new detergent as regeneration agent. It is important to note that a pH of 9.4 was measured shortly before starting the experiment and the solution was prepared fresh, since the active enzyme present is slowly inactivated in aqueous mixtures. As can be noticed from the graph, the signal is far from achieving stability, this time gradually increasing until it reaches a peak, and then slowly decreasing to 45% and 50% of its peak value for the AFB₂-CMO-peptide and the OTA-peptide, respectively.

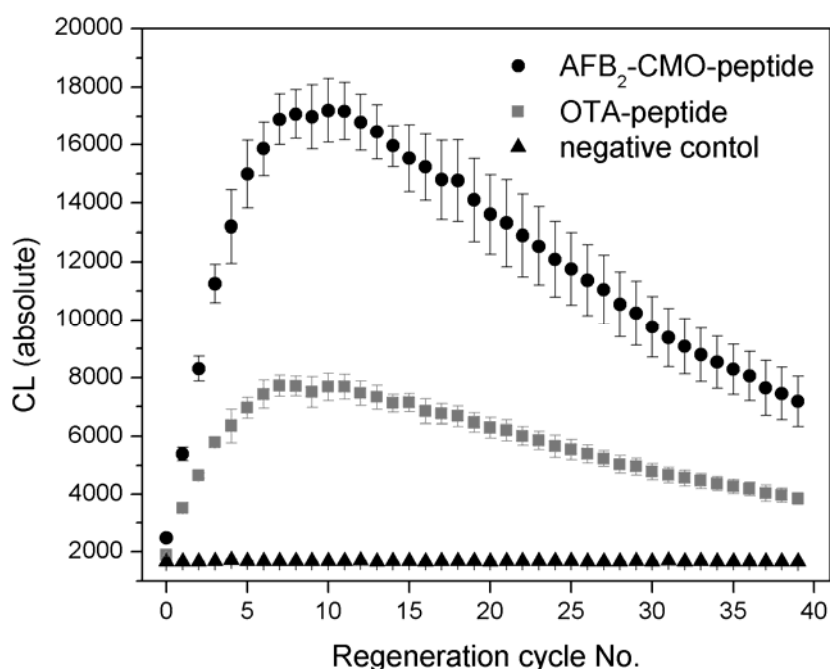


Figure 51 Non-competitive, regeneration assay in blank peanut extract for the simultaneous detection of OTA and AFB. Signal decrease along 40 cycles. New regeneration buffer: Tergazyme.

In conclusion, the specialty-detergent solution tried for regeneration does not seem to improve the regenerability of the biochip sensor or remove possible peanut matrix components that might be accumulating on the chip surface. This might make antibody access to both immobilized haptens difficult. Since it was not possible to obtain a fairly constant CL signal for the biochip along a number of measuring cycles that would at least allow for system calibration and sample determination, the system was deemed too unreliable and further development must be carried out in this respect. The reason for the signal instability is not

completely clear, but increasing the washing steps or modifying the already optimized program for the MCR 3 would have inevitably resulted in longer assay times. Nevertheless, under the present conditions, proof of principle was still provided that at least two toxin-like haptens with a peptide-linker anchoring motive can be simultaneously immobilized and used for ic-immunoassay formats on the MCR 3 for the detection of AFB₁ (AFB₂, or AFB₁+AFB₂) and OTA. As with most ELISA-based procedures, sample preparation and/or sample cleanup may need to be optimized and adapted in order to obtain a reproducible signal. On the other hand, the double-toxin assay may still be successful for other type of foods where AFB₁, AFB₂ and OTA are usually present. Grains such as wheat, oats and rice are examples of such crops. Since the fat content in these products is considerably less than in peanuts, an MCR 3-based application to detect multiple toxins might be better realizable.

3.3.3 Further Developments in MCR 3 Assay Formats for Reducing Measuring Time

Another possibility to shorten the measuring time in the MCR 3 is the use of HRP-labeled specific antibodies for immunoassays: both for the indirect competitive format and for other non-competitive assay types. Regardless of the format, crucial for the success of the assay is, of course, that the antibodies also present high affinity and selectivity towards their target. This type of variation involving HRP-tagged antibodies was also explored in the present work in order to provide proof of principle of the assay functionality. For this purpose, the antibody 3A7, AFB₂-specific and also produced and characterized at the IWC was put to the test in an ic-immunoassay. This antibody is cross-reactive with AFB₁ only to an extent of 37%, therefore the immunoaffinity experiments were conducted exclusively in the presence of AFB₂. Under optimized conditions, (MTP-based ic-ELISA) the minimum AFB₂ concentration at half-dose response was $30 \pm 10 \text{ ng L}^{-1}$.^[153] Figure 52 presents a brief scheme of the standard procedure used to couple HRP and the antibody 3A7. In this method, the polysaccharide component of HRP, a glycoprotein, is submitted to a mild oxidation to generate free aldehyde groups, which in turn react spontaneously with the amino groups present in the antibody to be conjugated.^[196] Activating the glycan portion (the polysaccharide component) of HRP is considered advantageous compared to other cross-linking procedures because this allows the conjugation reaction to be directed away from amino acids in the polypeptide chain that may be critical for protein activity.^[197] In particular, the mild oxidant sodium *meta*-periodate selectively cleaves the bond between two adjacent *cys*-glycols,

effectively oxidating them to the aldehyde and leaving other functional groups in the HRP intact. Coupling to the antibody of interest follows through imine formation and subsequent reduction of the bond with sodium cyanoborohydride to effectively convert the aldehyde into a secondary amine.

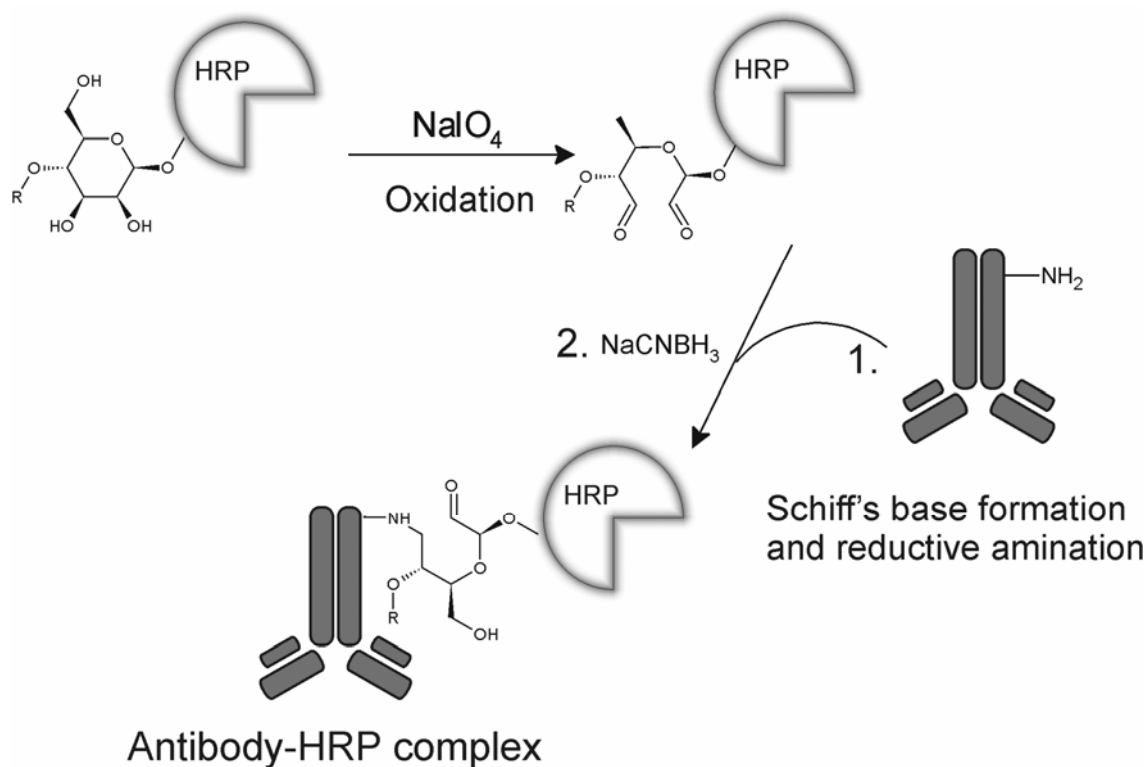


Figure 52 Antibody coupling with HRP.

After carrying out the coupling reaction between HRP and the specific antibody the product was extensively dialyzed against buffer with the aid of centrifugal filters. This step served the purpose of eliminating excess reagents (particularly unreacted HRP). The resulting solution was finally purified by size exclusion chromatography on dextran gel. The coupling of HRP to the antibody was confirmed by matrix-assisted laser desorption/ionization time-of-flight mass spectrometry (MALDI-TOF-MS). The single HRP-antibody conjugation product was detected in the purified sample with an m/z of 63749 ($[\text{M}+3\text{H}]^{3+}$, AB-HRP calculated m/z of 63774). Although the presence of a triple charged ion in MALDI-MS may sound unusual, examples are available where this is nevertheless the case.^[198] As frequently observed for most coupling procedures, the extent of conjugation depends on the number of surface-accessible reactive groups (amino groups, in the case of the antibody), as well as on the coupling technique and on the coupling time.^[199-201] In this case, a 1 to 1.9 ratio of antibody to activated HRP was used.

The amount of generated HR-labeled antibody was measured by carrying out a quantitative colorimetric protein assay, a so-called “bicinchoninic acid assay” (BCA).^[202, 203] The assay’s principle is that the peptide bond and the amino acid residues tryptophan, cysteine and tyrosine present in proteins are capable of reducing Cu^{2+} to Cu^+ in basic solution. Cu^+ then forms a violet complex with BCA that presents an absorbance maximum at 562 nm. This protein assay is calibrated with known amounts of BSA and is also useful for determining the amount of protein concentration in an antibody solution. It was important to know the approximate concentration of the final HRP-labeled antibody because only then was it possible to compare its efficiency against the original, unlabeled antibody.

After determining the concentration of the original antibody solutions (3A7 and 3A7-HRP) parallel ic-immunoassays were carried out for the two antibodies, both in microtiter plate format and in the MCR 3. The final concentrations of the work solutions were approximately 180 and 200 $\mu\text{g L}^{-1}$ for 3A7 and 3A7-HRP, respectively. The detailed optimized procedures to determine coating-conjugate and antibody concentrations for ELISA and for the MCR3 were very similar to that described for OTA in the previous chapter. The optimization also considered a final MeOH content of 20% (v/v), taking into account that extraction of a matrix would most likely be conducted out in a MeOH solution and should be further diluted for the immunoassay.^[204]

Figure 53, 54 and table 17 present the dose-response curves and assay parameters for 3A7 and 3A7-HRP performed in each case with the microtiter plate format and the MCR 3 format. It is to be noticed that in both methods the AFB_2 concentration at half-dose response is significantly lower for the HRP-labeled antibody than for the unlabeled counterpart. Emphasis should be made that, to the best of our knowledge, very similar concentrations of both antibodies were used for the comparison and the experimental conditions were identical. The maximum signal intensity at zero AFB_2 concentration is nevertheless different for the two methods: in the MCR 3-based ic-immunoassay, the 3A7-HRP method (labeled primary antibody) delivers a higher signal than its unlabeled counterpart. This order is reversed for the MTP-based methods, where the highest signal is afforded by the unlabeled antibody procedure, which could mean that blocking the surface to avoid unspecific binding of HRP-labeled antibodies is probably more efficient in the MCR 3 assay. Surprisingly enough, the flow-through assay affords better sensitivity and lower IC_{50} concentrations, as well as lower LOQs. Needless to say, the influence of matrix effects would also need to be tested in order to confirm these preliminary results.

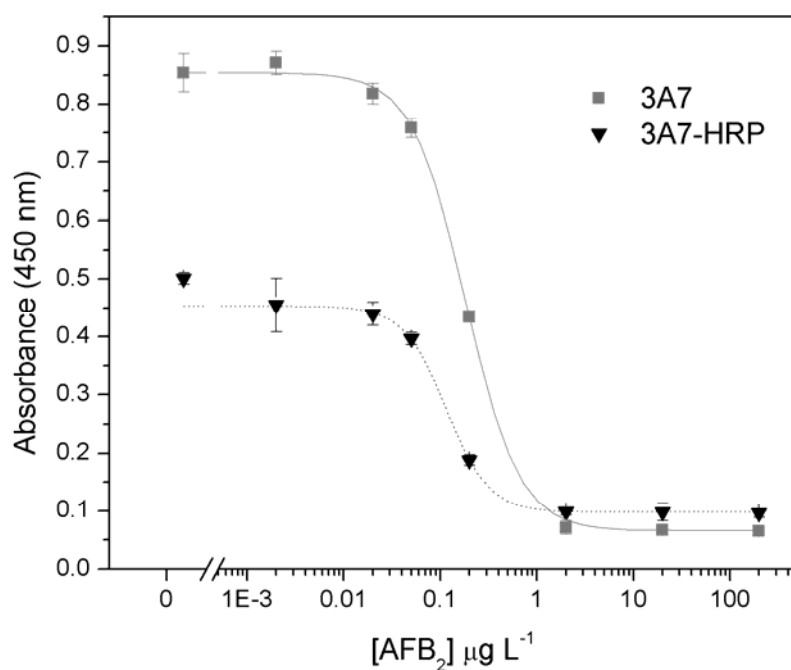


Figure 53 MTP-based ic-ELISA for the detection of AFB₂ in peanut matrix: comparison of antibodies 3A7 and 3A7-HRP.

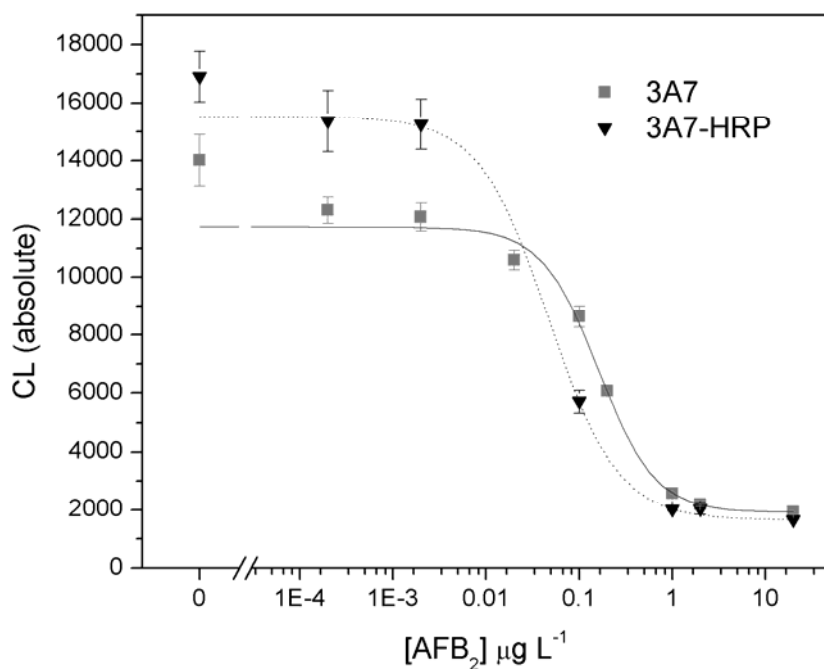


Figure 54 MCR 3-based ic-ELISA for the detection of AFB₂ in buffer-MeOH solution: comparison of antibodies 3A7 and 3A7-HRP.

Table 17 Summary of parameters for ic-immunoassays for the detection of AFB2: comparison of methods using the antibodies 3A7 and 3A7-HRP.

	ELISA IC₅₀ (µg L⁻¹)	LOD (µg L⁻¹)	LOQ (µg L⁻¹)
3A7	0.18 ± 0.01	0.03	0.08
3A7-HRP	0.12 ± 0.01	0.05	0.06
	MCR 3 IC₅₀ (µg L⁻¹)	LOD (µg L⁻¹)	LOQ (µg L⁻¹)
3A7	0.16 ± 0.01	0.03	0.06
3A7-HRP	0.05 ± 0.01	0.01	0.01

Finally, one benefit of the method developed for the HRP-labeled primary antibody over the regular, two-step method (specific antibody followed by secondary HRP-labeled antibody) is that the first method effectively saves three minutes of assay time per sample. This is because the time-saving sequence omits one washing step and the secondary HRP-labeled antibody tracing step. Therefore, proof of principle has been given that for the MCR 3 method, the use of labeled specific antibodies affords better LODs and LOQs than the equivalent 2-step procedure with non-labeled antibodies, both in the ELISA format and in the MCR 3 format. An improvement in the measuring time is also an advantage for applications where the measuring has to be kept to a minimum. In this case, the assay time could be further reduced by three minutes.

4 Summary and Outlook

Access to safe food sources is a universal right of individuals that requires the establishment and application of quality standards in every aspect of the food production chain. Mycotoxin contamination of important food crops has been known to pose a serious threat to human health since 1960. Therefore, efforts to limit the ingestion of mycotoxins by human beings have motivated the development of several analytical methods for their detection, as well as the harmonization of legislation prescribing maximum permissible contamination levels for relevant foods in most of the industrialized world. In particular, the mycotoxin ochratoxin A (OTA) is a common contaminant of important grains, dried fruits, wine, beer, nuts and coffee. OTA is a proven nephrotoxic substance, causes urinary tract tumors and is most likely responsible for the fatal disease known as “Balkan Endemic Nephropathy”. Furthermore, it is strongly suspected to be carcinogenic and genotoxic as well. Although several analytical procedures have already been optimized to detect and quantify OTA in the relevant food matrices, the need still exists for fast, reliable, and if possible fully automatized screening methods capable of delivering results in the μg per kg of product range.

Most of the validated methods for the detection of OTA and other mycotoxins in food samples comprise several steps that may include the removal of interfering matrix components before the actual analysis is performed. HPLC-based procedures with either spectroscopic or mass spectrometric detection are usually carried out after immunoaffinity chromatography enrichment. Not only are these procedures time-consuming and labor-intensive, but the cartridges are expensive and can only be used once. In recent examples that apply LC-MS/MS to highly diluted food samples, the enrichment step has been successfully eliminated. Nevertheless, the cost of the equipment is prohibitive for most analysis facilities and measuring must be conducted inside a well equipped laboratory. It is in this context that immunoaffinity-based techniques such as the Enzyme Linked Immunosorbent Assay (ELISA) have proven very useful and versatile. In comparison to other instrumental methods they are inexpensive, fast and may even be used in complex samples without the need of immunoaffinity cleanup. The MCR 3 technology developed at the IWC combines a miniaturized version of the heterogeneous immunoassay in the shape of a small glass sensor and the analytical instrument designed to store and automatically dispense the required reagent solutions in a user-programmable way. The general aim of this project was to explore some of the possibilities that this technology offers for the efficient screening of mycotoxins – particularly OTA –in complex food matrices.

Part one of this work dealt with modifications made to the MCR 3, considered necessary for mycotoxin determination. The original instrument was developed to screen for the relatively water-soluble antimicrobial residues in raw, undiluted milk. Not only are mycotoxins such as OTA and the aflatoxins considerably less hydrophilic, but they typically contaminate solid products. In this case, sample extraction needs to be carried out with a mixture of water and an organic solvent, usually methanol. In order to avoid cross-contamination and carry-over along different assay steps, the one-time-use plastic syringe for sample input of the originally developed MCR 3 unit was exchanged with the more inert glass equivalent. Instrument programming was accordingly modified in order to guarantee sufficient washing (and therefore avoid carry-over) and to make the most of measuring time. The differences consistently observed in signal intensity distribution along the two measuring chambers of the flow cell could not be overcome for the originally planned format that would simultaneously use two measuring chambers. Nevertheless, the problem was avoided by consistently using one cell for measuring and the remaining cell for washing. Regarding the chip biosensor, a novel method for receptor immobilization adequate for small analytes was designed by means of a 4-residue peptide linker presenting one nucleophilic lysine residue at the opposite end from the coupled toxins (OTA and a modified version of AFB₂). This linker proved adequate for immobilization on the previously developed amino-PEG surface. The random structure of the linker, as well as the covalent nature of the bond to the glass surface, opened the doors to a truly regenerable sensor, sufficiently robust to withstand the relatively harsh regeneration conditions that would otherwise denature a protein-hapten conjugate and negatively influence the reusability of the biochip. Several choices of regeneration buffer were considered and removal of the detection antibodies was ensured with experiments that tested all possibilities. Most importantly, the problem of signal decrease along sequential and independent non-competitive immunoassays was successfully dealt with in order to guarantee a stable signal along at least 20 regeneration cycles. Finally, the technical details pertaining to the biochip production (spotting conditions and chip treatment) were also fine-tuned.

Part two of this work regarded one practical application of the developed immobilization method and the perfected programming of the MCR 3 for the detection of OTA in green coffee samples. First of all, a suitable anti-OTA antibody was selected. For this purpose, a classical microtiter plate-based ELISA (indirect competitive format) was used as a means to compare the half-dose response of four available specific monoclonal antibodies. The three commercial antibodies tested showed similar affinities at optimized plate conditions and only the fourth antibody (made available as a kind gift from Prof. Märtlbauer) presented

comparatively lower affinity. The ELISA method proved to be useful for the measuring of OTA in raw green coffee extract as well. To guarantee the constant supply of blank green coffee along the MCR 3 development phase, a batch of 1 kg of commercial goods was tested for OTA contamination with a well-established, IAC-HPLC (FD) procedure. After the sample was confirmed free of OTA (LOD of method 0.08 μg OTA per kg coffee), it was consequently used for OTA spiking and calibration in combination with the MCR 3-based procedure.

Instrumental development included the search for an adequate positive control on the biochip. A peptide-derivatized biotin was immobilized and a constant positive control signal was achieved by supplementing an HRP-labeled anti-biotin antibody with the secondary HRP-marked tracer in the MCR 3 functional assay. Other controls tested for this purpose (immobilized DNP detected with anti-DNP antibody and immobilized biotin detected with HRP-coupled streptavidin) proved unsuitable. Preliminary dose-response curves were generated for OTA in spiked buffered methanol solutions, showing an adequate IC_{50} value of 0.48 $\mu\text{g L}^{-1}$ and a constant signal along multiple regeneration cycles. This was not the case with green coffee extract, where a decrease in the signal intensity in sequential individual (non-competitive) assays was recorded. The decrease amounted to 23% absolute signal loss along 20 regeneration cycles. It was concluded that the green coffee extract had a detrimental effect on the surface properties of the biosensor chip that could not be avoided. Because signal consistency had been previously demonstrated for a methanol-buffer system, the possibility that the receptor immobilization and/or the solutions used along the assay might be causing the signal decrease could be reasonably excluded. Regardless of the slight but constant signal loss, it was judged that the system should still be put to the test in recovery rate experiments. Solid green coffee samples were spiked with known amounts of OTA and extracted according to usual procedure. After calibrating the instrument and measuring these samples, recovery rates ranging from 100 % to 210 % were obtained. It must be pointed out that no false negatives were detected. Mainly, the least contaminated samples were the ones that tended to be overestimated; the cause of this would be the slight but constant signal decrease when one single biochip is used for system calibration and sample measurement. Nevertheless, the recovery rates encountered are not unusual for immunoaffinity-based procedures. Going one step further, 18 naturally contaminated and extracted samples were also measured in the MCR 3. Overall, the results show a tendency to overestimate the OTA content in the measured real samples. However, the results were considered inconclusive, since the samples were stored and shipped at least two weeks after extraction had taken place

and the author of this work noticed a significant change of their appearance during the time needed for sample processing and measurement. In order to better appreciate the applicability of the developed method, measurements must be conducted shortly after real sample extraction, preferably in cooperation with the project partner in Hamburg, Eurofins WEJ Contaminants GmbH. To complete this section, a comparison of the optimized method was made with other methods reported in the literature specific for OTA detection in coffee. The developed assay presents the advantages of cost-efficiency, making use of a reusable, regenerable sensor biochip. The time needed for one measurement, 12 min after instrument calibration, is considered adequate and competitive. Values in the range of 4 – 6 and 2 – 6 µg OTA per kg green coffee for the LOQ and LOD, respectively (daily fluctuations included) were also determined.

Part three of this work explored new assay formats in which the MCR 3 can be used for the screening of foods and food products. In particular, the possibility of measuring simultaneously two different toxins, total content of AFB₁ + AFB₂ and OTA, in one single experiment was tested. Proof of principle was given that simultaneous calibration is possible in 20% MeOH-buffer solution, with lower limits of quantification (80% maximum signal intensity) below the legal MRL of both OTA and AFB₁. These limits were calculated taking into consideration the associated dilution of the food extract. However, when a real peanut extract was tested for signal consistency (e.g. that the maximum CL signal remains constant for a number of measuring / regeneration cycles), it was evident that the signal loss would not allow for calibration and subsequent sample measurement. Changing the regeneration buffer from the original acidic solution to an enzyme-based, basic solution did not improve the signal consistency. It was concluded that further optimization (i.e. the use of a pre-clean-up step for this difficult matrix) needs to be carried out. On a side note, it should be mentioned that peanuts were chosen as a test matrix because they are susceptible to both OTA and AFB (AFB₁ and AFB₂) contamination and a good representative of nuts and nut products. Because of the positive results obtained in MeOH-buffer solution, it is predicted that the simultaneous measurement of at least AFB and OTA are possible in other, less complicated matrices, such as wheat, oats or rice (also susceptible of multitoxin contamination).

Finally, the last section of part three suggests an assay format that effectively shortens the measuring time per sample by three minutes. This was achieved by directly coupling the primary, selective antibody used in the ic-immunoassay to HRP. The assay was tested for the mycotoxin AFB₂, with an antibody that presented only 37% cross-reactivity to AFB₁.

Calibration was possible in MeOH-buffer solution, as well. It was also compared to the standard MTP-based ic-ELISA and the results were consistent. If specific antibodies are available, and provided that the cross-reactivities towards other analytes that may be present in the sample are small, the multiple screening of toxins on the MCR 3 platform can be made more time-efficient using this strategy.

5 Experimental

Instruments

Analytical balance (AT261 Mettler Delta Range, Mettler-Toledo, Gießen)

Bio-Odyssey Calligrapher Miniarrayer (Bio-Rad, Munich)

Centrifuge (Universal 320R, Hettich Centrifuges, Tuttlingen)

Drying cabinet (Type UM 400, Memmert, Schwabach)

Microplate reader (Synergy HT, Bio-Tek Instruments, Bad Friedrichshall)

Microplate washer, 96 channels (ELx405 Select, Bio-Tek Instruments, Bad Friedrichshall)

Munich Chip Reader 3 (GWK Präzisionstechnik GmbH)

pH-meter (Hanna, Eurotronik, Friedewald)

Rotary evaporator (RE 111, Büchi, Flawil, Switzerland)

Schlenk line

Shaker for microtiter plates (EAS 2/4, SLT, Crailsheim)

Shaker incubator (C24KC, Edison, New York, USA)

Stem blender (IKA-Werk A10, 180 W)

Ultrapure water filter (Millipore, Schwalbach)

Ultrasonic bath (Sonorex RK 102, Bandelin, Berlin)

UV-vis spectrophotometer (DU 650 UV, Beckman, Fullerton, USA)

Vortexer (REAX top, Heidolph, Schwabach)

Analytical HPLC:

(for OTA detection in green coffee)

Analytical HPLC-column Luna C18, 5 μ m, 250 x 4.60 mm ID (Phenomenex, Aschaffenburg)

Autosampler SIL-20A (Shimadzu, Neufahrn)

Column guard Gemini C18, 10 x 10 mm ID (Phenomenex, Aschaffenburg)

Column oven CTO-20A (Shimadzu, Neufahrn)

Degassing unit DGU-20A (Shimadzu, Neufahrn)

Fluorescence and UV/Vis detector RF-10AxL (Shimadzu, Neufahrn)

High-pressure mixing system with ternary gradient pump LC-20 (Shimadzu, Neufahrn)

Liquid chromatograph unit LC-20AT (Prominence, Shimadzu, Neufahrn)

Preparative HPLC:

(for analyte-peptide conjugate purification)

Degassing unit ERC-3415? (ERC Inc., Saitama, Japan)

Fraction collector INTEE (Polymer Laboratories, Shropshire, United Kingdom)

High-pressure mixing system with dual gradient pump L-6200° (Merck, Darmstadt)

PC-card LC421 (Software für Chromatographie und Prozessanalytik GmbH, Weyhe-Leeste)

Semipreparative HPLC-column Gemini C18, 5 µm, 150 x 10 mm ID (Phenomenex, Torrance, USA)

Six-port valve injector 7125 (Rheodyne, Rohnert Park, USA)

UV/vis-detector L-4250 (Merck, Darmstadt)

Mass Spectrometry:

LC-ESI/APPI-Orbitrap-mass spectrometer (Exactive, Thermo Scientific, Inc.)

LCT-ESI-TOF-mass spectrometer with Z-spray source (Waters/Micromass, Milford, MA)

Software

ACD/ChemSketch Freeware (ACD/Labs, Toronto, Canada)

Avis FITS Viewer (MSB di F. Cavicchio, Ravenna, Italy)

BioOdyssey Calligrapher 2.0 (Bio-Rad Laboratories GmbH, Munich)

Chromstar 6.3 (Software für Chromatographie und Prozessanalytik GmbH, Weyhe-Leeste)

Gen5 (BioTek, Bad Friedrichshall)

ImageJ (National Institute of Mental Health, Bethesda, MD, USA)

LabVIEW 8.2 (National Instruments, Austin, TX, USA)

LCsolution (Shimadzu, Neufahrn)

Origin 7G (MicroCal Inc., Northampton, MA, USA)

SIP 0.4 (Karsunke Softwarebüro, Wolnzach)

Antibodies and Antigens

Commercially available:

anti-biotin, polyclonal antibody, goat, HRP-linked (7075, New England BioLabs, Beverly, MA, USA)

anti-mouse Ab IgG, H+L, horse, HRP-linked (VC-PI-2000, AXXORA Germany GmbH, Lörrach)

anti-OTA: MAb (LC Tech GmbH, Dorfen)

anti-OTA: MAb 5E2 (Soft Flow Biotechnology, Gödöllő, Hungary)
anti-OTA: MAb 5G9 (Soft Flow Biotechnology, Gödöllő, Hungary)
anti-TNT: MAb A1 (D1930M000-AM, Strategic Diagnostics Inc., Newark, DE, USA)
streptavidin, HRP-linked (VC-SA-5004, AXXORA Germany GmbH, Lörrach)

In-house produced:

AFB₂-CMO-BSA

AFB₂-CMO-TG

anti-AFB₁, AFB₂: Mab 3A7

anti-AFB₁: Mab 1F2

anti-AFB₂-HRP: Mab 3A7, HRP-linked

OTA-BSA

Chemicals

2,4,6-trinitrobenzenesulfonic acid solution, 1% in DMF (92824, Sigma-Aldrich, Steinheim)
3,3',5,5'-tetramethylbenzidine (860336, Sigma-Aldrich, Steinheim)
3-glycidyloxypropyltrimethoxysilane (50040, Sigma-Aldrich, Steinheim)
4-(dimethylamino)pyridine (29224, Sigma-Aldrich, Steinheim)
acetic acid (320099, Sigma-Aldrich, Steinheim)
acetone, laboratory reagent (179973, Sigma-Aldrich, Steinheim)
acetonitrile, HPLC grade (34998, Sigma-Aldrich, Steinheim)
acetonitrile, LC-MS grade (34967, Sigma-Aldrich, Steinheim)
aflatoxin B₁, solid (A6636, Sigma-Aldrich, Steinheim)
aflatoxin B₂, solid (A6636, Sigma-Aldrich, Steinheim)
albumin from chicken egg white (A5503, Sigma-Aldrich, Steinheim)
argon 4.6 (Air Liquide, Munich)
bovine serum albumin (A3059, Sigma-Aldrich, Steinheim)
casein (C5890, Sigma-Aldrich, Steinheim)
diamino poly(ethyleneglycol), M~2000 g/mol (XTJ 502, Huntsman, Rotterdam, The Netherlands)
dichlormethane, for peptide synthesis (66738, Sigma-Aldrich, Steinheim)
diethyl ether (32203, Sigma-Aldrich, Steinheim)
dimethylsulfoxide (41647, Sigma-Aldrich, Steinheim)
dioxane (42510, Sigma-Aldrich, Steinheim)

ethanol (32205, Sigma-Aldrich, Steinheim)
ethanolamine (02400, Sigma-Aldrich, Steinheim)
formic acid, p.a. for MS (94318, Sigma-Aldrich, Steinheim)
glycerol (G5516, Sigma-Aldrich, Steinheim)
glycine (G6201, Sigma-Aldrich, Steinheim)
Hellmanex II solution (Hellma, Müllheim)
horseradish peroxidase (814393, Roche, Basel, Switzerland)
hydrochloric acid, fuming, 37% (84422, Sigma-Aldrich, Steinheim)
hydrogen peroxide 30% (95321, Sigma-Aldrich, Steinheim)
hydrogen peroxide solution for chemiluminescence imaging (XLSE2L, 0250, Cyanagen, Bologna, Italy)
luminol solution for chemiluminescence imaging (XLSE2L, 0250, Cyanagen, Bologna, Italy)
N,N'-dicyclohexylcarbodiimide (D80002, Sigma-Aldrich, Steinheim)
N,N'-diisopropylethylamine (496219, Sigma-Aldrich, Steinheim)
N,N'-dimethylformamide (40258, Sigma-Aldrich, Steinheim)
N,N'-disuccinimidyl carbonate (43720, Sigma-Aldrich, Steinheim)
NI-(2,4-dinitrophenyl)-1,2-ethanediamine (15083, ChemPur Feinchemikalien, Karlsruhe)
N-hydroxysuccinimide (130672, Sigma-Aldrich, Steinheim)
N- α -Fmoc-glycine (04-12-1001, Novabiochem, Darmstadt)
N- α -Fmoc-*N*- ϵ -biotinyl-L-lysine (04-12-1237, Novabiochem, Darmstadt)
N- α -Fmoc- ϵ -tboC-L-lysine (04-12-1026, Novabiochem, Darmstadt)
N- α -Fmoc- ϵ -tbutyl-O-L-serine (04-12-1033, Novabiochem, Darmstadt)
nitrogen 5.0 (Air Liquide, Munich)
O-(benzotriazol-1-yl)-*N,N,N',N'*-tetramethyluronium hexafluorophosphate (85100600, Merck, Darmstadt)
O-(carboxymethyl)hydroxylamine hemihydrochloride (C13408, Sigma-Aldrich, Steinheim)
ochratoxin A, certified standard, 10 μ g mL⁻¹ in acetonitrile (13620, LGC Standards, Luckenwalde)
ochratoxin A, solid (O1877, Sigma-Aldrich, Steinheim)
poly(ethyleneglycol) diglycidyl ether 526 Da (475696, Sigma-Aldrich, Steinheim)
potassium dihydrogen citrate (60214, Sigma-Aldrich, Steinheim)
potassium dihydrogen phosphate (60220, Sigma-Aldrich, Steinheim)
potassium hydrogen phosphate (04248, Sigma-Aldrich, Steinheim)
potassium sorbate (85520, Sigma-Aldrich, Steinheim)

rink amide resin (NovaPEG, 01-64-0473, Novabiochem, Darmstadt)
sodium azide (S2002, Sigma-Aldrich, Steinheim)
sodium carbonate (71628, Sigma-Aldrich, Steinheim)
sodium chloride (13565, Sigma-Aldrich, Steinheim)
sodium cyanoborohydride, 5M solution in 1M NaOH (296945, Sigma-Aldrich, Steinheim)
sodium dodecylsulfate (71728, Sigma-Aldrich, Steinheim)
sodium hydrogen carbonate (71628, Sigma-Aldrich, Steinheim)
sodium hypochlorite solution, 10% (71696, Sigma-Aldrich, Steinheim)
sodium periodate (311448, Sigma-Aldrich, Steinheim)
sulfuric acid, concentrated, 95-98 % (435589, Sigma-Aldrich, Steinheim)
Tergazyme, enzyme detergent (860336, Sigma-Aldrich, Steinheim)
tetrahydrofuran (34865, Sigma-Aldrich, Steinheim)
thyroglobulin (89385, Sigma-Aldrich, Steinheim)
trifluoroacetic acid, for synthesis and HPLC (91707, Sigma-Aldrich, Steinheim)
triisopropylsilane (92095, Sigma-Aldrich, Steinheim)
Trizma base, Tris (T6066, Sigma-Aldrich, Steinheim)
Tween 20 (8.17072, Merck, Darmstadt)

Miscellaneous

Double-sided adhesive sheets (ARcare 90106, Adhesive Research Ireland Ltd., Limerick, Ireland)
Immunoaffinity columns for OTA determination (OchraTest, Vicam, Watertown, MA, USA)
Microtiter plate, 384-well, 30 μ L, polystyrene, flat bottom (788101, Greiner Bio-One, Frickenhausen)
Microtiter plate, 96-well, 300 μ L, high binding, flat bottom (655061, Greiner Bio-One, Frickenhausen)
Microtiter plate, 96-well, 300 μ L, low binding, flat bottom (655201, Greiner Bio-One, Frickenhausen)
PMMA opaque slide supports (in-house produced)
Protein assay reagent kit (Micro BCATM 23235, Thermo Fisher Scientific, Rockford, USA)
Solid printing heads SNS 9, 12 and 15 for Bio-Odyssey Caligrapher (Array-it Corporation, Sunnyvale, California, USA)

Buffer solutions

For this work, only ultrapure, demineralized water was used in the preparation of the required buffers.

Substrate solution:

273 μL of the TMB stock solution (375 mg of TMB in 5.00 mL DMSO), 138 μL of a 1% H_2O_2 water solution (v/v) and 15.0 mL of substrate buffer were mixed shortly before plate development.

Stop solution:

5 % conc. sulfuric acid in water (v/v)

TRIS regeneration buffer (pH 8,5):

121.14 g Trizma®Base dissolved to a total volume of 1000 mL in water, pH adjusted with concentrated hydrochloric acid

Carbonate buffer (pH 9,6):

42.01 g NaHCO_3 dissolved to a total volume of 2500 mL in water

Coating buffer:

3.98 g Na_2CO_3

7.33 g NaHCO_3

0.50 g NaN_3

dissolved to a total volume of 2500 mL in water

Coating buffer concentrate (without NaN_3 , 10 times concentrated):

1.59 g Na_2CO_3

2.93 g NaHCO_3

dissolved to a total volume of 100 mL in water

PBS buffer:

3.40 g KH_2PO_4

30.48 g K_2HPO_4

21.25 g NaCl

dissolved to a total volume of 2500 mL in water

Regeneration buffer (pH 3,0):

15.014 g glycine

11.688 g NaCl

0.1 % SDS (w/v)

dissolved to a total volume of 2000 mL in water

Substrate buffer:

115.10 g potassium dihydrogen citrate

0.25 g potassium sorbate

dissolved to a total volume of 2500 mL in water

Washing buffer concentrate:

8.17 g KH_2PO_4

73.16 g K_2HPO_4

52.60 g NaCl

30.0 mL Tween 20

dissolved to a total volume of 1000 mL in water

Washing buffer:

42 mL of washing buffer concentrate dissolved to a total volume of 2500 mL in water

Standard Procedures

Synthesis of mycotoxin-protein conjugates for ELISA on microtiter plates

OTA-protein conjugates for ELISA immobilization were synthesized by OTA activation and further coupling to ϵ -amino groups of the lysine residues on BSA, TG and OVA.

Synthesis of OTA-NS

The N-oxysuccinimide ester of OTA (OTA-NS) was synthesized according to the following procedure: 10 μl of an NHS solution (390.7 mM, 3.91×10^{-3} mmol, 1.13 equivalents in dioxane) and 10 μL of a DCC solution (319.8 mM, 3.20×10^{-3} mmol, 0.92 equivalents in dioxane) were given to 1.42 mg of OTA (3.47×10^{-3} mmol, 1.00 equivalents) in 200 μL of dry dioxane. The reaction was shaken and kept under argon atmosphere for 20 h. After ca. 45

min the formation of fine needles became apparent; most likely the insoluble side product dicyclohexylurea. After removing from shaker, the reaction solution was placed in the freezer (-20 °C) and used up within the next 4 days. The supernatant of the solution containing the activated ester of OTA was used to synthesize the OTA-protein conjugates. Assuming 100% of conversion, the concentration of OTA-NS was calculated to be 15.98 mM.

Synthesis of AFB₂-CMO

Aflatoxin B₂ was derivatized via a carboxymethyl oxime as previously described in the literature.^[154] Briefly, 10 mg of AFB₂ (0.0318 mmol, 1 equivalent) and 30 mg *O*-(carboxymethyl)hydroxylamine hemihydrochloride (0.2744 mmol, 8.6 equivalents) were dissolved in 12 mL of a 1:4:1 mixture of pyridine:MeOH:water. The mixture was refluxed for 3 h and then allowed to stand overnight at room temperature. Later, the solvent was removed by rotary evaporation, followed by drying under vacuum. The solid product was dissolved in 5 mL DCM and was washed three times with 7 mL of a 5% acetic acid solution in water (v/v). After washing, the remaining solvent was evaporated with the aid of a rotary evaporator. Finally, the solid product was dissolved in 6 mL of MeOH, filtered, and crystallized from a 5% acetic acid solution in water (v/v) at 4 °C, overnight. The final product yield afforded 6.0 mg (0.0155 mmol, 49% yield) of a light yellow product.

Synthesis of OTA-BSA protein conjugate

1 mg of BSA (1.5×10^{-5} mmol, 1.00 eq) was dissolved in 125 μ L of 0.71 M NaHCO₃ buffer, pH 8.0 – 8.5, ice-cold. 41.1 μ L of OTA-NS solution (6.61×10^{-4} mmol, 44 equivalents) were added dropwise to the reaction mixture. Immediately upon addition, the solution turned yellow and cloudy. The reaction was stirred at room temperature for 3.5 h. After the reaction was judged complete, the mixture was further diluted with PBS to a total volume of 500 μ L and applied to a PD-10 size exclusion column (previously equilibrated with 50 mL of PBS) for purification. Eluting fractions (ca. 4 drops/fraction) were collected on a 96-well polystyrene microtiter plate. Absorbance was measured at 280 and 333 nm and the fractions that showed a distinct peak in both regions were pooled together in a total volume of 1 mL of PBS supplemented with 0.01% of NaN₃. Similar procedures were applied for producing and purifying the TG-OTA and OVA-OTA conjugates.

Synthesis of AFB₂-CMO-TG protein conjugate

This was carried out in two stages. Stage one consisted of the activation of the previously generated AFB₂-CMO molecule with NHS. For this purpose, 20 μL of a 0.29 M NHS solution in dioxane (5.87×10^{-3} mmol, 1.14 equivalents) were added to 400 μL of a 12.9 mM solution of AFB₂-CMO (5.15×10^{-3} mmol, 1.00 equivalent). Next, 25 μL of a 0.19 M dioxane solution of *N,N'*-dicyclohexylcarbodiimide (4.75×10^{-3} mmol, 0.92 equivalents) were added. The mixture was stirred under argon at room temperature for 20 h. The crystallization of the side product, *N,N'*-dicyclohexylurea was noticed in the shape of white needles. Of the remaining solution, 100 μL were added to 227 μL of a 0.13 mM solution of TG in buffer in the second step where the TG and the activated AFB₂-CMO-NS were conjugated. The buffer consisted of a 0.70 M solution of NaHCO₃ in water, adjusted to a pH of 7.5. The mixture was allowed to warm to room temperature and was shaken for 2 h. The protein conjugate was finally purified by size exclusion chromatography on a Sephadex G-25 column, previously equilibrated with 25 mL of PBS solution. After measuring absorbance at 360 nm of the collected fractions, the relevant fractions were pooled together, lyophilized, and further diluted to a concentration of approximately 1 mg mL⁻¹. The solution was supplemented with 0.1% sodium azide to inhibit microorganism growth.

Synthesis of HRP-anti-AFB₂ conjugate: 3A7-HRP

10 mg of HRP (2.5×10^{-4} mmol) were dissolved in 1 mL of phosphate buffer. 100 μL of a water solution of NaIO₄ (88 mM) were added to the HPR solution and allowed to react under gentle shaking in the dark for 20 min (RT). The solution changed color from brown to green upon oxidation of HRP. A Sephadex G-25 size exclusion cartridge was equilibrated with 25 mL of phosphate buffer. Upon reaction, the HRP-sodium periodate mixture was diluted to 2.5 mL with phosphate buffer and applied to the gel filtration column. 5 mL of PBS were further given to the column and fractions were collected on an MTP (6 drops / fraction). Absorption was measured at 403 nm and the absorbing fractions were pooled together. The buffer of the cleaned HRP solution was exchanged to carbonate buffer with the aid of centrifugal filtration (MWCO 10000) and the volume after concentration added up to 1 mL (to give an HRP concentration of ca. 10 mg mL⁻¹). 100 μL of monoclonal antibody 3A7 in carbonate buffer (ca. 20 mg mL⁻¹, carbonate buffer consisting of 50 mM NaHCO₃, pH 9.6) were mixed with 100 μL of the oxidized HRP solution and allowed to react under gentle shaking for 2 h (RT). After the elapsed time, 2 μL of a 5M NaBH₃CN solution in 1 M NaOH were added to the mixture and the reaction proceeded for 30 minutes. The unreacted aldehyde groups were

quenched adding 10 μL of a 1 M ethanolamine solution (pH 9.6), which was left to react for 30 additional min. The reaction solution was further diluted to a total volume of 2.5 mL and cleaned by sephadex gel filtration as previously described. The filtered conjugate solution was further concentrated to a total volume of 100 μL by means of centrifugal filtration (MWCO 50000). Finally, the conjugate concentration was determined to be $16.0 \pm 3.5 \text{ mg mL}^{-1}$ with the aid of the BCA test.^[203, 205] It is important to notice that antibodies are usually stored in phosphate buffer containing 0.02% NaN_3 , in order to prevent contamination of the solutions with bacteria or fungi^[206]. By no means should azide come into contact with HRP, since it binds irreversibly to its heme group, particularly in the presence of H_2O_2 , inhibiting its catalytic mechanism.^[207] Therefore, the storing buffer of antibody solutions must be exchanged before performing any coupling reactions with heme-containing proteins, such as HRP.

BCA assay to determine concentration of 3A7-HRP

A Micro Bicinchoninic Acid Assay (BCA) was used for this purpose.^[202] The assay was optimized for determining protein concentrations in the range of 0.5 – 20 $\mu\text{g mL}^{-1}$. For calibration, the enclosed BSA standards were diluted to concentrations from 200 to 0.50 $\mu\text{g mL}^{-1}$ (a dilution row was used). The working reagent was mixed according to the kit's instructions. The original solution of the antibody 3A7 was diluted in a proportion of 1:100 and 1:500 with PBS. The original solution of the antibody-HRP conjugate 3A7-HRP was diluted as well in a proportion of 1:100 and 1:1000 with PBS. 150 μL of the BSA calibrants and the antibody unknowns were dispensed in a 96-well MTP, followed by the addition of 150 μL per well of the freshly prepared working solution. The plate was shaken for 30 s in order to mix the reagents and was further incubated at 37 °C for 2 h. Finally, absorbance was measured at 562 nm.

Synthesis of peptide linker for mycotoxins

19 mg of rink-amide resin (0.0127 mmol, 1 equivalent) were pre-swelled for 1 h in DMF. First, the peptide linker was synthesized and stored attached to the resin for subsequent coupling to the toxins or to Fmoc-Lys(biotin)-OH. The peptide sequence Gly-Ser-Gly-Lys (GSGK) was produced by dissolving the corresponding Fmoc- and / or side chain-protected amino acid in 1 mL of a DIPEA / DMF solution (0.062 mmol or 5 equivalents of each amino acid, 22 μL DIPEA, 978 μL DMF; 2 equivalents DIPEA / equivalent amino acid, or 10 equivalent DIPEA / equivalent resin). HBTU was added to the mixture (0.061 mmol; 4.9

equivalent HBTU / equivalent resin) and the whole was given to the pre-swelled resin. Additionally, 1 mL of DMF was used to rinse the container and given likewise to the resin. The mixture was bubbled under a gentle stream of nitrogen for 20 min and then rinsed 5 times with portions of DMF (2 mL). After coupling of the Fmoc-protected amino acid, a TNBS test was carried out to check for complete coupling. For this purpose, a small aliquot of the resin was removed from the reactor and reacted with a solution of TNBS and DIPEA in DMF (20 μ L of a 1% (w/v) TNBS in DMF solution + 20 μ L of a 10% (v/v) DIPEA in DMF solution). If coupling was complete, resin beads presented a transparent appearance, otherwise they turned red. If the later was the case, the coupling was performed a second time. After satisfactory coupling, the Fmoc group was cleaved for further coupling with the next amino acid by bubbling 3 mL of a 20% (v/v) piperidine solution in DMF. The TNBS test was also carried out on the deprotected resin beads after thorough washing with five 2-mL portions of DMF. In this case, deprotection was judged complete when the few resin beads turned red immediately with the TNBS solution. After the last amino acid was coupled, the resin was successively rinsed several times with DMF, methanol, and DCM, dried under vacuum overnight and stored in a closed container at 6 °C until coupling to OTA or Fmoc-Lys(biotin)-OH took place.

Synthesis of OTA-peptide conjugates for MCR 3 measurement

5 mg of OTA (0.01241 mmol, 1 equivalent) were coupled to 1 equivalent of deprotected peptide resin. OTA was dissolved in a total of 2 mL DMF / DIPEA solution (10 equivalents DIPEA / equivalent OTA) and 0.9 equivalents of HBTU (4.2 mg) were added. The mixture was given to the resin and bubbled with nitrogen for 45 min. After coupling, the resin was successively washed with DMF, methanol, and DCM, and dried under vacuum overnight, to prepare for deprotection and product cleavage. For cleavage and deprotection, the derivatized resin beads were worked up at different concentrations of TFA. First, the resin was slurried for ca. 2 min with 5 mL of a TFA / TIS / DCM solution (10:2.5:87.5, v/v). The solution was allowed to percolate slowly through the resin bed and collected in an evaporation flask. Next, 5 mL of a TFA / TIS / DCM solution (5:2.5:92.5, v/v) were allowed to percolate slowly through the resin bed and collected with the previous 5 mL. The solution was evaporated to ca. 1 mL by blowing a gentle stream of nitrogen on the solution surface. Finally, a more concentrated TFA / TIS / DCM solution (95:2.5:2.5, v/v) was given to the resin and allowed to incubate for 30 min. The filtered solution was pooled together with the two fractions and evaporated slowly with the aid of a nitrogen stream. When the total volume had been reduced

to approximately 200 μL , the solution was transferred to a centrifuge tube and 4 mL of cold diethyl ether were added. The formation of a precipitate was immediately noticed. The mixture was shaken and subsequently centrifuged at 850 g_n for 3 min. The supernatant was discarded, another aliquot of diethyl ether was added, and the whole extraction procedure was repeated four more times. Finally, the pellet was dried and redissolved in 1 mL of 10% methanol solution in water. All the synthetic and/or evaporation steps were carried out under a closed fume hood. The product was purified by semipreparative RP-HPLC (C-18). Flow rate: 3.76 mL min^{-1} ; mobile phase: first min at 10% MeOH/water (v/v, 0.1% TFA), followed by gradient from 10% to 90% MeOH/water (v/v, 0.1% TFA) in 50 min; retention time: 15.613 min. Identity of the peptide-linked OTA hapten was confirmed by HRMS ((ESI)⁺, calculated for $\text{C}_{33}\text{H}_{42}\text{ClN}_7\text{O}_{10}$: 732.27544 [$M + \text{H}^+$]; found: 732.2746).

Synthesis of biotin-peptide conjugate for MCR 3 measurement

30 mg of Fmoc-Lys(Biotin)-OH (0.0504 mmol, 5.2 equivalents) were coupled to 1 equivalent of deprotected peptide resin. Fmoc-Lys(biotin)-OH was dissolved in 1 mL of DIPEA / DMF solution, 4.9 equivalents of HBTU (94 mg) were added and the mixture was poured in the resin bed and bubbled with nitrogen for 20 min. The resin was washed and the coupling procedure was repeated. After a negative TNBS test, the resin was deprotected again. End acetyl capping proceeded by bubbling a 50% (v/v) acetic anhydride in DCM solution for 20 min. The resin was extensively washed and dried as described above. Cleavage and deprotection followed in the same way as for the peptide-linked OTA hapten. The product was purified by semipreparative RP-HPLC (C-18). Flow rate: 3.76 mL min^{-1} ; mobile phase: first 3 min at 10% ACN/water (v/v, 0.1% TFA), followed by gradient from 10% to 90% ACN : water (v/v, 0.1% TFA) in 25 min; retention time: 10.099 min. Identity of peptide-linked biotin was confirmed by HRMS ((ESI)⁺, calculated for $\text{C}_{31}\text{H}_{55}\text{N}_{10}\text{O}_9\text{S}$: 743.3868 [$M + \text{H}^+$]; found: 743.3891).

Synthesis of AFB₂-CMO-peptide conjugate for MCR3 measurement

For peptide derivatization of the modified AFB₂, 5 mg of AFB₂-CMO (0.0129 mmol, 1 equivalent) were dissolved in 2 mL of DMF / DIPEA, as described previously. 4.4 mg of HBTU (0.0116 mmol, 0.9 equivalents) and the solution was immediately added to 1 equivalent of the Fmoc-deprotected peptide-resin bed. The mixture was bubbled with nitrogen for 2 h, then washed thoroughly with DMF, methanol, and DCM, and dried overnight under vacuum for further deprotection / cleavage. The resin was extensively washed and dried as

described above. Cleavage and deprotection followed in the same way as for the peptide-linked OTA hapten. The product was purified by semipreparative RP-HPLC (C-18). Flow rate: 3.76 mL min⁻¹; mobile phase: first min at 10% MeOH/water (v/v, 0.1% TFA), followed by gradient from 10% to 90% MeOH/water (v/v, 0.1% TFA) in 50 min; retention time: 15.613 min. Identity of the peptide-linked OTA hapten was confirmed by HRMS ((ESI)⁺, calculated for C₃₃H₄₂ClN₇O₁₀: 732.27544 [M + H⁺]; found: 732.2746).

Glass functionalization for immuno-biochip production for MCR3 measurements (epoxy, StarPEG, DSC)

Amino poly(ethyleneglycol) functionalization

Glass chip functionalization was carried out according to the SOP developed at the IWC and adapted from a previously published procedure.^[94] Briefly, commercially available glass slides were engraved with a number on one side, immersed in a 2% (v/v) Hellmanex-water solution and sonicated for 1 h before incubating under mild shaking overnight. The slides were thoroughly rinsed with ultrapure water until no residue of detergent was detectable and submerged and shaken sequentially in 1) a mixture of methanol/hydrochloric acid (1:1, v/v), and 2) concentrated sulfuric acid, for 1 h each time, with copious water rinsing in between. After the slides had been blow-dried under a stream of nitrogen followed by incubating for 15 min at 80 °C in a drying cabinet, silanization of the surface was carried out by dispensing 600 µL of 3-glycidyloxypropyltrimethoxysilane (GOPTS) and covering with another equally treated slide, in a “sandwich” format. The slides were allowed to react for 45 min, after which they were rinsed and sonicated for 15 min in ethanol. The rinsing solvent was replaced by fresh ethanol and the glass slides were sonicated one more time for 15 min. The glass slides were again dried under a stream of nitrogen and placed in the oven at 60 °C for 30 min for curing. After silanization, approximately 600 µL of molten diamino poly(ethyleneglycol) (DAPEG) were dispensed on the surface of one slide that was immediately covered in a “sandwich” format by a second slide. The “sandwiches” were incubated at 95 – 100 °C for 15 h. Finally, the “sandwiches” were separated and rinsed several times with ultrapure water before drying with a stream of nitrogen and storing in a desiccator under vacuum, protected from light, until further use.

Epoxy functionalization of amino-PEG derivatized glass slides

Epoxy-functionalization was carried out according to the literature.^[208] 800 μL of poly(ethyleneglycol) diglycidyl ether (diepoxy-PEG) were pipetted on the activated surface of an amino-PEG derivatized glass slide and covered immediately with a second slide. These “sandwiches” were incubated for ca. 15 hours at 95 – 100 °C. Afterwards, the glass slides were rinsed and sonicated in methanol for 15 min, followed by drying under a stream of nitrogen. If the slides showed any smearing on the surface, the procedure was repeated as needed, until the slides showed no trace of visual contamination. Analyte microcontact printing followed immediately afterwards.

Succinimidyl functionalization of amino-PEG derivatized glass slides

For succinimidyl functionalization of the glass slides, a previously published procedure was used.^[151] 80 mg of DSC and 4 mg of DMAP were dissolved in 1.6 mL DMF and 125 μL of triethylamine. A volume of 600 μL of this mixture was given to the amino-PEG derivatized surface of a functionalized glass chip. The slide was covered with a second slide, as described for the epoxy-activated glass slides. The “sandwiches” were incubated in covered Petri dishes for 4 h and after this time the separated slides were rinsed with methanol. A second wash and sonication for 15 min in fresh methanol followed. Finally, the slides were dried under a stream of nitrogen and analyte microcontact printing followed immediately afterwards.

Star-PEG functionalization of amino-PEG derivatized glass slides

The “Star-PEG” isocyanate end-functionalized pre-polymer reagent was kindly donated by Prof. Groll (DWI / RWTH Aachen e.V.). This reagent is suitable for coupling to surfaces that display end-functional amino groups. 50 mg of star-PEG were dissolved and stirred in 2 mL of tetrahydrofurane (THF) for 10 min. 600 μL of the solution were pipetted directly onto the glass slides and covered immediately with a second slide in the “sandwich” format. After an incubation time of 3 min, the slides were carefully separated by hand and vortexed for 5 min in ultrapure water in order to stop the cross-linking. The slides were dried under a gentle flow of nitrogen, further incubated in a Petri dish for 20 min, and immediately spotted. After 20 min they were ready for antigen immobilization.

Contact spotting of analyte conjugates

Unless otherwise indicated, microcontact printing of the analytes (OTA-peptide conjugate, AFB₂-CMO-peptide conjugate and biotin-peptide conjugate) was performed with an SNS 12 solid printing head. The manufacturer reports a spot diameter of 400 μm , an uptake volume of

0.25 μL and a delivery volume of 5.1 nL. Solutions of 1 mg mL^{-1} for the peptide-linked OTA, AFB₂-CMO and biotin conjugates were prepared in spotting buffer. These solutions as well as plain spotting buffer (25 μL each) were placed in individual wells of a 384-well microtiter plate and were spotted on the activated amino-PEG glass chips (either epoxy or DSC). An array of a particular analyte consisted on either 5 or 6 spots of the same solution. For the optimized green coffee procedure an array of 6 x 4 spots was defined with the analytes consisting of biotin-peptide (positive control), OTA-peptide, blank buffer (negative control) and AFB₂-CMO-peptide. Chamber humidity was set at 45% and temperature on the plate was kept at 21 °C. After spotting, the glass slides were incubated overnight and deactivated by shaking in 3M tris buffer for 15 min, then washing thoroughly with water. Finally, glass chips were kept overnight in PBS, before being used for the assays.

Biotin immobilization on complete biosensor surface to study signal distribution

The synthesized biotin peptide was dissolved in spotting buffer at a final concentration of 0.1 mg mL^{-1} . 800 μL of this solution were pipetted on an epoxy-functionalized glass slide that was immediately covered with a second slide in a “sandwich” format. The slides were kept in covered Petri dishes overnight (15 h), thoroughly rinsed with ultrapure water the following day, and subsequently deactivated by shaking in 3M tris buffer for 15 min. After a final wash with water, the slides were dried under a gentle stream of nitrogen and immediately used for the assay with streptavidin-HRP (1:10 000 dilution, original solution concentration 1 mg mL^{-1}).

CL data processing

For analysis and quantification of the images captured by the CCD camera, the program Spot Image Processor 0.4 (SIP0.4, Karsunke Softwarebüro, Wolnzach, Germany) was used. For the present study, the intensity of a 9 x 9 pixel area corresponding to the chemiluminescent spot was averaged and plotted against the competing analyte concentration (as in the dose-response curve for OTA), or against the number of regeneration cycles (as in the signal reproducibility curve). The area taken for signal quantification corresponds to $0.1348 \pm 0.0052 \text{ mm}^2$. Dose-response curve data were fitted to the four parameter logistic equation (using instrumental weighing of the uncertainty) with the aid of the program Origin (version 7.5). The no-dose response was always monitored, but it was not taken into consideration for the fit. LODs in the green coffee method were calculated by taking three times the standard

deviation associated to the fitted dose response at zero analyte concentration and subtracting from the maximum intensity signal.

MTP-based indirect competitive ELISA: AFB₂ and antibody 3A7

The MTP was coated with 200 μL per well of an AFB₂-CMO-TG solution (1:40 000 dilution, original solution concentration approximately 1 mg mL⁻¹) in coating buffer and incubated overnight at 4 °C. The plate was then washed 3 times with washing buffer and the cavities filled with 300 μL per well of a 1% casein solution in PBS (w/v). Blocking took place for 30 min, after which the plate was washed again three times with washing buffer. The AFB₂ calibrant solutions were originally spiked with an AFB₂ content of 0, 0.002, 0.02, 0.2, 2, 20 and 200 $\mu\text{g L}^{-1}$ and were mixed with the antibody solution (1:10 000 dilution, original solution concentration approximately 1.78 mg mL⁻¹) separately, in a low-binding polypropylene MTP, at a 1:1 ratio (v/v), the total volume added to 240 μL of solution per well. This was done to ensure that all coated wells of the work MTP would come in contact with the AB/competing analyte solution at approximately the same time. Care was taken to perform this step as quick as possible, since the AFB₂ calibrant solutions were prepared in 20% MeOH in PBS (v/v) and MeOH denatures the antibodies. After pipetting 200 μL per well of the AB/competing analyte mixture to the working MTP, the system was incubated under mild shaking for exactly 30 min. 3 x washing was carried out again, followed by the addition of 200 μL of secondary antibody solution (anti-mouse IgG-HRP, 1:10 000 dilution, original solution concentration of 1 mg mL⁻¹). This last incubation step of the tracer proceeded for 1h under gentle shaking. The plate was washed in triplicate for a final time and 100 μL per well of substrate solution (TMB, and H₂O₂ mixture) were dispensed. Blue color development was allowed to proceed for 15 to 20 min, judging visually from the intensity of the color. The reaction was finally stopped with 5% H₂SO₄ in water (v/v), which generated a yellow color. Absorbance was measured at 450 nm.

MTP-based indirect competitive ELISA: AFB₂ and antibody 3A7-HRP

Aside from the following modifications, the procedure was similar to the previous detection of AFB₂ with 3A7. The antibody solution used for competition was in this case the 3A7-HRP (1:80 000 dilution, original solution concentration approximately 16.5 mg mL⁻¹). After incubation with 3A7-HRP and calibrant solutions, the plate was washed 3 times with washing buffer and developed with the substrate solution (no secondary anti-mouse IgG-HRP step was necessary).

MTP-based ELISA: OTA indirect competitive

Unless otherwise indicated (for example in the optimization of plate conditions, for the 2-D assay), plates were coated with a 1:5000 dilution of the synthesized OTA-BSA conjugate (original solution concentration approximately 1 mg mL⁻¹). When OTA calibrants were spiked in PBS incubation in the competition step lasted 1 h. If real coffee samples were measured, the total MeOH concentration (original from coffee extract: 80% v/v) was diluted to 20 % v/v by adding 1% NaHCO₃ solution in water, pH 9.4 (w/v). The dilution with NaHCO₃, instead of PBS was important, since some of the samples had been stored for longer periods of time and dilution with PBS usually caused precipitation of green matter and an inhomogeneous appearance of the final solution. It was determined that the NaHCO₃ solution was more adequate to this end, preventing precipitation. Also, when MeOH was present in the competition step, this was allowed to proceed for only 30 min. Otherwise, the ic-ELISA was carried out exactly as previously described for the detection of AFB₂ with antibody 3A7.

Green coffee extraction

For in-house green coffee extraction, 1 kg of green coffee bought from a coffee roasting facility in Munich was ground with the aid of a food mill to a fine powder. This could only be accomplished at low temperature: the beans were first cooled with liquid nitrogen and then ground in small portions in the cooled mill. The powder thus obtained was thoroughly mixed and kept frozen at -20 °C until the time of use.

To prepare our own blank green coffee extracts for calibration (both MCR 3 and MTP-based assays), 18.75 g of green coffee powder were supplemented with 56.25 mL water, 100 mL MeOH and 2.5 g NaHCO₃ and extracted by gentle magnetic stirring for 30 min. The slurry was centrifuged at 1924 g_n for 15 min and the supernatant was filtered with filter paper. The MeOH content of this solution was assumed to be 64% (v/v). The solution was further diluted to 20% total MeOH by adding enough volume of a NaHCO₃ aqueous solution (1% w/v) (as specifically mentioned in the “Results and Discussion” section of this work). It was found that antibodies tolerated MeOH content in this range, both for the MCR 3 and for the MTP-ic-ELISA. The final sample-to-solution ratio (i.e. the factor by which directly determined OTA concentrations have to be multiplied in order to obtain the final contamination level in µg kg⁻¹) was 1 g of coffee in 26.666 mL of final extract.

In the case of samples obtained from our work partner, Eurofins WEJ Contaminants, two types of samples were received. The first type of samples consisted of GREEN COFFEE

SLURRIES (coffee beans blended with water). According to our work partner, these were prepared by blending green coffee beans with water in a 3:1 ratio (w/w). The slurries were to be kept frozen, but they arrived already thawed. Since all of them presented OTA contamination levels, they could not be used for calibration, either in the MCR 3 or in the MTP ic-ELISA. Indeed, the values determined by these techniques (not shown in this work) were always overestimated by large and very variable factors. The samples had been stored for over 3 months; therefore they were considered inadequate for measuring. Multiple thawing and freezing might have contributed to these sources of uncertainty. The second type of sample received consisted of green coffee extracts. As indicated by our partner, these were produced by blending exactly 75 g of green coffee slurry with 100 mL of MeOH and 2.5 g of NaHCO₃ at high speed with a stem blender. This composition is the same as what was used for the in-house production of blank, green coffee extract, in order to make the samples comparable. As with our in-house produced samples, the MeOH content of these extracts was brought down to 20% (v/v) by adding enough volume of a NaHCO₃ aqueous solution (1% w/v).

Peanut extraction

100 g blank peanuts were ground to a fine powder and mixed with 150 mL water. This “slurry” then homogenized and further divided into 7.5 g portions that were frozen at -20 °C. The portions were used as needed. For the extraction, the thawed sample (7.5 g) was extracted with 18 mL MeOH by magnetic stirring for 1h. The mixture was filtered by passing through filter paper and the MeOH concentration of the filtrate was assumed to be 80% (v/w). This filtrate was further diluted to a total MeOH content of 20% by adding a BSA solution (1% w/v) in PBS. In this case, the BSA was proven to be of help in diminishing the unspecific matrix effects that arise when conducting immunoaffinity assays.^[190] The total sample-to-solution ratio of the final, diluted extract was 1 g of peanuts to 30 mL solution.

Immunoaffinity enrichment of OTA in green coffee

Please note that the extraction procedure is slightly different to the one used for measuring green coffee samples either by MTP-ic-ELISA or by MCR 3. The reason for this is that the details of the standardized DIN procedure were followed in this case. Immunoaffinity enrichment also needs to be carried out at very different conditions: the toxin needs to be highly diluted and the MeOH content needs to be brought down to a minimum of 5% or lower, otherwise this might affect binding of the toxin to the immobilized antibodies. 25 g of

finely ground coffee bean powder were extracted with 250 mL of a 50:50 mixture (v/v) of methanol:sodium bicarbonate, aq. (3% w/v) by gentle magnetic stirring for 30 min. The slurry was centrifuged at 1924 g_n for 15 min and the supernatant was filtered with filter paper. The filtrate was further diluted with PBS (10 mL of extract + 200 mL of PBS). A volume of 210 mL of the diluted filtrate (equivalent to 1 g of coffee) were applied to an immunoaffinity column at a flow rate of 2-3 mL per min. The column was further washed with 2 x 10 mL of water, dried with a gentle nitrogen flow and eluted step-wise with 4 mL methanol. The eluate was evaporated to dryness under nitrogen and redissolved in 1 mL of HPLC mobile phase (HPLC method 1).

HPLC determination of OTA in green coffee

Method 1, isocratic:

acetonitrile, 45% (v/v)

4 mM sodium acetate / acetic acid (19:1, v/v), 55%

Injection volume: 20 μ L; column T = 27°C, running time: 20 min.

Fluorescence detection, 330 nm (excitation); 470 nm (emission)

Method 2, isocratic:

acetonitrile, 48%

water, 51%

glacial acetic acid, 1% (in volume composition)

Injection volume: 100 μ L; column T = 45°C, running time: 20 min.

Fluorescence detection, 330 nm (excitation); 460 nm (emission)

OTA standards ([OTA]: 0.1 – 100 μ g L⁻¹) were prepared in mobile phase (method 1) or in 30:70:1 methanol:water:glacial acetic acid (v/v) (method 2). For calibration, standards were measured in triplicate.

MCR 3 code for green coffee assay

(please note: the program code is given in the original German commands)

Line No.	Command
0	Initialisieren
1	Do
2	Ventil 6 auf Position 4 im Uhrzeigersinn

3	LoadPump Pump: 2 Pickup: 250 ul Speed: 250 ul/s
4	ReadyCheck
5	Ventil 6 auf Position 2 gegen Uhrzeigersinn
6	DispensePump Pump: 2 Dispense: 250 ul Speed: 250 ul/s
7	ReadyCheck
8	Loop for 2times
9	ReadyCheck
10	Ventil 6 auf Position 4 im Uhrzeigersinn
11	LoadPump Pump: 2 Pickup: 1000 ul Speed: 250 ul/s
12	ReadyCheck
13	Ventil 6 auf Position 2 gegen Uhrzeigersinn
14	Ventil 7 auf Position B
15	Ventil 5 auf Position 1 im Uhrzeigersinn
16	Ventil 4 auf Position I
17	Ventil 2 auf Position 3 im Uhrzeigersinn
18	Ventil 1 auf Position 4 im Uhrzeigersinn
19	DispensePump Pump: 2 Dispense: 300 ul Speed: 500 ul/s
20	LoadPump Pump: 4 Pickup: 5000 ul Speed: 1500 ul/s
21	ReadyCheck
22	Wait for 1000 ms
23	ReadyCheck
24	Ventil 2 auf Position 5 im Uhrzeigersinn
25	DispensePump Pump: 4 Dispense: 1000 ul Speed: 500 ul/s
26	ReadyCheck
27	Ventil 5 auf Position 6 gegen Uhrzeigersinn
28	Ventil 6 auf Position 1 gegen Uhrzeigersinn
29	DispensePump Pump: 2 Dispense: 200 ul Speed: 100 ul/s
30	ReadyCheck
31	Ventil 7 auf Position O
32	DispensePump Pump: 2 Dispense: 500 ul Speed: 60 ul/s
33	DispensePump Pump: 1 Dispense: 500 ul Speed: 60 ul/s
34	LoadPump Pump: 5 Pickup: 960 ul Speed: 1500 ul/s
35	ReadyCheck
36	Ventil 7 auf Position B
37	Ventil 5 auf Position 5 gegen Uhrzeigersinn
38	ReadyCheck
39	Do
40	Ventil 6 auf Position 6 im Uhrzeigersinn
41	Ventil 3 auf Position 3 gegen Uhrzeigersinn
42	LoadPump Pump: 2 Pickup: 1000 ul Speed: 250 ul/s
43	LoadPump Pump: 3 Pickup: 50 ul Speed: 300 ul/s
44	ReadyCheck
45	Ventil 6 auf Position 2 gegen Uhrzeigersinn
46	Ventil 3 auf Position 4 im Uhrzeigersinn
47	DispensePump Pump: 2 Dispense: 1000 ul Speed: 250 ul/s
48	LoadPump Pump: 3 Pickup: 50 ul Speed: 300 ul/s
49	ReadyCheck
50	Loop for 2times
51	Ventil 6 auf Position 5 im Uhrzeigersinn
52	Ventil 3 auf Position 3 gegen Uhrzeigersinn

53	LoadPump Pump: 2 Pickup: 1000 ul Speed: 250 ul/s
54	LoadPump Pump: 3 Pickup: 50 ul Speed: 300 ul/s
55	ReadyCheck
56	Ventil 6 auf Position 2 gegen Uhrzeigersinn
57	Ventil 3 auf Position 4 im Uhrzeigersinn
58	DispensePump Pump: 2 Dispense: 1000 ul Speed: 250 ul/s
59	LoadPump Pump: 3 Pickup: 50 ul Speed: 300 ul/s
60	ReadyCheck
61	Ventil 6 auf Position 3 gegen Uhrzeigersinn
62	Ventil 3 auf Position 3 gegen Uhrzeigersinn
63	LoadPump Pump: 2 Pickup: 1000 ul Speed: 250 ul/s
64	LoadPump Pump: 3 Pickup: 50 ul Speed: 300 ul/s
65	ReadyCheck
66	Ventil 6 auf Position 2 gegen Uhrzeigersinn
67	Ventil 3 auf Position 4 im Uhrzeigersinn
68	DispensePump Pump: 2 Dispense: 1000 ul Speed: 250 ul/s
69	LoadPump Pump: 3 Pickup: 50 ul Speed: 300 ul/s
70	ReadyCheck
71	ReadyCheck
72	Ventil 5 auf Position 6 im Uhrzeigersinn
73	Ventil 6 auf Position 3 im Uhrzeigersinn
74	LoadPump Pump: 2 Pickup: 1000 ul Speed: 250 ul/s
75	ReadyCheck
76	Ventil 6 auf Position 1 gegen Uhrzeigersinn
77	DispensePump Pump: 2 Dispense: 1000 ul Speed: 100 ul/s
78	ReadyCheck
79	Ventil 2 auf Position 5 im Uhrzeigersinn
80	Ventil 5 auf Position 1 gegen Uhrzeigersinn
81	DispensePump Pump: 4 Dispense: 2000 ul Speed: 500 ul/s
82	ReadyCheck
83	Ventil 5 auf Position 4 im Uhrzeigersinn
84	DispensePump Pump: 0 Dispense: 200 ul Speed: 100 ul/s
85	DispensePump Pump: 0 Dispense: 800 ul Speed: 10 ul/s
86	ReadyCheck
87	Ventil 5 auf Position 1 gegen Uhrzeigersinn
88	DispensePump Pump: 4 Dispense: 2000 ul Speed: 500 ul/s
89	ReadyCheck
90	Ventil 5 auf Position 2 im Uhrzeigersinn
91	Ventil 3 auf Position 2 gegen Uhrzeigersinn
92	DispensePump Pump: 3 Dispense: 400 ul Speed: 150 ul/s
93	ReadyCheck
94	Ventil 5 auf Position 5 gegen Uhrzeigersinn
95	Take Photo with: 2 x 2 and 60000 ms
96	ReadyCheck
97	Do
98	Ventil 5 auf Position 6 im Uhrzeigersinn
99	Ventil 6 auf Position 5 im Uhrzeigersinn
100	LoadPump Pump: 2 Pickup: 1000 ul Speed: 250 ul/s
101	ReadyCheck
102	Ventil 6 auf Position 1 gegen Uhrzeigersinn

103	DispensePump Pump: 2 Dispense: 1000 ul Speed: 250 ul/s
104	ReadyCheck
105	Loop for 2 times
106	Do
107	Ventil 6 auf Position 6 im Uhrzeigersinn
108	LoadPump Pump: 2 Pickup: 1000 ul Speed: 250 ul/s
109	ReadyCheck
110	Ventil 6 auf Position 1 gegen Uhrzeigersinn
111	DispensePump Pump: 2 Dispense: 1000 ul Speed: 250 ul/s
112	ReadyCheck
113	Loop for 2 times
114	Do
115	Ventil 6 auf Position 5 im Uhrzeigersinn
116	LoadPump Pump: 2 Pickup: 1000 ul Speed: 250 ul/s
117	ReadyCheck
118	Ventil 6 auf Position 1 gegen Uhrzeigersinn
119	DispensePump Pump: 2 Dispense: 1000 ul Speed: 250 ul/s
120	ReadyCheck
121	Loop for 2 times
122	Ventil 4 auf Position O
123	Ventil 1 auf Position 5 im Uhrzeigersinn
124	Do
125	Ventil 6 auf Position 6 im Uhrzeigersinn
126	Ventil 5 auf Position 6 im Uhrzeigersinn
127	LoadPump Pump: 2 Pickup: 1000 ul Speed: 250 ul/s
128	DispensePump Pump: 5 Dispense: 60 ul Speed: 10 ul/s
129	ReadyCheck
130	Ventil 6 auf Position 1 im Uhrzeigersinn
131	DispensePump Pump: 2 Dispense: 1000 ul Speed: 250 ul/s
132	DispensePump Pump: 5 Dispense: 60 ul Speed: 10 ul/s
133	ReadyCheck
134	Loop for 5times
135	Do
136	Ventil 6 auf Position 3 gegen Uhrzeigersinn
137	LoadPump Pump: 2 Pickup: 1000 ul Speed: 250 ul/s
138	DispensePump Pump: 5 Dispense: 60 ul Speed: 10 ul/s
139	ReadyCheck
140	Ventil 6 auf Position 1 im Uhrzeigersinn
141	DispensePump Pump: 2 Dispense: 1000 ul Speed: 250 ul/s
142	DispensePump Pump: 5 Dispense: 60 ul Speed: 10 ul/s
143	ReadyCheck
144	Loop for 3times
145	Do
146	Ventil 1 auf Position 4 gegen Uhrzeigersinn
147	LoadPump Pump: 5 Pickup: 300 ul Speed: 1500 ul/s
148	ReadyCheck
149	Ventil 1 auf Position 5 im Uhrzeigersinn
150	ReadyCheck
151	Do
152	DispensePump Pump: 5 Dispense: 100 ul Speed: 100 ul/s

153	LoadPump Pump: 5 Pickup: 100 ul Speed: 100 ul/s
154	Loop for 5times
155	ReadyCheck
156	DispensePump Pump: 5 Dispense: 300 ul Speed: 500 ul/s
157	ReadyCheck
158	Loop for 5times
159	ReadyCheck
160	Do
161	Ventil 1 auf Position 2 gegen Uhrzeigersinn
162	LoadPump Pump: 5 Pickup: 500 ul Speed: 1500 ul/s
163	ReadyCheck
164	Ventil 1 auf Position 5 im Uhrzeigersinn
165	DispensePump Pump: 5 Dispense: 500 ul Speed: 500 ul/s
166	ReadyCheck
167	Loop for 3times
168	ReadyCheck
169	Ventil 1 auf Position 6 im Uhrzeigersinn
170	LoadPump Pump: 5 Pickup: 1500 ul Speed: 1500 ul/s
171	ReadyCheck
172	Ventil 1 auf Position 5 gegen Uhrzeigersinn
173	DispensePump Pump: 5 Dispense: 1500 ul Speed: 500 ul/s
174	ReadyCheck
175	Do
176	Ventil 1 auf Position 2 gegen Uhrzeigersinn
177	LoadPump Pump: 5 Pickup: 1500 ul Speed: 1500 ul/s
178	ReadyCheck
179	Ventil 1 auf Position 5 im Uhrzeigersinn
180	DispensePump Pump: 5 Dispense: 1500 ul Speed: 500 ul/s
181	ReadyCheck
182	Loop for 2times
183	ReadyCheck
184	Ventil 4 auf Position I
185	Ventil 1 auf Position 2 gegen Uhrzeigersinn
186	LoadPump Pump: 5 Pickup: 1500 ul Speed: 1500 ul/s
187	ReadyCheck
188	Ventil 1 auf Position 5 im Uhrzeigersinn
189	DispensePump Pump: 5 Dispense: 1500 ul Speed: 500 ul/s
190	ReadyCheck
	ENDFILE

6 Abbreviations

ACN	acetonitrile
AFB1	aflatoxin B ₁
AFB2	aflatoxin B ₂
AP	alkaline phosphatase
APTS	aminopropyltriethoxysilane
ASE	accelerated solvent extraction
BCA	bicinchoninic acid assay
Boc	<i>tert</i> -butyloxycarbonyl
	benzotriazol-1-yl-oxy-tris-(dimethylamino) phosphonium
BOP	hexafluorophosphate
BSA	bovine serum albumin
BW	body weight
CCD	charged coupled device
CL	chemiluminescence
CMO	carboxymethyl oxime
CV	coefficient of variation
DAPEG	polyethyleneglycol diamine
DCC	N,N'-dicyclohexylcarbodiimide
DCM	dichloromethane
diepoxy-PEG	polyethyleneglycol diglycidyl ether
DIPEA	N,N'-diisopropylethylamine
DMAP	4-(dimethylamino)pyridine
DMF	N,N'-dimethylformamide
DMSO	dimethylsulfoxide
DNP	N1-(2,4-dinitrophenyl)-1,2-ethanediamine
DSC	N,N'-disuccinimidyl carbonate
DVB	divinylbenzene
ELISA	enzyme-linked immunosorbent assay
ESI	electrospray ionization
EU	European Union
FAO	Food and Agriculture Organization of the United Nations
FD	fluorescence detection
Fmoc	fluorenylmethoxycarbonyl
FPIA	fluorescence polarization immunoassay
GOPTS	3-glycidyoxypropyltrimethoxysilane
HBTU	O-benzotriazol-1-yl)-N,N,N',N'-tetramethyluronium hexafluorophosphate
HMPA	hexamethyl phosphoric triamide
HPTLC	high performance thin layer chromatography
HRMS	high resolution mass spectrometry
HRP	horseradish peroxidase
IAC	immunoaffinity chromatography
IARC	International Agency for Research on Cancer
ic-ELISA	indirect competitive ELISA
ID	internal diameter
LC	liquid chromatography

LFD	lateral flow device
LC-MS/MS	liquid chromatography-tandem mass spectrometry
LOD	limit of detection
LOQ	limit of quantitation
Mab	monoclonal antibody
MALDI-MS	matrix-assisted laser desorption/ionization mass spectrometry
MeOH	methanol
MERCOSUR	Mercado Común del Sur (Southern Common Market)
MPTS	mercaptopropyltrimethoxysilane
MRL	maximum residual limit
MTP	microtiter plate
MWCO	molecular weight cut off
NHS	N-hydroxysuccinimide
NMP	N-Methyl-2-pyrrolidone
OTA	ochratoxin A
OVA	ovalbumin, albumin from chicken egg white
OWLS	optical waveguide lightmode spectroscopy
PASA	Parallel Assay Sensor Array
PBS	phosphate buffered saline (solution)
PDMS	polydimethylsiloxane
PEG	polyethylene glycol
pK _a	negative logarithm of the acid dissociation constant
PMMA	polymethylmethacrylate
PTFE	polytetrafluoroethylene
PTWI	provisional tolerable weekly intake
PyBOP	benzotriazol-1-yl-oxytripyrrolidino phosphonium hexafluorophosphate
R _f	retardation factor (planar chromatography)
RP-HPLC	reversed-phase high performance liquid chromatography
RT	room temperature
SOP	standard operating procedure
SPE	solid phase extraction
SPME	solid phase micro extraction
SPPS	solid phase peptide synthesis
SPR	surface plasmon resonance
TBTU	O-(benzotriazol-1-yl)-1,1,3,3-tetramethyluronium tetrafluoroborate
TFA	trifluoroacetic acid
TG	thyroglobulin
THF	tetrahydrofuran
TIS	triisopropylsilane
TLC	thin layer chromatography
TMB	3,3',5,5'-tetramethylbenzidine
TNBS	2,4,6-trinitrobenzenesulfonic acid
TNT	trinitrotoluene
WHO	World Health Organization

7 Bibliography

1. Shephard, G. S., *Determination of mycotoxins in human foods*. Chem. Soc. Rev. **2008**, 37, (11), 2468-2477.
2. Calvo, A. M., Wilson, R. A., Bok, J. W., Keller, N. P., *Relationship between secondary metabolism and fungal development*. Microbiol. Mol. Biol. R. **2002**, 66, (3), 447-459.
3. Harris, J. P., Mantle, P. G., *Biosynthesis of ochratoxins by Aspergillus ochraceus*. Phytochemistry **2001**, 58, (5), 709-716.
4. Steyn, P. S., Holzapfel, C. W., Ferreira, N. P., *Biosynthesis of ochratoxins, metabolites of Aspergillus ochraceus*. Phytochemistry **1970**, 9, (9), 1977-1983.
5. Frisvad, J. C., Thrane, U., Samson, R. A., Pitt, J. I., *Important mycotoxins and the fungi which produce them*. Adv. Exp. Med. Biol. **2006**, 571, 3-31.
6. Reddy, L., Bhoola, K., *Ochratoxins - food contaminants: impact on human health*. Toxins **2010**, 2, (4), 771-779.
7. Kuiper-Goodman, T., Scott, P. M., *Risk assessment of the mycotoxin ochratoxin A*. Biomed. Environ. Sci. **1989**, 2, (3), 179-248.
8. Dall'Asta, C., Galaverna, G., De Dea Lindner, J., Virgili, R., Neviani, E., Dossena, A., *A new validated HPLC-FLD method for detecting ochratoxin A in dry-cured meat and in blue cheese*. Mycotoxin Res. **2007**, 23, (3), 132-137.
9. Zimmerli, B., Dick, R., *Determination of ochratoxin A at the ppt level in human blood, serum, milk and some foodstuffs by high-performance liquid-chromatography with enhanced fluorescence detection and immunoaffinity column cleanup - methodology and Swiss data*. J. Chromatogr. B. **1995**, 666, (1), 85-99.
10. Abrunhosa, L., Paterson, R. R., Venâncio, A., *Biodegradation of ochratoxin A for food and feed decontamination*. Toxins **2010**, 2, (5), 1078-1099.
11. IARC, *Some naturally occurring substances: food items and constituents, heterocyclic aromatic amines and mycotoxins*. International Agency for Research on Cancer Monographs on the Evaluation of Carcinogenic Risks to Humans **1993**, 53, 489-521.
12. Faucet, V., Pfohl-Leszkowicz, A., Dai, J., Castegnaro, M., Manderville, R. A., *Evidence for covalent DNA adduction by ochratoxin A following chronic exposure to rat and subacute exposure to pig*. Chem. Res. Toxicol. **2004**, 17, (9), 1289-1296.

13. Hult, K., Plestina, R., Habazinovak, V., Radic, B., Ceovic, S., *Ochratoxin A in human blood and Balkan endemic nephropathy*. Arch. Toxicol. **1982**, 51, (4), 313-321.
14. WHO *Safety evaluation of certain mycotoxins in food*; 2001.
15. Mantle, P. G., Faucet-Marquis, V., Manderville, R. A., Squillaci, B., Pfohl-Leszkowicz, A., *Structures of covalent adducts between DNA and ochratoxin A: a new factor in debate about genotoxicity and human risk assessment*. Chem. Res. Toxicol. **2010**, 23, (1), 89-98.
16. Dai, J., Park, G., Perry, J. L., Il'ichev, Y. V., Bow, D. A. J., Pritchard, J. B., Faucet, V., Pfohl-Leszkowicz, A., Manderville, R. A., Simon, J. D., *Molecular aspects of the transport and toxicity of ochratoxin A*. Accounts Chem. Res. **2004**, 37, (11), 874-881.
17. Faucet-Marquis, V., Pont, F., Stormer, F. C., Rizk, T., Castegnaro, M., Pfohl-Leszkowicz, A., *Evidence of a new dechlorinated ochratoxin A derivative formed in opossum kidney cell cultures after pretreatment by modulators of glutathione pathways: correlation with DNA-adduct formation*. Mol. Nutr. Food Res. **2006**, 50, (6), 530-542.
18. Mally, A., Zepnik, H., Wanek, P., Eder, E., Dingley, K., Ihmels, H., Vokel, W., Dekant, W., *Ochratoxin A: lack of formation of covalent DNA adducts*. Chem. Res. Toxicol. **2004**, 17, (2), 234-242.
19. FAO/WHO *Evaluation of certain food additives and contaminants (37th report of the Joint FAO/WHO Committee on Food Additives)*; 806; 1991.
20. FAO/WHO *Evaluation of certain food additives and contaminants (44th report of the Joint FAO/WHO Committee on Food Additives)*; 859; 1995.
21. Codex Alimentarius Commission *Report of the 38th session of the Codex Committee on food additives and contaminants*; 2006.
22. Directorate-General Health and Consumer Protection *Assessment of dietary intake of ochratoxin A by the population of EU Member States*; Rome, 2002.
23. WHO *Safety evaluation of certain food additives and contaminants*; Geneva, 2008; pp 1-471.
24. FAO *Worldwide regulations for mycotoxins in food and feed in 2003*; Rome, 2003; p 165.
25. Shephard, G. S., Berthiller, F., Dorner, J., Krska, R., Lombaert, G. A., Malone, B., Maragos, C., Sabino, M., Solfrizzo, M., Trucksess, M. W., van Egmond, H. P.,

- Whitaker, T. B., *Developments in mycotoxin analysis: an update for 2007-2008*. World Mycotoxin Journal **2009**, 2, (1), 3-21.
26. Höchstmengenregelungen für Mykotoxine in Lebensmitteln in der Europäische Union und in Deutschland, 2008.
27. Food Quality and Standards Service of the FAO *Enhancement of coffee quality through the prevention of mould formation*; Rome, 2006; p 91.
28. Biselli, S., *Analytische Methoden für die Kontrolle von Lebens- und Futtermitteln auf Mykotoxine*. J.V.L. **2006**, 1, 106-114.
29. 1998/35/EC (Commission Directive of 16 July 1998) Laying down the sampling methods and the methods of analysis for the official control of the levels for certain contaminants in foodstuffs, 1998.
30. Spanjer, M., Stroka, J., Patel, S., Buechler, S., Pittet, A., Barel, S., *Non-destructive automated sampling of mycotoxins in bulk food and feed - A new tool for required harmonization*. Mycotoxin Res. **2001**, 17, (0), 198-201.
31. Stroka, J., Spanjer, M., Buechler, S., Barel, S., Kos, G., Anklam, E., *Novel sampling methods for the analysis of mycotoxins and the combination with spectroscopic methods for the rapid evaluation of deoxynivalenol contamination*. Toxicol. Lett. **2004**, 153, (1), 99-107.
32. Dall'Asta, C., Galaverna, G., Dossena, A., Marchelli, R., *Reversed-phase liquid chromatographic method for the determination of ochratoxin A in wine*. J. Chromatogr. A. **2004**, 1024, (1-2), 275-279.
33. DIN EN 14133 Foodstuffs - Determination of ochratoxin A in barley and roasted coffee - HPLC method with clean-up on an immunoaffinity column, 2003.
34. Richter, B. E., Jones, B. A., Ezzell, J. L., Porter, N. L., Avdalovic, N., Pohl, C., *Accelerated solvent extraction: a technique for sample preparation*. Anal. Chem. **1996**, 68, (6), 1033-1039.
35. Juan, C., Gonzalez, L., Soriano, J. M., Molto, J. C., Manes, J., *Accelerated solvent extraction of ochratoxin A from rice samples*. J. Agric. Food Chem. **2005**, 53, (24), 9348-9351.
36. Lattanzio, V. M. T., Solfrizzo, M., Powers, S., Visconti, A., *Simultaneous determination of aflatoxins, ochratoxin A and fusarium toxins in maize by liquid chromatography/tandem mass spectrometry after multitoxin immunoaffinity cleanup*. Rapid Commun. Mass Spectrom. **2007**, 21, (20), 3253-3261.

37. Senyuva, H. Z., Gilbert, J., *Immunoaffinity column clean-up techniques in food analysis: a review*. J. Chromatogr. B. **2010**, 878, (2), 115-132.
38. Nesheim, S., Stack, M. E., Trucksess, M. W., Eppley, R., *Rapid solvent-efficient method for liquid chromatographic determination of ochratoxin A in corn, barley, and kidney: collaborative study*. J. AOAC Int. **1992**, 75, (3), 481-487.
39. Hinkel, C., Koelling-Speer, I., Speer, K., *Automating the solid-phase extraction for the determination of ochratoxin A*. Mycotoxin Res. **2005**, 21, (2), 128-131.
40. Sibanda, L., De Saeger, S., Van Peteghem, C., *Optimization of solid-phase clean-up prior to liquid chromatographic analysis of ochratoxin A in roasted coffee*. J. Chromatogr. A. **2002**, 959, (1-2), 327-330.
41. Ventura, M., Vallejos, C., Anaya, I. N. A., Broto-Puig, F., Agut, M., Comellas, L., *Analysis of ochratoxin A in coffee by solid-phase cleanup and narrow-bore liquid chromatography-fluorescence detector-mass spectrometry*. J. Agric. Food Chem. **2003**, 51, (26), 7564-7567.
42. Romer Labs Diagnostic GmbH MycoSep® Clean-up columns. <http://www.romerlabs.com/en/products/columns.html>, accessed November 9 2010
43. Buttinger, G., Fuchs, E., Knapp, H., Berthiller, F., Schuhmacher, R., Binder, E. M., Krska, R., *Performance of new clean-up column for the determination of ochratoxin A in cereals and foodstuffs by HPLC-FLD*. Food Addit. Contam. A **2004**, 21, (11), 1107-1114.
44. Maier, N. M., Buttinger, G., Welhartizki, S., Gavioli, E., Lindner, W., *Molecularly imprinted polymer-assisted sample clean-up of ochratoxin A from red wine: merits and limitations*. J. Chromatogr. B. **2004**, 804, (1), 103-111.
45. Jodlbauer, J., Maier, N. M., Lindner, W., *Towards ochratoxin A selective molecularly imprinted polymers for solid-phase extraction*. J. Chromatogr. A. **2002**, 945, (1-2), 45-63.
46. Zhou, S. N., Lai, E. P. C., *N-phenylacrylamide functional polymer with high affinity for ochratoxin A*. React. Funct. Polym. **2004**, 58, (1), 35-42.
47. Yu, J. C. C., Krushkova, S., Lai, E. P. C., Dabek-Zlotorzynska, E., *Molecularly-imprinted polypyrrole-modified stainless steel frits for selective solid phase preconcentration of ochratoxin A*. Anal. Bioanal. Chem. **2005**, 382, (7), 1534-1540.
48. Turner, N. W., Piletska, E. V., Karim, K., Whitcombe, M., Malecha, M., Magan, N., Baggiani, C., Piletsky, S. A., *Effect of the solvent on recognition properties of*

- molecularly imprinted polymer specific for ochratoxin A*. Biosens. Bioelectron. **2004**, 20, (6), 1060-1067.
49. Maragos, C. M., *Recent advances in the development of novel materials for mycotoxin analysis*. Anal. Bioanal. Chem. **2009**, 395, (5), 1205-1213.
50. Gilbert, J., Anklam, E., *Validation of analytical methods for determining mycotoxins in foodstuffs*. TrAC Trend. Anal. Chem. **2002**, 21, (6-7), 468-486.
51. Göbel, R., Lusky, K., *Simultaneous determination of aflatoxins, ochratoxin A, and zearalenone in grains by new immunoaffinity column/liquid chromatography*. J. AOAC Int. **2004**, 87, (2), 411-416.
52. Scott, P. M., Trucksess, M. W., *Application of immunoaffinity columns to mycotoxin analysis*. J. AOAC Int. **1997**, 80, (5), 941-949.
53. Vargas, E. A., dos Santos, E. A., Pittet, A., *Determination of ochratoxin A in green coffee by immunoaffinity column cleanup and liquid chromatography: collaborative study*. J. AOAC Int. **2005**, 88, (3), 773-779.
54. Krska, R., Schubert-Ullrich, P., Molinelli, A., Sulyok, M., MacDonald, S., Crews, C., *Mycotoxin analysis: an update*. Food Addit. Contam. A **2008**, 25, (2), 152 - 163.
55. Sulyok, M., Krska, R., Schuhmacher, R., *Application of a liquid chromatography-tandem mass spectrometric method to multi-mycotoxin determination in raw cereals and evaluation of matrix effects*. Food Addit. Contam. **2007**, 24, (10), 1184-1195.
56. Reinsch, M., Topfer, A., Lehmann, A., Nehls, I., Panne, U., *Determination of ochratoxin A in beer by LC-MS/MS ion trap detection*. Food Chem. **2007**, 100, (1), 312-317.
57. Nesheim, S., *Analysis of ochratoxins A and B and their esters in barley, using partition and thin-layer chromatography 2. Collaborative study*. J. AOAC Int. **1973**, 56, (4), 822-826.
58. Santos, E. A., Vargas, E. A., *Immunoaffinity column clean-up and thin layer chromatography for determination of ochratoxin A in green coffee*. Food Addit. Contam. **2002**, 19, (5), 447-458.
59. Lee, K. Y., Poole, C. F., Zlatkis, A., *Simultaneous multi-mycotoxin determination by high-performance thin-layer chromatography*. Anal. Chem. **1980**, 52, (6), 837-842.
60. Köhler, G., Milstein, C., *Continuous cultures of fused cells secreting antibody of predefined specificity*. Nature **1975**, 256, (5517), 495-497.

61. Knopp, D., Niessner, R., Biomonitoring based on immunological principles. In *Solid Waste: Assessment, Monitoring and Remediation*, Twardowska, I.; Allen, H. E.; Kettrup, A. A. E.; Lacy, W. J., Eds. Elsevier: Amsterdam, 2004; Vol. 4, pp 505-537.
62. Goldberg, M. E., Djavadiohanian, L., *Methods for measurement of antibody antigen affinity based on ELISA and RIA*. *Curr. Opin. Immunol.* **1993**, 5, (2), 278-281.
63. Chu, F. S., Mycotoxin analysis: immunological techniques. In *Foodborne Disease Handbook, Plant Toxicants*, Hui, Y. H.; Smith, R. A.; Spoerke, D. G., Eds. Marcel Dekker: New York, 2001; Vol. 3, pp 683-713.
64. BarnaVetro, I., Solti, L., Teren, J., Gyongyosi, A., Szabo, E., Wolfling, A., *Sensitive ELISA test for determination of ochratoxin A*. *J. Agric. Food Chem.* **1996**, 44, (12), 4071-4074.
65. Thirumala-Devi, K., Mayo, M. A., Reddy, G., Reddy, S. V., Delfosse, P., Reddy, D. V. R., *Production of polyclonal antibodies against ochratoxin A and its detection in chilies by ELISA*. *J. Agric. Food Chem.* **2000**, 48, (10), 5079-5082.
66. Prieto-Simón, B., Campàs, M., Marty, J.-L., Noguer, T., *Novel highly-performing immunosensor-based strategy for ochratoxin A detection in wine samples*. *Biosens. Bioelectron.* **2008**, 23, (7), 995-1002.
67. Fujii, S., Ono, E. Y. S., Ribeiro, R. M. R., Assuncao, F. G. A., Takabayashi, C. R., de Oliveira, T., Itano, E. N., Ueno, Y., Kawamura, O., Hirooka, E. Y., *A comparison between enzyme immunoassay and HPLC for ochratoxin A detection in green, roasted and instant coffee*. *Braz. Arch. Biol. Techn.* **2007**, 50, (2), 349-359.
68. Fujii, S., Ribeiro, R. M. R., Scholz, M. B. D., Ono, E. Y. S., Prete, C. E. C., Itano, E. N., Ueno, Y., Kawamura, O., Hirooka, E. Y., *Reliable indirect competitive ELISA used for a survey of ochratoxin A in green coffee from the North of Parana State, Brazil*. *Food Addit. Contam.* **2006**, 23, (9), 902-909.
69. Taitt, C. R., Shriver-Lake, L. C., Ngundi, M. M., Ligler, F. S., *Array biosensor for toxin detection: continued advances*. *Sensors* **2008**, 8, (12), 8361-8377.
70. Ngundi, M. M., Shriver-Lake, L. C., Moore, M. H., Lassman, M. E., Ligler, F. S., Taitt, C. R., *Array Biosensor for Detection of Ochratoxin A in Cereals and Beverages*. *Anal. Chem.* **2004**, 77, (1), 148-154.
71. Ngundi, M. M., Shriver-Lake, L. C., Moore, M. H., Ligler, F. S., Taitt, C. R., *Multiplexed detection of mycotoxins in foods with a regenerable array*. *J. Food Prot.* **2006**, 69, (12), 3047-3051.

72. De Saeger, S., Sibanda, L., Paepens, C., Lobeau, M., Delmulle, B., Barna-Vetro, I., Van Peteghem, C., *Novel developments in rapid mycotoxin detection*. *Mycotoxin Res.* **2006**, 22, (2), 100-104.
73. Liu, B.-H., Tsao, Z.-J., Wang, J.-J., Yu, F.-Y., *Development of a monoclonal antibody against ochratoxin A and its application in enzyme-linked immunosorbent assay and gold nanoparticle immunochromatographic strip*. *Anal. Chem.* **2008**, 80, (18), 7029-7035.
74. Shim, W. B., Kolosova, A. Y., Kim, Y. J., Yang, Z. Y., Park, S. J., Eremin, S. A., Lee, I. S., Chung, D. H., *Fluorescence polarization immunoassay based on a monoclonal antibody for the detection of ochratoxin A*. *Int. J. Food Sci. Technol.* **2004**, 39, (8), 829-837.
75. Smith, D. S., Eremin, S. A., *Fluorescence polarization immunoassays and related methods for simple, high-throughput screening of small molecules*. *Anal. Bioanal. Chem.* **2008**, 391, (5), 1499-1507.
76. Zezza, F., Longobardi, F., Pascale, M., Eremin, S. A., Visconti, A., *Fluorescence polarization immunoassay for rapid screening of ochratoxin A in red wine*. *Anal. Bioanal. Chem.* **2009**, 395, (5), 1317-1323.
77. Robelek, R., *Surface plasmon resonance sensors in cell biology: basics and application*. *B.A.R.* **2009**, 1, (1), 57-72.
78. van der Gaag, B., Spath, S., Dietrich, H., Stigter, E., Boonzaaijer, G., van Osenbruggen, T., Koopal, K., *Biosensors and multiple mycotoxin analysis*. *Food Control* **2003**, 14, (4), 251-254.
79. Grieshaber, D., MacKenzie, R., Voros, J., Reimhult, E., *Electrochemical biosensors - Sensor principles and architectures*. *Sensors* **2008**, 8, (3), 1400-1458.
80. Adanyi, N., Levkovets, I. A., Rodriguez-Gil, S., Ronald, A., Varadi, M., Szendro, I., *Development of immunosensor based on OWLS technique for determining Aflatoxin B1 and Ochratoxin A*. *Biosens. Bioelectron.* **2007**, 22, (6), 797-802.
81. Beyer, M., Felgenhauer, T., Bischoff, F. R., Breitling, F., Stadler, V., *A novel glass slide-based peptide array support with high functionality resisting non-specific protein adsorption*. *Biomaterials* **2006**, 27, (18), 3505-3514.
82. Radi, A. E., Munoz-Berbel, X., Cortina-Ping, M., Marty, J. L., *Novel protocol for covalent immobilization of horseradish peroxidase on gold electrode surface*. *Electroanal.* **2009**, 21, (6), 696-700.

83. Schmid, A. H., Stanca, S. E., Thakur, M. S., Thampi, K. R., Suri, C. R., *Site-directed antibody immobilization on gold substrate for surface plasmon resonance sensors*. Sens. Actuators, B **2006**, 113, (1), 297-303.
84. Pasche, S., Voros, J., Griesser, H. J., Spencer, N. D., Textor, M., *Effects of ionic strength and surface charge on protein adsorption at PEGylated surfaces*. J. Phys. Chem. B **2005**, 109, (37), 17545-17552.
85. Schlapak, R., Armitage, D., Saucedo-Zeni, N., Hohage, M., Howorka, S., *Dense passivating poly(ethylene glycol) films on indium tin oxide substrates*. Langmuir **2007**, 23, 10244-10253.
86. Ohtsuka, K., Uemura, K., Nojima, T., Waki, M., Takenaka, S., *Immobilization of RNase S-peptide on a single-stranded DNA-fixed gold surface and effective masking of its surface by an acridinyl poly(ethylene glycol)*. Analyst **2006**, 131, (1), 55-61.
87. Butler, J. E., *Solid supports in enzyme-linked immunosorbent assay and other solid-phase immunoassays*. Methods **2000**, 22, (1), 4-23.
88. Angenendt, P., Glokler, J., Murphy, D., Lehrach, H., Cahill, D. J., *Toward optimized antibody microarrays: a comparison of current microarray support materials*. Anal. Biochem. **2002**, 309, (2), 253-260.
89. Yakovleva, J., Davidsson, R., Lobanova, A., Bengtsson, M., Eremin, S., Laurell, T., Emneus, J., *Microfluidic enzyme immunoassay using silicon microchip with immobilized antibodies and chemiluminescence detection*. Anal. Chem. **2002**, 74, (13), 2994-3004.
90. North, S. H., Lock, E. H., King, T. R., Franek, J. B., Walton, S. G., Taitt, C. R., *Effect of physicochemical anomalies of soda-lime silicate slides on biomolecule immobilization*. Anal. Chem. **2010**, 82, (1), 406-412.
91. North, S. H., Lock, E. H., Taitt, C. R., Walton, S. G., *Critical aspects of biointerface design and their impact on biosensor development*. Anal. Bioanal. Chem. **2010**, 397, 925-933.
92. Shriver-Lake, L. C., *Silane-modified surfaces for biomaterial immobilization*. In *Immobilized Biomolecules in Analysis: A Practical Approach*, Cass, T.; Ligler, F. S., Eds. Oxford University Press: NY, 1998; pp 1-14.
93. Cloarec, J. P., Deligianis, N., Martin, J. R., Lawrence, I., Souteyrand, E., Polychronakos, C., Lawrence, M. F., *Immobilization of homooligonucleotide probe layers onto Si/SiO₂ substrates: characterization by electrochemical impedance measurements and radiolabelling*. Biosens. Bioelectron. **2002**, 17, (5), 405-412.

94. Piehler, J., Brecht, A., Valiokas, R., Liedberg, B., Gauglitz, G., *A high-density poly(ethylene glycol) polymer brush for immobilization on glass-type surfaces.* Biosens. Bioelectron. **2000**, 15, (9-10), 473-481.
95. Gauthier, S., Aime, J. P., Bouhacina, T., Attias, A. J., Desbat, B., *Study of grafted silane molecules on silica surface with an atomic force microscope.* Langmuir **1996**, 12, (21), 5126-5137.
96. Halliwell, C. M., Cass, A. E. G., *A factorial analysis of silanization conditions for the immobilization of oligonucleotides on glass surfaces.* Anal. Chem. **2001**, 73, (11), 2476-2483.
97. Luzinov, I., Julthongpiput, D., Liebmann-Vinson, A., Cregger, T., Foster, M. D., Tsukruk, V. V., *Epoxy-terminated self-assembled monolayers: molecular glues for polymer layers.* Langmuir **2000**, 16, (2), 504-516.
98. Knecht, B. G., Strasser, A., Dietrich, R., Maertlbauer, E., Niessner, R., Weller, M. G., *Automated microarray system for the simultaneous detection of antibiotics in milk.* Anal. Chem. **2004**, 76, (3), 646-654.
99. Elbs, M., Brock, R., *Determination of binding constants on microarrays with confocal fluorescence detection.* Anal. Chem. **2003**, 75, (18), 4793-4800.
100. Schlapak, R., Caruana, D., Armitage, D., Howorka, S., *Semipermeable poly(ethylene glycol) films: the relationship between permeability and molecular structure of polymer chains.* Soft Matter **2009**, 5, (21), 4104-4112.
101. Metzger, S. W., Natesan, M., Yanavich, C., Schneider, J., Lee, G. U., *Development and characterization of surface chemistries for microfabricated biosensors.* J. Vac. Sci. Technol. A-Vac. Surf. Films **1999**, 17, (5), 2623-2628.
102. Rapp Polymere GmbH, Tübingen. <http://www.rapp-polymere.com/>, accessed November 10, 2010
103. Groll, J., Haubensak, W., Ameringer, T., Moeller, M., *Ultrathin coatings from isocyanate terminated star PEG prepolymers: patterning of proteins on the layers.* Langmuir **2005**, 21, (7), 3076-3083.
104. Groll, J., Amirgoulova, E. V., Ameringer, T., Heyes, C. D., Rocker, C., Nienhaus, G. U., Moller, M., *Biofunctionalized, ultrathin coatings of cross-linked star-shaped poly(ethylene oxide) allow reversible folding of immobilized proteins.* JACS **2004**, 126, (13), 4234-4239.

105. Groll, J., Ameringer, T., Spatz, J. P., Moeller, M., *Ultrathin coatings from isocyanate-terminated star PEG prepolymers: layer formation and characterization*. *Langmuir* **2005**, 21, (5), 1991-1999.
106. Gasteier, P., Reska, A., Schulte, P., Salber, J., Offenhausser, A., Moeller, M., Groll, J., *Surface grafting of PEO-based star-shaped molecules for bioanalytical and biomedical applications*. *Macromol. Biosci.* **2007**, 7, (8), 1010-1023.
107. Diamandis, E. P., Christopoulos, T. K., *The biotin (strept)avidin system - principles and applications in biotechnology*. *Clin. Chem.* **1991**, 37, (5), 625-636.
108. Green, N. M., *Avidin and streptavidin*. *Method. Enzymol.* **1990**, 184, 51-67.
109. Li, Y.-J., Bi, L.-J., Zhang, X.-E., Zhou, Y.-F., Zhang, J.-B., Chen, Y.-Y., Li, W., Zhang, Z.-P., *Reversible immobilization of proteins with streptavidin affinity tags on a surface plasmon resonance biosensor chip*. *Anal. Bioanal. Chem.* **2006**, 386, 1321-1326.
110. Birkert, O., Haake, H. M., Schutz, A., Mack, J., Brecht, A., Jung, G., Gauglitz, G., *A streptavidin surface on planar glass substrates for the detection of biomolecular interaction*. *Anal. Biochem.* **2000**, 282, (2), 200-208.
111. Kolb, H. C., Finn, M. G., Sharpless, K. B., *Click chemistry: diverse chemical function from a few good reactions*. *Angew. Chem., Int. Ed.* **2001**, 40, (11), 2004-2021.
112. Ciampi, S., Boecking, T., Kilian, K. A., James, M., Harper, J. B., Gooding, J. J., *Functionalization of acetylene-terminated monolayers on Si(100) surfaces: a click chemistry approach*. *Langmuir* **2007**, 23, (18), 9320-9329.
113. Wang, Q., Chan, T. R., Hilgraf, R., Fokin, V. V., Sharpless, K. B., Finn, M. G., *Bioconjugation by copper(I)-catalyzed azide-alkyne [3+2] cycloaddition*. *JACS* **2003**, 125, (11), 3192-3193.
114. Quan, S., Xuesi, C., Tiancheng, L., Xiabin, J., *The immobilization of proteins on biodegradable polymer fibers via click chemistry*. *Biomaterials* **2008**, 29, (8), 1118-1126.
115. Lin, P. C., Ueng, S. H., Tseng, M. C., Ko, J. L., Huang, K. T., Yu, S. C., Adak, A. K., Chen, Y. J., Lin, C. C., *Site-specific protein modification through Cu-I-catalyzed 1,2,3-triazole formation and its implementation in protein microarray fabrication*. *Angew. Chem., Int. Ed.* **2006**, 45, (26), 4286-4290.
116. Matsumoto, E., Yamauchi, T., Fukuda, T., Miura, Y., *Sugar microarray via click chemistry: molecular recognition with lectins and amyloid beta(1-42)*. *Sci. Technol. Adv. Mat.* **2009**, 10, (3).

117. Rozkiewicz, D. I., Gierlich, J., Burley, G. A., Gutmiedl, K., Carell, T., Ravoo, B. J., Reinhoudt, D. N., *Transfer printing of DNA by "Click" chemistry*. *ChemBiochem* **2007**, 8, 1997-2002.
118. Chevlot, Y., Bouillon, C., Vidal, S., Morvan, F., Meyer, A., Cloarec, J. P., Jochum, A., Praly, J. P., Vasseur, J. J., Souteyrand, E., *DNA-based carbohydrate biochips: a platform for surface glyco-engineering*. *Angew. Chem., Int. Ed.* **2007**, 46, (14), 2398-2402.
119. Frank, R., *The SPOT synthesis technique - synthetic peptide arrays on membrane supports - principles and applications*. *J. Immunol. Methods* **2002**, 267, (1), 13-26.
120. Reineke, U., Volkmer-Engert, R., Schneider-Mergener, J., *Applications of peptide arrays prepared by the SPOT-technology*. *Curr. Opin. Biotechnol.* **2001**, 12, (1), 59-64.
121. Barbulovic-Nad, I., Lucente, M., Sun, Y., Zhang, M., Wheeler, A. R., Busmann, M., *Bio-microarray fabrication techniques - a review*. *CRC Cr. Rev. Biotechn.* **2006**, 26, (4), 237-259.
122. Quist, A. P., Pavlovic, E., Oscarsson, S., *Recent advances in microcontact printing*. *Anal. Bioanal. Chem.* **2005**, 381, (3), 591-600.
123. Geissler, M., Bernard, A., Bietsch, A., Schmid, H., Michel, B., Delamarche, E., *Microcontact-printing chemical patterns with flat stamps*. *JACS* **2000**, 122, (26), 6303-6304.
124. Avseenko, N. V., Morozova, T. Y., Ataulakhanov, F. I., Morozov, V. N., *Immunoassay with multicomponent protein microarrays fabricated by electrospray deposition*. *Anal. Chem.* **2002**, 74, (5), 927-933.
125. Avseenko, N. V., Morozova, T. Y., Ataulakhanov, F. I., Morozov, V. N., *Immobilization of proteins in immunochemical microarrays fabricated by electrospray deposition*. *Anal. Chem.* **2001**, 73, (24), 6047-6052.
126. Duocastella, M., Fernandez-Pradas, J. M., Morenza, J. L., Zafra, D., Serra, P., *Novel laser printing technique for miniaturized biosensors preparation*. *Sens. Actuators, B*, 145, (1), 596-600.
127. Merrifield, R. B., *Solid-phase peptide synthesis. III. Improved synthesis of bradykinin*. *Biochemistry* **1964**, 3, (9), 1385-&.
128. Merrifield, R. B., *Solid phase peptide synthesis. I. Synthesis of a tetrapeptide*. *JACS* **1963**, 85, (14), 2149-&.

129. Mitchell, A. R., *Invited review: Bruce Merrifield and solid-phase peptide synthesis: a historical assessment*. *Biopolymers* **2008**, 90, (3), 175-184.
130. Lemieux, G. A., Bertozzi, C. R., *Chemoselective ligation reactions with proteins, oligosaccharides and cells*. *Trends Biotechnol.* **1998**, 16, (12), 506-513.
131. Fields, G., *Solid-phase peptide synthesis*. In *Molecular Biomethods Handbook*, Walker, J. M.; Rapley, R., Eds. Humana Press: Totowa, NJ, 1998; pp 527-545.
132. Amblard, M., Fehrentz, J.-A., Martinez, J., Subra, G., *Methods and protocols of modern solid phase peptide synthesis*. *Mol. Biotechnol.* **2006**, 33, (3), 239-254.
133. Sheppard, R., *The fluorenylmethoxycarbonyl group in solid phase synthesis*. *J. Pept. Sci.* **2003**, 9, (9), 545-552.
134. Isidro-Llobet, A., Alvarez, M., Albericio, F., *Amino acid-protecting groups*. *Chem. Rev.* **2009**, 109, (6), 2455-2504.
135. Walker, J. M., Aitken, A., Learmonth, M., *Protein determination by UV absorption*. In *The Protein Protocols Handbook*, Humana Press: 1996; pp 3-6.
136. Wellings, D. A., Atherton, E., *Standard Fmoc protocols*. *Method. Enzymol.* **1997**, 289, 44-67.
137. Gude, M., Ryf, J., White, P. D., *An accurate method for the quantitation of Fmoc-derivatized solid phase supports*. *Lett. Pept. Sci.* **2002**, 9, (4), 203-206.
138. Palasek, S. A., Cox, Z. J., Collins, J. M., *Limiting racemization and aspartimide formation in microwave-enhanced Fmoc solid phase peptide synthesis*. *J. Pept. Sci.* **2007**, 13, (3), 143-148.
139. Nicolas, E., Pedroso, E., Giralt, E., *Formation of aspartimide peptides in Asp-Gly sequences*. *Tetrahedron Lett.* **1989**, 30, (4), 497-500.
140. Yang, Y., Sweeney, W. V., Schneider, K., Thornqvist, S., Chait, B. T., Tam, J. P., *Aspartimide formation in base-driven 9-fluorenylmethoxycarbonyl chemistry*. *Tetrahedron Lett.* **1994**, 35, (52), 9689-9692.
141. Dolling, R., Beyermann, M., Haenel, J., Kernchen, F., Krause, E., Franke, P., Brudel, M., Bienert, M., *Piperidine-mediated side product formation for Asp(Obu(T))-containing peptides*. *J. Chem. Soc. Chem. Comm.* **1994**, (7), 853-854.
142. Packman, L. C., *N-2 hydroxy-4-methoxybenzyl (Hmb) backbone protection strategy prevents double aspartimide formation in a difficult peptide sequence*. *Tetrahedron Lett.* **1995**, 36, (41), 7523-7526.

143. Fall, B. I., Eberlein-Konig, B., Behrendt, H., Niessner, R., Ring, J., Weller, M. G., *Microarrays for the screening of allergen-specific IgE in human serum*. Anal. Chem. **2003**, 75, (3), 556-562.
144. Weller, M. G., Schuetz, A. J., Winklmaier, M., Niessner, R., *Highly parallel affinity sensor for the detection of environmental contaminants in water*. Anal. Chim. Acta **1999**, 393, (1-3), 29-41.
145. Rieger, M., Cervino, C., Saucedo, J. C., Niessner, R., Knopp, D., *Efficient hybridoma screening technique using capture antibody based microarrays*. Anal. Chem. **2009**, 81, (6), 2373-2377.
146. Lin, Z., Saucedo-Friebe, J. C., Lin, J. M., Niessner, R., Knopp, D., *Double-codified nanogold particles based automated flow-through CLEIA for 2,4-dinitrotoluene*. Anal. Methods **2010**, 2, 824-830.
147. Kloth, K., Rye-Johnsen, M., Didier, A., Dietrich, R., Märklbauer, E., Niessner, R., Seidel, M., *A regenerable immuno-chip for the rapid determination of 13 different antibiotics in raw milk*. Analyst **2009**, 134, (7), 1433-1439.
148. Kloth, K., *Entwicklung eines regenerierbaren Mikroarray-Chips zur simultanen Detektion von 13 Antibiotika in Milch*, PhD thesis, Technische Universität München **2009**.
149. Seidel, M., Niessner, R., *Automated analytical microarrays: a critical review*. Anal. Bioanal. Chem. **2008**, 391, (5), 1521-1544.
150. Squires, T. M., Messinger, R. J., Manalis, S. R., *Making it stick: convection, reaction and diffusion in surface-based biosensors*. Nat. Biotechnol. **2008**, 26, (4), 417-426.
151. Wolter, A., Niessner, R., Seidel, M., *Preparation and characterization of functional poly(ethylene glycol) surfaces for the use of antibody microarrays*. Anal. Chem. **2007**, 79, (12), 4529-4537.
152. Cervino, C., Knopp, D., Weller, M. G., Niessner, R., *Novel aflatoxin derivatives and protein conjugates*. Molecules **2007**, 12, (3), 641-653.
153. Cervino, C., *Entwicklung von immunoanalytischen, chromatographischen und massenspektrometrischen Methoden zur Bestimmung von Aflatoxinen in Lebensmitteln*, PhD thesis, Technische Universität München **2009**.
154. Hastings, K. L., Hagler, W. M., Harris, T. M., Voyksner, R. D., Dean, J. H., *Production and characterization of aflatoxin-B₂ oximinoacetate*. J. Agric. Food Chem. **1989**, 37, (2), 393-400.

155. Kandimalla, V. B., Neeta, N. S., Karanth, N. G., Thakur, M. S., Roshini, K. R., Rani, B. E. A., Pasha, A., Karanth, N. G. K., *Regeneration of ethyl parathion antibodies for repeated use in immunosensor: a study on dissociation of antigens from antibodies.* Biosens. Bioelectron. **2004**, 20, (4), 903-906.
156. Gonzalez-Martinez, M. A., Puchades, R., Maquieira, A., Ferrer, I., Marco, M. P., Barcelo, D., *Reversible immunosensor for the automatic determination of atrazine. Selection and performance of three polyclonal antisera.* Anal. Chim. Acta **1999**, 386, (3), 201-210.
157. Fitzpatrick, B., O'Kennedy, R., *The development and application of a surface plasmon resonance-based inhibition immunoassay for the determination of warfarin in plasma ultrafiltrate.* J. Immunol. Methods **2004**, 291, (1-2), 11-25.
158. Raz, S. R., Bremer, M., Haasnoot, W., Norde, W., *Label-free and multiplex detection of antibiotic residues in milk using imaging surface plasmon resonance-based immunosensor.* Anal. Chem. **2009**, 81, (18), 7743-7749.
159. Dong, M. W., *Modern HPLC for practicing scientists*, John Wiley & Sons, Inc., 1. ed., Hoboken, N.J. **2006**.
160. Schlapak, R., Pammer, P., Armitage, D., Zhu, R., Hinterdorfer, P., Vaupel, M., Fruhwirth, T., Howorka, S., *Glass surfaces grafted with high-density poly(ethylene glycol) as substrates for DNA oligonucleotide microarrays.* Langmuir **2006**, 22, (1), 277-285.
161. Emoto, K., Van Alstine, J. M., Harris, J. M., *Stability of poly(ethylene glycol) graft coatings.* Langmuir **1998**, 14, (10), 2722-2729.
162. Wutz, K., *Quantifizierung von Antibiotika in Milch und Honig mittels eines Chemilumineszenz-Durchfluss-Mikroarray-Chip-Auslesesystems*, MSc Thesis, Technische Universität München **2009**.
163. Pittet, A., Tornare, D., Huggett, A., Viani, R., *Liquid chromatographic determination of ochratoxin A in pure and adulterated soluble coffee using an immunoaffinity column cleanup procedure.* J. Agric. Food Chem. **1996**, 44, (11), 3564-3569.
164. Foley, J., Dorsey, J., *Clarification of the limit of detection in chromatography.* Chromatographia **1984**, 18, (9), 503-511.
165. *OchraTest & OchraTest WB Instruction Manual (for HPLC use)*, VICAM, Waterton, MA **2008**.

166. Cervino, C., Weber, E., Knopp, D., Niessner, R., *Comparison of hybridoma screening methods for the efficient detection of high-affinity hapten-specific monoclonal antibodies*. J. Immunol. Methods **2008**, 329, (1-2), 184-193.
167. Ekins, R. P., Chu, F., *Developing multianalyte assays*. Trends Biotechnol. **1994**, 12, (3), 89-94.
168. Pesce, A. J., Michael, J. G., *Artifacts and limitations of enzyme-immunoassay*. J. Immunol. Methods **1992**, 150, (1-2), 111-119.
169. Findlay, J. W. A., Dillard, R. F., *Appropriate calibration curve fitting in ligand binding assays*. AAPS Journal **2007**, 9, (2), E260-E267.
170. Clifford, M. N., *Chlorogenic acids and other cinnamates - nature, occurrence, dietary burden, absorption and metabolism*. J. Sci. Food Agric. **2000**, 80, (7), 1033-1043.
171. Daglia, M., Papetti, A., Aceti, C., Sordelli, B., Spini, V., Gazzani, G., *Isolation and determination of alpha -dicarbonyl compounds by RP-HPLC-DAD in green and roasted coffee*. J. Agric. Food Chem. **2007**, 55, (22), 8877-8882.
172. Savage, M. D., *Avidin-biotin chemistry: a handbook*, Pierce Chemical Co., Rockford, Illinois **1992**.
173. Dudley, R. A., Edwards, P., Ekins, R. P., Finney, D. J., McKenzie, I. G. M., Raab, G. M., Rodbard, D., Rodgers, R. P. C., *Guidelines for immunoassay data processing*. Clin. Chem. **1985**, 31, (8), 1264-1271.
174. Zheng, Z. M., Hanneken, J., Houchins, D., King, R. S., Lee, P., Richard, J. L., *Validation of an ELISA test kit for the detection of ochratoxin A in several food commodities by comparison with HPLC*. Mycopathologia **2005**, 159, (2), 265-272.
175. Lobeau, M., De Saeger, S., Sibanda, L., Barna-Vetro, I., Van Peteghem, C., *Development of a new clean-up tandem assay column for the detection of ochratoxin A in roasted coffee*. Anal. Chim. Acta **2005**, 538, (1-2), 57-61.
176. Sibanda, L., De Saeger, S., Barna-Vetro, I., Van Peteghem, C., *Development of a solid-phase cleanup and portable rapid flow-through enzyme immunoassay for the detection of ochratoxin A in roasted coffee*. J. Agric. Food Chem. **2002**, 50, (24), 6964-6967.
177. Berthiller, F., Sulyok, M., Krska, R., Schuhmacher, R., *Chromatographic methods for the simultaneous determination of mycotoxins and their conjugates in cereals*. Int. J. Food Microbiol. **2007**, 119, (1-2), 33-37.
178. Sulyok, M., Krska, R., Schuhmacher, R., *A liquid chromatography/tandem mass spectrometric multi-mycotoxin method for the quantification of 87 analytes and its*

- application to semi-quantitative screening of moldy food samples. Anal. Bioanal. Chem.* **2007**, 389, (5), 1505-1523.
179. Entwisle, A. C., Williams, A. C., Mann, P. J., Russell, J., Slack, P. T., Gilbert, J., *Combined phenyl silane and immunoaffinity column cleanup with liquid chromatography for determination of ochratoxin A in roasted coffee: collaborative study. J. AOAC Int.* **2001**, 84, (2), 444-450.
180. Vargas, E. A., Whitaker, T. B., Santos, E. A., Slate, A. B., Lima, F. B., Franca, R. C. A., *Testing green coffee for ochratoxin A, part I: estimation of variance components. J. AOAC Int.* **2004**, 87, (4), 884-891.
181. Vatinno, R., Aresta, A., Zambonin, C. G., Palmisano, F., *Determination of ochratoxin A in green coffee beans by solid-phase microextraction and liquid chromatography with fluorescence detection. J. Chromatogr. A.* **2008**, 1187, (1-2), 145-150.
182. Eisert, R., Pawliszyn, J., *Automated in-tube solid-phase microextraction coupled to high-performance liquid chromatography. Anal. Chem.* **1997**, 69, (16), 3140-3147.
183. Zhang, Z. Y., Yang, M. J., Pawliszyn, J., *Solid-phase microextraction. Anal. Chem.* **1994**, 66, (17), A844-A853.
184. Aresta, A., Cioffi, N., Palmisano, F., Zambonin, C. G., *Simultaneous determination of ochratoxin A and cyclopiazonic, mycophenolic, and tenuazonic acids in cornflakes by solid-phase microextraction coupled to high-performance liquid chromatography. J. Agric. Food Chem.* **2003**, 51, (18), 5232-5237.
185. Aresta, A., Palmisano, F., Vatinno, R., Zambonin, C. G., *Ochratoxin A determination in beer by solid-phase microextraction coupled to liquid chromatography with fluorescence detection: a fast and sensitive method for assessment of noncompliance to legal limits. J. Agric. Food Chem.* **2006**, 54, (5), 1594-1598.
186. Aresta, A., Vatinno, R., Palmisano, F., Zambonin, C. G., *Determination of ochratoxin A in wine at sub ng/mL levels by solid-phase microextraction coupled to liquid chromatography with fluorescence detection. J. Chromatogr. A.* **2006**, 1115, (1-2), 196-201.
187. Ligler, F. S., Sapsford, K. E., Golden, J. P., Shriver-Lake, L. C., Taitt, C. R., Dyer, M. A., Barone, S., Myatt, C. J., *The array biosensor: portable, automated systems. Anal. Sci.* **2007**, 23, (1), 5-10.
188. Saucedo-Friebe, J. C., Karsunke, X. Y. Z., Vazac, S., Biselli, S., Niessner, R., Knopp, D., *Regenerable immuno-biochip for screening ochratoxin A in green coffee extract*

- using an automated microarray chip reader with chemiluminescence detection. *Anal. Chim. Acta* **2011**, 689, (2), 234-242.
189. Roth, L., Frank, H., Kormann, K., *Giftpilze, Pilzgifte, Schimmelpilze, Mykotoxine. Vorkommen, Inhaltsstoffe, Pilzallergien, Nahrungsmittelvergiftungen.*, Ecomed, Landsberg am Lech **1990**.
190. Lee, N. A., Wang, S., Allan, R. D., Kennedy, I. R., *A rapid aflatoxin B₁ ELISA: Development and validation with reduced matrix effects for peanuts, corn, pistachio, and soybeans.* *J. Agric. Food Chem.* **2004**, 52, (10), 2746-2755.
191. Stroka, J., Anklam, E., *New strategies for the screening and determination of aflatoxins and the detection of aflatoxin-producing moulds in food and feed.* *TrAC Trend. Anal. Chem.* **2002**, 21, (2), 90-95.
192. Soares, L. M. V., Rodriguezamaya, D. B., *Screening and quantitation of ochratoxin-A in corn, peanuts, beans, rice, and cassava.* *J. AOAC Int.* **1985**, 68, (6), 1128-1130.
193. Sangare-Tigori, B., Dem, A. A., Kouadio, H. J., Betbeder, A. M., Dano, D. S., Moukha, S., Creppy, E. E., *Preliminary survey of ochratoxin A in millet, maize, rice and peanuts in Cote d'Ivoire from 1998 to 2002.* *Hum. Exp. Toxicol.* **2006**, 25, (4), 211-216.
194. Sangare-Tigori, B., Moukha, S., Kouadio, H. J., Betbeder, A. M., Dano, D. S., Creppy, E. E., *Co-occurrence of aflatoxin B-1, fumonisin B-1, ochratoxin A and zearalenone in cereals and peanuts from Cote d'Ivoire.* *Food Addit. Contam.* **2006**, 23, (10), 1000-1007.
195. Sultan, Y., Magan, N., *Mycotoxigenic fungi in peanuts from different geographic regions of Egypt.* *Mycotoxin Res.* **2010**, 26, (2), 133-140.
196. Hermanson, G. T., *Bioconjugate Techniques*, Academic Press, San Diego **1996**.
197. Pierce Biotechnology's description and instructions to sodium *meta*-periodate (product No. 20504), 2010.
198. Kononikhin, A. S., Nikolaev, E. N., Frankevich, V., Zenobi, R., *Letter: Multiply charged ions in matrix-assisted laser desorption/ionization generated from electrosprayed sample layers.* *Eur. J. Mass Spectrom.* **2005**, 11, 257-259.
199. Dhawan, S., *Design and construction of novel molecular conjugates for signal amplification (II): use of multivalent polystyrene microparticles and lysine peptide chains to generate immunoglobulin-horseradish peroxidase conjugates.* *Peptides* **2002**, 23, (12), 2099-2110.

200. Boorsma, D. M., Streefkerk, J. G., *Peroxidase-conjugate chromatography isolation of conjugates prepared with glutaraldehyde or periodate using polyacrylamide-agarose gel*. J. Histochem. Cytochem. **1976**, 24, (3), 481-486.
201. Boorsma, D. M., Kalsbeek, G. L., *Comparative study of horseradish-peroxidase conjugates prepared with a one-step and a two-step method*. J. Histochem. Cytochem. **1975**, 23, (3), 200-207.
202. Smith, P. K., *Measurement of protein using bicinchoninic acid*. United States Patent No.4839295, Pierce Chemical Company (Rockford, IL), **1989**.
203. Wiechelman, K. J., Braun, R. D., Fitzpatrick, J. D., *Investigation of the bicinchoninic acid protein assay: identification of the groups responsible for color formation*. Anal. Biochem. **1988**, 175, (1), 231-237.
204. Ott, S., *Synthese und Charakterisierung eines Antikörper-Enzym-Konjugats für die immunologische Bestimmung von Aflatoxinen in Nahrungsmitteln*, MSc thesis, Technische Universität München **2009**.
205. Smith, P. K., Krohn, R. I., Hermanson, G. T., Mallia, A. K., Gartner, F. H., Provenzano, M. D., Fujimoto, E. K., Goeke, N. M., Olson, B. J., Klenk, D. C., *Measurement of protein using bicinchoninic acid*. Anal. Biochem. **1985**, 150, (1), 76-85.
206. Harlow, E., Lane, D., *Antibodies: a laboratory manual*, Cold Spring Harbor Laboratory, 1st ed., New York **1988**.
207. Brill, A. S., Weinryb, I., *Reactions of horseradish peroxidase with azide. Evidence for a methionine residue at the active site*. Biochemistry **1967**, 6, (11), 3528-3535.
208. Kloth, K., Niessner, R., Seidel, M., *Development of an open stand-alone platform for regenerable automated microarrays*. Biosens. Bioelectron. **2009**, 24, (7), 2106-2112.